

2018

SENSORS FOR CERAMIC MATRIX COMPOSITE (CMC) ENGINE COMPONENTS

Kevin Rivera
University of Rhode Island, ryuzaki24@my.uri.edu

Follow this and additional works at: <https://digitalcommons.uri.edu/theses>

Terms of Use

All rights reserved under copyright.

Recommended Citation

Rivera, Kevin, "SENSORS FOR CERAMIC MATRIX COMPOSITE (CMC) ENGINE COMPONENTS" (2018).
Open Access Master's Theses. Paper 1408.
<https://digitalcommons.uri.edu/theses/1408>

This Thesis is brought to you by the University of Rhode Island. It has been accepted for inclusion in Open Access Master's Theses by an authorized administrator of DigitalCommons@URI. For more information, please contact digitalcommons-group@uri.edu. For permission to reuse copyrighted content, contact the author directly.

SENSORS FOR CERAMIC MATRIX COMPOSITE (CMC)

ENGINE COMPONENTS

BY

KEVIN RIVERA

A THESIS SUBMITTED IN PARTIAL FULFILLMENT OF THE

REQUIREMENTS FOR THE DEGREE OF

MASTER OF SCIENCE

IN

CHEMICAL ENGINEERING

UNIVERSITY OF RHODE ISLAND

2018

ABSTRACT

The focus of this thesis is to investigate alternative approaches to measure temperature and strain in the gas turbine engines. Within the hot section of gas turbine engines most components are made of nickel based superalloys however, next generation gas turbine engines will utilize ceramic matrix composites (CMCs) in the hot section. The CMCs consist of ceramic strand bundled into fibers and the fibers are then woven and embedded in a continuous ceramic matrix. Traditionally ceramic materials were not used for engine components because they were not lack ductility which is important with the shear and tensile forces that the engine components experience. Due to their superior thermomechanical properties, CMCs will soon replace nickel superalloys. The ability to instrument the CMC components with conventional wire based instrumentation including flame spray and thermal spray instrumentation is not an option for CMCs.

ACKNOWLEDGMENTS

I would like to humbly acknowledge Professor Otto J. Gregory for being an exceptional mentor to me the past five years as both an undergraduate student and masters student. Through high expectation and patience he has helped me to grow tremendously in the time I've worked with him and I owe my success, past or future, to the invaluable guidance and knowledge he has given.

I thank Michael Platek for being a great support in the lab. I specially thank Matthew Ricci for being someone whom I could always rely on and the members of my thesis committee: Professor Alan Davis and Professor Everett Crisman. Brenda Moyer, Mary Lou, and Deborah Brielmaier of the Chemical Engineering department have all been supportive and very helpful. I thank Vince Wnuk from HPI for providing mullite cement any time I needed because without it none of my research could have been possible. Very importantly, I thank my mother for being a visionary for what I could be capable of and pushing me forward.

PREFACE

This thesis is written in manuscript format and contains an introduction chapter, seven manuscript chapters, a conclusions chapter and a future work chapter. Manuscript one, two, three and four focus on thermocouples compatible with SiC-SiC ceramic matrix composites (CMCs). Manuscript five explores thermocouples, strain gages and resistance temperature detectors (RTDs) compatible with SiC-SiC CMCs. Manuscript six investigates the strain gage concept more in depth and chapter seven does the same with the RTD.

Manuscript one: “Novel Temperature Sensors for CMC Engine Components” was published in the Journal of Materials Research by Kevin Rivera, Tommy Muth, John Rhoat, Matthew Ricci, and Otto J. Gregory discusses thermocouples compatible with SiC-SiC CMCs. The SiC-SiC CMC substrates are used as part of the thermocouple and platinum thin films are used as the other part. The SiC-SiC CMC substrates provided also have varying ceramic fiber orientations and the effect of varying orientation on thermocouple performance is investigated.

Manuscript two: “ITO:SiC CMC Thermocouples for CMC Engine Components” by Kevin Rivera and Otto J. Gregory is currently being reviewed for publication in IEEE Electron Device Letters. The article focuses on the fabrication of thermocouples compatible with the SiC-SiC CMCs that incorporate indium tin oxide (ITO) as one thermoelement and the SiC-SiC CMC substrate as the other thermoelement making up the thermocouple.

Manuscript three: “Embedded Thermocouples for CMC Engine Components” was published in IEEE Sensors by Kevin Rivera, Matthew Ricci and Otto J. Gregory.

The article investigates protective barrier coatings in an attempt to improve the high temperature stability of the Pt:SiC CMC thermocouples developed previously.

Manuscript four: “Diffusion Barrier Coatings for CMC Thermocouples” was published in Surface & Coatings Technology by Kevin Rivera, Matthew Ricci and Otto Gregory. The article revisits the Pt:SiC CMC thermocouples that were developed in the first manuscript and improves their high temperature stability so that they can perform near 1000°C. Protective barrier coatings are employed, and a final barrier scheme is defined that allows the thermocouples to survive to 930°C.

Manuscript five: “Advanced Sensors for CMC Engine Components” was published in ICACC 2018 by Kevin Rivera and Otto J. Gregory. The article discusses thermocouples as well as introduces strain gages and RTDs that are compatible with SiC-SiC CMCs and have been tested. This chapter serves as a precursor to the next two chapters.

Manuscript six: “Strain Gages for CMC Engine Components” was published in IEEE Sensors Letters by Kevin Rivera and Otto Gregory. The article explores Pt:SiC CMC strain gages which are compatible with SiC-SiC CMCs. The strain gages are tested to determine gage factor and high temperature performance.

Manuscript seven: “Resistance Temperature Detectors for CMC Engine Components” by Kevin Rivera and Otto Gregory is currently being prepared for publication in IEEE Electron Devices. In this article the SiC-SiC CMCs are used as resistors and their negative temperature coefficient of resistance is taken advantage of in conjunction with a four point resistance measurement technique in order to develop high temperature RTDs.

TABLE OF CONTENTS

| | |
|--|------------|
| ABSTRACT | ii |
| ACKNOWLEDGMENTS | iii |
| PREFACE..... | iv |
| TABLE OF CONTENTS..... | vi |
| LIST OF TABLES | x |
| LIST OF FIGURES | xi |
| 1 Introduction | 1 |
| 1.1 Background | 1 |
| 2 Novel Temperature Sensors for CMC Engine Components | 4 |
| 2.1 Abstract | 5 |
| 2.2 Introduction..... | 5 |
| 2.3 Experimental..... | 9 |
| 2.4 Results and Discussion | 14 |
| 2.5 Conclusions..... | 22 |
| List of References..... | 23 |
| 3 ITO:SiC CMC Thermocouples for CMC Engine Components..... | 26 |
| 3.1 Abstract | 27 |
| 3.2 Introduction..... | 27 |
| 3.3 Experimental..... | 29 |
| 3.3.1 Fabrication Process..... | 29 |
| 3.3.2 Testing Procedures | 31 |
| 3.3.3 Thermoelectric Characterization | 32 |
| 3.4 Results..... | 33 |
| 3.4.1 Thermoelectric Performance | 33 |
| 3.4.2 Thermocouple Measurement Drift..... | 35 |
| 3.5 Conclusions..... | 36 |

| | |
|---|-----------|
| List of References..... | 36 |
| 4 Embedded Thermocouples for CMC Engine Components..... | 39 |
| 4.1 Abstract | 40 |
| 4.2 Introduction..... | 40 |
| 4.3 Experimental..... | 42 |
| 4.3.1 Preparation of the CMC Substrate Overcoat | 42 |
| 4.3.2 Pt:SiC (CMC) Thermocouple Fabrication | 42 |
| 4.3.3 SiC Fiber Orientation..... | 44 |
| 4.3.4 Protective Barrier Testing..... | 44 |
| 4.4 Results..... | 46 |
| 4.4.1 SiC Fiber Orientation Effect Testing | 46 |
| 4.4.2 Protective Barrier Testing..... | 47 |
| 4.4.3 Governing Equations..... | 49 |
| 4.5 Conclusions..... | 50 |
| List of References..... | 50 |
| 5 Diffusion Barrier Coatings for CMC Thermocouples..... | 52 |
| 5.1 Abstract | 53 |
| 5.2 Introduction..... | 54 |
| 5.3 Experimental..... | 57 |
| 5.3.1 Fabrication | 57 |
| 5.3.2 Thermocouple Testing..... | 58 |
| 5.4 Results and Discussion | 60 |
| 5.4.1 Pt:SiC (CMC) TC with No Diffusion Barriers..... | 60 |
| 5.4.2 Pt:SiC (CMC) TC with An Oxygen Barrier | 61 |
| 5.4.3 Pt:SiC (CMC) TC with Oxygen and Platinum Silicide Barriers..... | 62 |
| 5.5 Conclusions..... | 64 |
| List of References..... | 65 |
| 6 Advanced Sensors for CMC Engine Components | 68 |
| 6.1 Abstract | 69 |
| 6.2 Introduction..... | 69 |
| 6.2.1 Temperature sensors | 70 |

| | | |
|-------|---|-----|
| 6.2.2 | Strain gages | 71 |
| 6.3 | Experimental..... | 72 |
| 6.3.1 | Preparation of the CMC Substrate Overcoat | 72 |
| 6.3.2 | Pt:SiC(CMC) Thermocouple Fabrication | 72 |
| 6.3.3 | SiC-SiC CMC RTD and Strain Gage Fabrication..... | 74 |
| 6.3.4 | Sensor Testing Procedures..... | 74 |
| 6.4 | Results and Discussion | 76 |
| 6.4.1 | Thermocouples with Protective Barrier Testing..... | 76 |
| 6.4.2 | SiC-SiC CMC RTD Testing..... | 78 |
| 6.4.3 | SiC-SiC CMC Strain Gage..... | 79 |
| 6.5 | Conclusions..... | 80 |
| | List of References..... | 80 |
| 7 | Strain Gages for CMC Engine Components | 83 |
| 7.1 | Abstract | 84 |
| 7.2 | Introduction..... | 84 |
| 7.3 | Experimental Results..... | 87 |
| 7.3.1 | Strain Gage Fabrication..... | 87 |
| 7.3.2 | Electrical Characterization of Contacts..... | 88 |
| 7.3.3 | Piezoresistance | 89 |
| 7.3.4 | SiC CMC Fiber Directionality Effect..... | 95 |
| 7.4 | Conclusion | 97 |
| | List of References..... | 98 |
| 8 | Resistance Temperature Detectors for CMC Engine Components..... | 101 |
| 8.1 | Abstract | 102 |
| 8.2 | Introduction..... | 102 |
| 8.3 | Experimental..... | 104 |
| 8.3.1 | Fabrication | 104 |
| 8.3.2 | Governing Equations..... | 105 |
| 8.3.3 | Diffusion Barrier Coatings..... | 105 |
| 8.3.4 | Testing Procedure..... | 106 |
| 8.4 | Results..... | 106 |

| | | |
|------|--|-----|
| 8.5 | Conclusion | 109 |
| | List of References..... | 109 |
| 9 | Conclusions | 111 |
| 9.1 | Thermocouples for CMC engine components..... | 111 |
| 9.2 | Strain Gages for CMC engine components | 111 |
| 10 | Future work | 113 |
| 10.1 | High Temperature CMC Thermocouples | 113 |
| 10.2 | High Temperature CMC Strain gages and RTDs | 113 |
| | APPENDICES | 115 |
| | BIBLIOGRAPHY | 116 |

LIST OF TABLES

| TABLE | PAGE |
|---|------|
| Table 1: Thermoelectric powers and drift rates of Pt:SiC CMC thermocouples with fiber orientation fibers perpendicular, parallel, and at a 45o to the long axis of the CMC substrate..... | 19 |
| Table 2: Tabulated results for SiC fiber orientation testing. | 46 |
| Table 3: Embedded SiC fiber orientation effect on gage factor using the four point ASTM C1341 and cantilever load methods at room temperature..... | 96 |

LIST OF FIGURES

| FIGURE | PAGE |
|--|------|
| Figure 1: Thermocouple schematic showing the two dissimilar conductors and the hot and cold temperature junctions. | 2 |
| Figure 2: Strain gage on a test piece which is held firmly at one end and flexed at the other end. The strain gage deforms with the target and its resistance is changed some measureable amount. In this case the strain gage exhibits piezoresistive effects and its | 3 |
| Figure 3: Schematic of a Pt:SiC CMC thermocouple, showing location of bond pads and interconnects (top view). Grey areas represent the CMC material while the dark grey represents the platinum bond pads and interconnects. | 10 |
| Figure 4: Photograph of three SiC-SiC CMC's beams used for the thermoelectric experiments. The SiC weaves in the CMC were (A) parallel to, (B) at a 45o angle to and (C) perpendicular to the long axis of the CMC beams. | 13 |
| Figure 5: Photograph of test bed used for thermoelectric testing. CMC beam is cantilever loaded to a chill block that keeps the cold junction at or near room temperature, while the hot junction temperature was varied from 100°C-1000°C. The heat shield produces a | 14 |
| Figure 6: Thermoelectric response of a Pt:SiC CMC thermocouple fabricated onto a SiC-SiC CMC substrate with fibers parallel to the long axis and tested for 20 hours. A peak hot junction temperature of 925°C was achieved. | 15 |

Figure 7: Thermoelectric response of a Pt:SiC CMC thermocouple and platinum:palladium thin film thermocouple upon heating and cooling; note the large difference in slopes for the two different thermocouples. There is almost no hysteresis between heating/cooling..... 16

Figure 8: (a) Thermoelectric response of a Pt:SiC CMC thermocouple with a SiC fiber weave that was at 45° diagonal relative to the long axis of the CMC beam, (b) Thermoelectric response of a Pt:SiC CMC thermocouple with a parallel SiC fiber weave relative to the..... 18

Figure 9: Thermoelectric response of a Pt:SiC CMC thermocouple at 530, 630, and 730°C fabricated with an ITON diffusion barrier. 21

Figure 10: Schematic of the ITO:SiC CMC thermocouple..... 31

Figure 11: Testing apparatus used for the thermocouples. The aluminum chill block induces a cold junction and the free floating end of the thermocouple is inserted into a tube furnace. Data is collected using a personal Daq54..... 32

Figure 12: Furnace test for the ITO:SiC CMC thermocouple. Temperature ramps from 20-660°C. 34

Figure 13: Hysteresis upon heating and cooling. Minimal hysteresis occurs at high temperature..... 34

Figure 14: Temperature limit testing for the ITO:SiC CMC thermocouple. Oxidation at the ITO:SiC CMC contact area causes oxidation and sensor failure past 700°C..... 35

Figure 15: Measurement drift test conducted at 600°C..... 36

Figure 16: Schematic top-down view of a Pt:SiC(CMC) thermocouple. 43

Figure 17: Cross section of a Pt:SiC(CMC) thermocouple with barrier coatings..... 43

| | |
|---|----|
| Figure 18: Photograph of different SiC fiber orientations in CMC. Note orientation (a) is horizontal, (b) at 45° to normal, and (c) parallel to the long axis of the substrate. .. | 45 |
| Figure 19: Photo of apparatus used for thermocouple testing and calibration..... | 45 |
| Figure 20: Pt:SiC(CMC) thermocouple with no diffusion barrier coating. | 48 |
| Figure 21: Pt:SiC(CMC) thermocouple utilizing a InON oxygen barrier coating. | 48 |
| Figure 22: Pt:SiC(CMC) thermocouple utilizing ITON oxygen and ITO platinum silicide barrier coatings. | 49 |
| Figure 23: Schematic of a Pt:SiC(CMC) thermocouple (top-view)..... | 55 |
| Figure 24: Schematic cross section of a Pt:SiC(CMC) thermocouple (cross section) showing the various sputtered films that serve as diffusion barriers and thermocouple legs (side view). | 56 |
| Figure 25: Apparatus used for testing Pt:SiC(CMC) thermocouples. | 60 |
| Figure 26: Thermoelectric response of a Pt:SiC(CMC) thermocouple with no diffusion barriers..... | 61 |
| Figure 27: Thermoelectric response of a Pt:SiC(CMC) thermocouple Utilizing an InON oxygen diffusion barrier..... | 62 |
| Figure 28: Thermoelectric response of a Pt:SiC(CMC) thermocouple that utilizes a ITON oxygen diffusion barrier and ITO platinum silicide diffusion barrier. | 63 |
| Figure 29: Schematic top-down view of a Pt:SiC(CMC) thermocouple. | 73 |
| Figure 30: Cross section of a Pt:SiC(CMC) thermocouple with barrier coatings..... | 73 |
| Figure 31: Schematic view of the design shared by SiC-SiC CMC RTD and strain gage. | 74 |
| Figure 32: Pt:SiC(CMC) thermocouple with no diffusion barrier coating | 77 |

| | |
|--|----|
| Figure 33: Pt:SiC(CMC) thermocouple utilizing a InON oxygen barrier coating..... | 78 |
| Figure 34: Pt:SiC(CMC) thermocouple utilizing ITON oxygen and ITO platinum silicide barrier coatings | 78 |
| Figure 35: RTD testing from 100-250°C. | 79 |
| Figure 36: SiC-SiC CMC strain gage test using an excitation current of 0.05A | 79 |
| Figure 37: Pt:SiC CMC strain gage design showing the two outer leads (current) and two inner leads (voltage). The pattern on the left is sensitive to longitudinal strain and the pattern on the right is sensitive to transverse strain. | 88 |
| Figure 38: I-V characteristics of a Pt:SiC CMC contact. The I-V characteristic in the forward bias and reverse bias conditions for the Pt:SiC-SiC CMC contacts at 20°C (left) and the I-V curve for the forward bias condition at temperatures ranging from 20°C-510°C | 89 |
| Figure 39: (Bottom) Plot showing resistance change as a function of applied strain in tension, Note; slight non-linear resistance change with applied strain. (Top) Portion of a test for a Pt:SiC CMC strain gage strained at $-600\mu\epsilon$ and 20°C. Gage factor of 112 is | 93 |
| Figure 40: The effect of temperature on the gage factor for the Pt:SiC CMC strain gage under compressive strain. | 93 |
| Figure 41: Photograph of SiC-SiC CMC substrates with differing fiber orientations. Relative to the long axis (Top) is 90°, (Middle) is 45°, and (Bottom) is parallel. | 94 |
| Figure 42: Photograph showing the testing tube furnace holding a Pt:SiC CMC strain gage in a cantilever fixture..... | 95 |

Figure 43: Pt/Rh:SiC CMC RTD design. Current is passed through the outer legs and voltage drop is measured across the inner legs..... 105

Figure 44: Resistance vs. temperature shows a linear relationship between resistance and temperature from 150°C to 450°C and nonlinear behavior at temperatures lower than 150°C and higher than 450°C. 107

Figure 45: TCR of the Pt/Rh:SiC CMC RTD as a function of temperature. 108

Figure 46: Cooldown of ITON/ITO:SiC CMC RTD. Large amount of thermal lag seen from 425°C-250°C..... 108

Figure 47: IV characteristics of ITO:SiC CMC contacts using the vanderpauw method. ITO forms an ohmic contact to the SiC-SiC CMC. 108

Figure 48: Concept for future RTD and strain gage showing a top and layered view. 114

CHAPTER 1

Introduction

Next generation gas turbine engines will utilize ceramic matrix composite (CMC) components rather than traditional nickel based superalloys due to their superior thermomechanical properties such as higher creep resistance and operating temperatures. CMC based components will permit higher engine operating temperatures and thus allows higher thermal efficiencies. Advanced instrumentation for these CMC components is needed to verify structural models and the structural integrity of the components. Wire sensors for temperature and strain measurement have been used extensively for nickel based superalloys since they can be welded directly to the components but they can affect the gas flow path and vibrational modes during operation due to their bulky nature, however, they cannot be welded to CMC components because the CMC is a ceramic material. Thin-film sensors can be deposited directly onto the surfaces of engine components and do not affect the gas flow path and vibrational modes during operation. However, thin-film sensors are prone to selective oxidation, dewetting, and metallurgical changes in the metallic films that lead to considerable signal drift.

1.1 Background

The goal of this project is to produce transducers which are able to convert a physical measurement (temperature or strain) to an electrical signal which can then be interpreted and stored. Thermocouples are comprised of two dissimilar conductors known as thermoelements (Fig. 1) and when connected, an electromotive force (emf) is produced due to the Seebeck effect. Strain gages are sensors used to measured

vibrations, displacement or applied forces. Strain gages come in a variety of types such resistors, capacitors, inductors, piezoelectric, etc. Piezoresistive strain gages consist of a resistor that exhibits a change in resistance when a force is applied on them (Fig. 2).

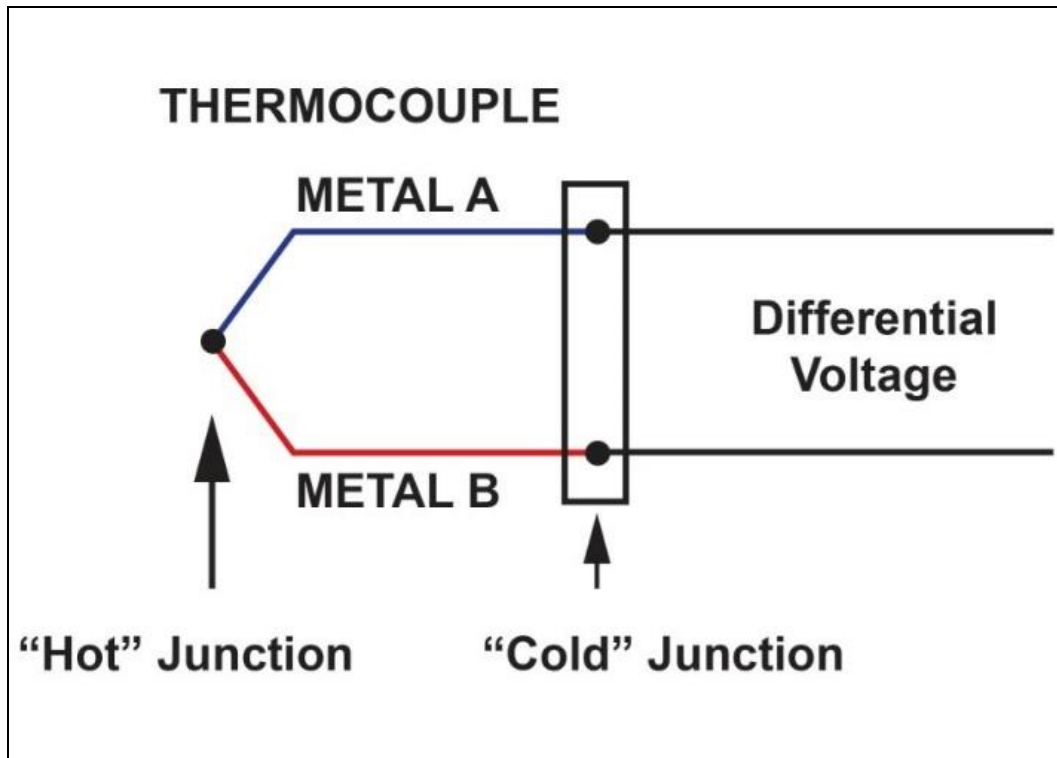


Figure 1: Thermocouple schematic showing the two dissimilar conductors and the hot and cold temperature junctions.

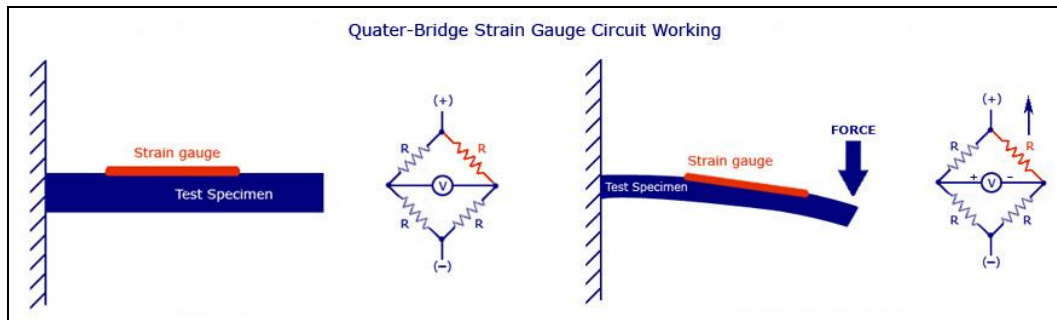


Figure 2: Strain gage located on a test piece which is held firmly at one end and flexed at the other end. As the strain gage deforms, its electrical resistance changes in a reproducible fashion. The magnitude of the change in resistance with strain is referred to as the piezoresistive effect and the metric is referred to as the gage factor.

CHAPTER 2

Novel Temperature Sensors for CMC Engine Components

Published in the Journal of Materials Research, September 2017

Kevin Rivera, Tommy Muth, John Rhoat, Matthew Ricci, Otto J. Gregory

Department of Chemical Engineering, University of Rhode Island, Kingston RI

K. Rivera, T. Muth, J. Rhoat, M. Ricci, O.J. Gregory, “Novel temperature sensors for CMC engine components,” Journal of Materials Research, vol. 32, pp. 3319-3325

2.1 Abstract

As more and more SiC-SiC ceramic matrix composites or CMC's are being used in the hot sections of gas turbine engines, there is a greater need for surface temperature measurement in these harsh conditions. Thin film sensors are ideally suited for this task since they have very small thermal masses and are non-intrusive due to their thickness. However, if the bulk properties of SiC contributed to the sensor performance (thermoelectric response) rather than those of the thin films, superior resolution and stability could be realized. Therefore, thermocouples utilizing the SiC-SiC CMC itself as one thermoelement and thin film platinum as the other thermoelement were developed. Large and stable thermoelectric powers ($\sim 180 \mu\text{V}/^\circ\text{K}$) were realized with these Pt:SiC(CMC) thermocouples. The advantages in using this approach for surface temperature measurement are presented as well as the effects of fiber orientation on thermoelectric response and drift.

2.2 Introduction

The next generation gas turbine engines will employ advanced materials that are specifically designed to handle the harsh environment inside the hot section of an engine. Thus, there is a need to develop instrumentation that can survive the higher operating temperatures associated with these advanced engine designs and monitor the conditions during operation. Specifically, engine components based on ceramic matrix composites or CMC's are lighter and have superior thermo-mechanical properties

compared to nickel-based superalloys [1]. Thus, they can operate at higher temperatures, which enable greater overall efficiencies. Advanced instrumentation must not only survive the rotational forces and high temperatures but must also be capable of accurately monitoring the temperature and strain of CMC engine components. Given the harsh conditions inside the gas turbine engine, it is becoming increasingly more difficult to instrument these CMC engine components to monitor structural integrity for extended periods of time, without adversely affecting operation of the engine.

Wire thermocouples, for example, are difficult to use on CMC's for temperature measurement, since they cannot be easily incorporated into the surfaces of environmental barrier coatings without affecting gas flow over the surface [1]. Typically, thin film sensors are deposited directly onto the surface of a component so that a true surface measurement is possible. In this way, thin film instrumentation becomes an integral part of the surface of a component. Thin film sensors have several advantages over conventional wire thermocouples. They do not interfere with gas flow paths through the engine because they have a low profile; i.e. they have thicknesses on the order of micrometers, which is well below the boundary layer thickness. Thin film sensors have extremely small masses (on the order of 10^{-6} g). With a minimal mass, this means that thin film sensors will not alter the vibrational modes of blades comprising the turbine. It also translates into faster response times [1] and there is no need for adhesives. However, thin film sensors also have some disadvantages including relatively small diffusion distances, which can lead to

decreased stability at elevated temperature.

Recent research has focused on developing thin film temperature and strain sensors for the next generation of ceramic matrix composites [1,18]. Much of this research has focused on platinum and palladium thin film thermocouples but these suffer from limitations associated with oxidation of the palladium at elevated temperatures [2]. Thin film thermocouples utilizing the SiC-SiC CMC itself as one of the thermoelements and platinum as the other thermoelement were fabricated on SiC-SiC CMC's and evaluated in terms of thermoelectric performance. Here, the bulk properties of SiC determine sensor performance (thermoelectric response) as opposed to the thin film properties of materials such as platinum and palladium. The Pt:SiC CMC thermocouples exhibit thermoelectric powers ranging from 130 $\mu\text{V/K}$ to 250 $\mu\text{V/K}$ depending on how the thermocouple is oriented with respect to the SiC fibers or weave in the CMC. These thermocouples can operate at significantly higher temperatures in the harsh environment of the gas turbine engine while maintaining low drift at temperature.

At high temperatures, the Pt:SiC interface comprising the hot junction of the Pt:SiC CMC thermocouple can undergo oxidation; i.e. oxygen can diffuse through the platinum film and react with the SiC to form an SiO_2 layer. This oxide changes the nature of the ohmic contact associated with the Pt:SiC junction and produces a rectifying junction, which ultimately contributes to the measured electromotive force (emf). This can lead to considerable signal drift that increases with increasing temperature. Thus, implementing an effective oxygen diffusion barrier is critical to the high temperature performance of these Pt:SiC CMC thermocouples. Increased stability

at high temperatures is a priority of this research since most thin film sensors fail due to the small diffusional distances associated with these devices. Bulk properties of the SiC in the CMC make Pt:SiC CMC thermocouples promising candidates for the extreme environments anticipated in advanced gas turbine engines. These thermocouples are also extremely sensitive, having a maximum thermoelectric voltage almost two orders of magnitude greater than those generated with type K wire thermocouples [3-9]. Yet the drift rates associated with these thermocouples were significantly lower than other types of thin film thermocouples. However, the hot junctions can also undergo platinum-silicide formation at temperatures greater than 600°C. The formation of platinum-silicides is normally inhibited by the diffusion of oxygen through the platinum [10] but when an oxygen diffusion barrier is employed, the thermodynamics shift in favor of the formation of platinum-silicides in the absence of oxygen at the Pt:SiC junction. At high temperatures (~1100C), a mixture of silicides are produced [11-13], but no carbides were formed since carbon precipitates migrate to the platinum-silicide grain boundaries [11,14]. Thus, a platinum-silicide diffusion barrier is necessary if these Pt:SiC (CMC) thermocouples are to be utilized for very high temperature applications.

The silicon-carbide fiber-reinforced silicon-carbide (SiC/SiC) composites were supplied by the NASA Glenn Research Center and are typically used for high temperature, structural applications. These fiber-reinforced materials show significantly improved toughness and damage tolerance in comparison to unreinforced monolithic ceramic materials with similar matrix compositions [15,16]. Other materials have been considered for these applications including: metallic super

alloys, carbon fiber composites, and oxide/oxide ceramic composites. For successful application, the ceramic matrix composite properties must be reproducible when fabricated in 3D shapes and maintain their strength at temperatures up to 1400C. Sylramic-iBN fibers (10- μm in diameter). These were processed via chemical vapor infiltration (CVI) of commercial Sylramic SiC [15,16]. These fibers are dense, polycrystalline, and exhibit stoichiometric ratios of Si and C. They also contain approximately 1% boron and 3% TIB_2 by weight [15,16]. The fibers are treated by the chemical vapor infiltration of boron nitride (BN), which allows excess boron in the bulk to diffuse to the fiber surface [16]. It then reacts with nitrogen to form an in situ boron nitride (BN) coating on the fiber surface improving creep resistance and thermal conductivity [16]. The BN coating also aids in increasing the oxidation resistance of the CMC at higher temperatures [17]. Coating the fibers provide matrix crack deflection and also prevents the growth of silica on fiber surfaces at high temperatures [15,16]. Undesired silica growth allows for strong mechanical bonds to form between the contacting fibers causing fracture or rupture stresses to be much lower than independently acting fibers [15,16]. SiC CMC's are also highly fatigue resistant [17] making them a much more attractive option for high temperature applications.

2.3 Experimental

A schematic of a Pt:SiC CMC thermocouple (top view) is shown in Figure 3. The thermocouple is comprised of a SiC-SiC CMC substrate that is coated with mullite or other dielectric for device isolation and two Pt:SiC junctions. In Figure 3, the light grey areas represent the CMC material while the dark grey areas represent the

platinum bond pads and interconnects. The SiC-SiC (CMC) beams measured 1 in x 7 in. Three different weave orientations were utilized for the thermoelectric experiments. Specifically, the SiC-SiC CMC beams had weaves parallel to, perpendicular to and at a 45° degree angle with respect to the long axis of the CMC beams, as shown in Figure 4. A mullite coating or other dielectric, approximately 200 μm thick was applied to the surface of the CMC and heat treated at 100C for 20 minutes, at 200C for 20 minutes and at 300C for 40 minutes followed by a 1000C heat treatment for 10 hours in a Deltech furnace. A dry negative MX5050™ Dupont™ photoresist was applied to the surface of the dielectric-coated beam and soft baked at 100C for one minute to pattern with thin film portion of the sensors.

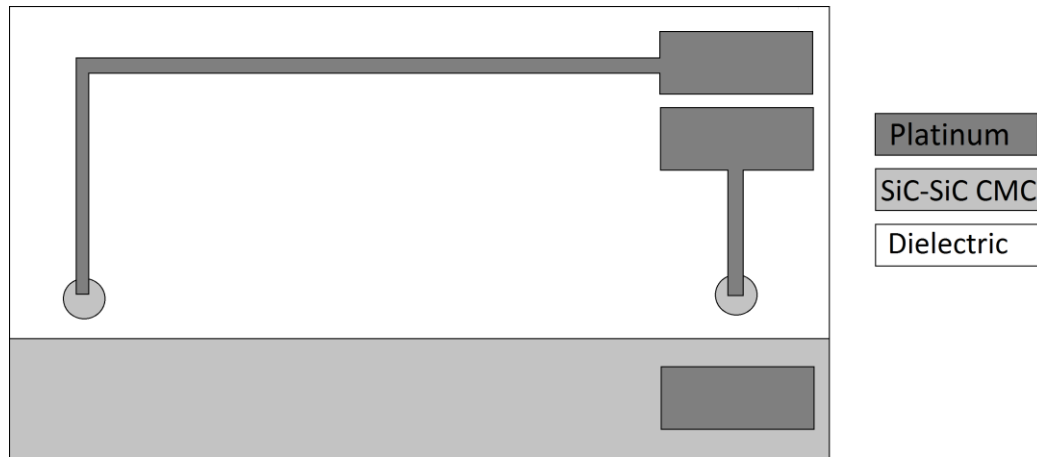


Figure 3: Schematic of a Pt:SiC CMC thermocouple, showing location of bond pads and interconnects (top view). Grey areas represent the CMC material while the dark grey represents the platinum bond pads and interconnects.

The photoresist-coated substrate was then exposed to ultraviolet light source (350 nm) using an AOI Aligner and developed using an ammonium hydroxide based developer.

The SiC-SiC CMC substrates were pre-etched using buffered HF to remove any native oxide layer that had formed on the surface during previous heating steps. Radio frequency (rf) sputtering was used to deposit platinum thin film interconnects and bond pads onto the surface of the SiC-SiC CMC substrates (see Figure 3). A chamber background pressure of $9 \times 10^{-3} \text{ mTorr}$ was maintained prior to sputter deposition. An rf power of 250W was used to deposit the platinum thin films. All platinum films were sputtered for 2 hours, resulting in a thickness of 1.5 μm . The furnace was programmed as follows: ramp to 700°C at a rate of 4°C/min and hold period of 30 minutes, a ramp to 200°C at a rate of 4°C/min and hold period of 30 minutes, a ramp back up to 700°C at a rate of 4°C/min and a hold period of 300 minutes, and finally a ramp back down to room temperature at a rate of 4°C/min. This protocol was used to determine the thermoelectric voltage as a function of temperature difference between the hot and cold junctions of the thermocouple. Drift was measured as a function of time while the furnace was held at a constant hot junction temperature. The test bed used for thermoelectric characterization is shown in Figure 5. Here, the SiC-SiC CMC beam was cantilever loaded to a chill block that uses ethylene glycol or chilled water to keep the block temperature at or near room temperature, while the hot junction temperature was varied from 100°C-1000°C. Platinum wires were used to connect the thermocouple to the PDAQ data acquisition system. Two type-K thermocouples were used to monitor the hot and cold junction temperatures on the instrumented SiC-SiC CMC beam, which was attached to the aluminum chill block (Figure 5). The assembly including the chill block was inserted into a horizontal tube furnace, with the heat

shield producing a temperature gradient along the beam. The thermoelectric voltage, V_t , was measured as a function of temperature according to equation (1) below:

$$V_t = \frac{\Delta V}{\Delta T} \quad (1)$$

where ΔV is the voltage difference between the SiC-SiC CMC and platinum and ΔT is the difference between the hot and cold junction temperatures. Drift rate, r , was also measured at temperature for the Pt:SiC CMC thermocouples, according to equation (2) below:

$$r = \frac{\Delta V}{V_i} \cdot \frac{T_c}{\Delta t} \quad (2)$$

where ΔV is the voltage difference measured at a constant temperature (T_c), V_i is the initial voltage measured and Δt is the time interval over which the voltage changes. Drift typically occurs due to the formation of an oxide layer between the platinum and SiC as a result of oxygen diffusion through the platinum interconnect. when the Pt:SiC (CMC) thermocouple that does not utilize an oxygen diffusion barrier. Drift could also be attributed to the formation of platinum-silicides of a Pt:SiC (CMC) thermocouple with an oxygen diffusion barrier but not a platinum-silicide barrier.

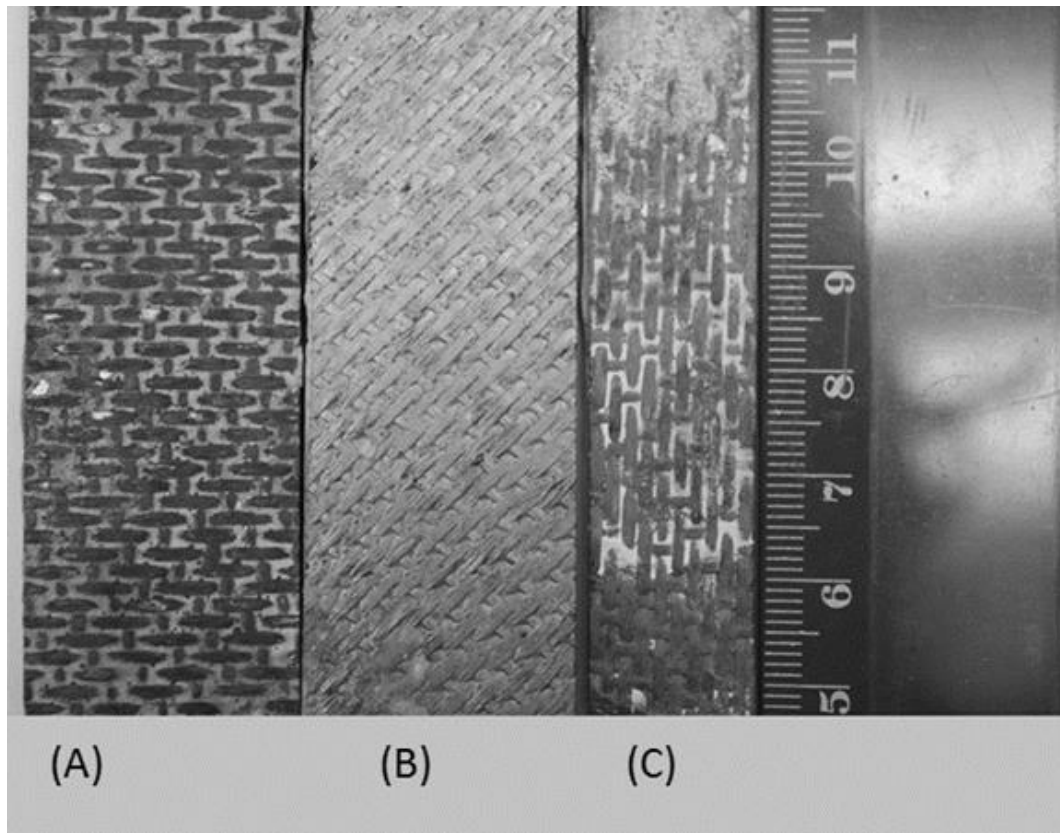


Figure 4: Photograph of three SiC-SiC CMC's beams used for the thermoelectric experiments. The SiC weaves in the CMC were (A) parallel to, (B) at a 45° angle to and (C) perpendicular to the long axis of the CMC beams.

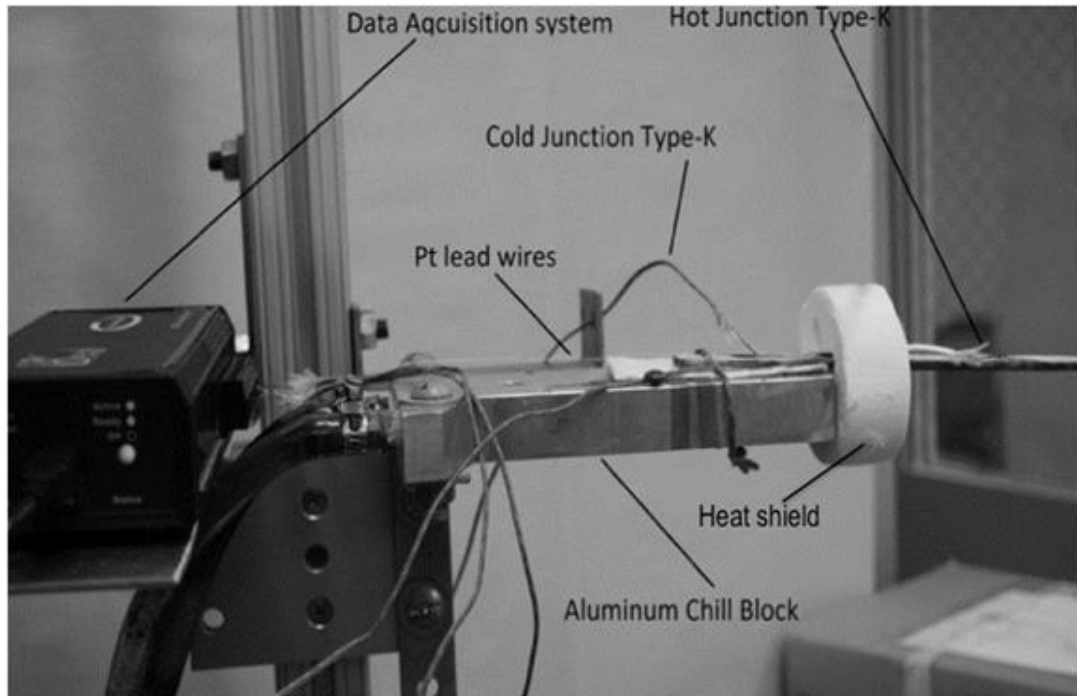


Figure 5: Photograph of test bed used for thermoelectric testing. CMC beam is cantilever loaded to a chill block that keeps the cold junction at or near room temperature, while the hot junction temperature was varied from 100°C-1000°C. The heat shield produces a

2.4 Results and Discussion

Figure 6 shows the thermoelectric response of a Pt:SiC CMC thermocouple as a function of temperature, with a peak hot junction temperature of 925°C. While the cold junction temperature varied from 25-100°C. The fiber orientation used in this test is the same as shown in figure 2(c) and a maximum voltage of 190 mV was observed for a peak temperature of 925°C. The thermoelectric response of the same Pt:SiC CMC thermocouple relative to a platinum:palladium thin film thermocouple is shown

in Figure 5. Here, The hysteresis upon heating and cooling (Figure 7) is minimal for the Pt:SiC CMC thermocouple as well as the platinum:palladium thin film thermocouple. The large difference in the slopes of the two curves is related to the difference in thermoelectric power for the two thermocouples. While both maintain very low hysteresis, the thermoelectric power of the Pt:SiC CMC thermocouple is almost two orders of magnitude greater than that of the platinum:palladium thermocouple due to the contribution of SiC-SiC CMC bulk properties to the thermoelectric power.

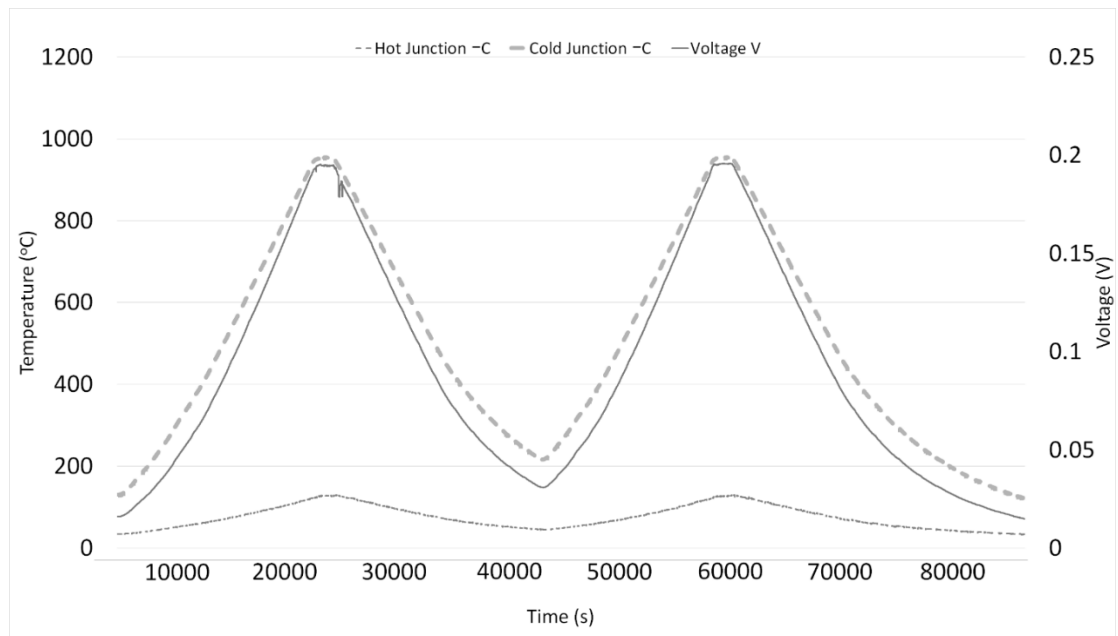


Figure 6: Thermoelectric response of a Pt:SiC CMC thermocouple fabricated onto a SiC-SiC CMC substrate with fibers parallel to the long axis and tested for 20 hours. A peak hot junction temperature of 925°C was achieved.

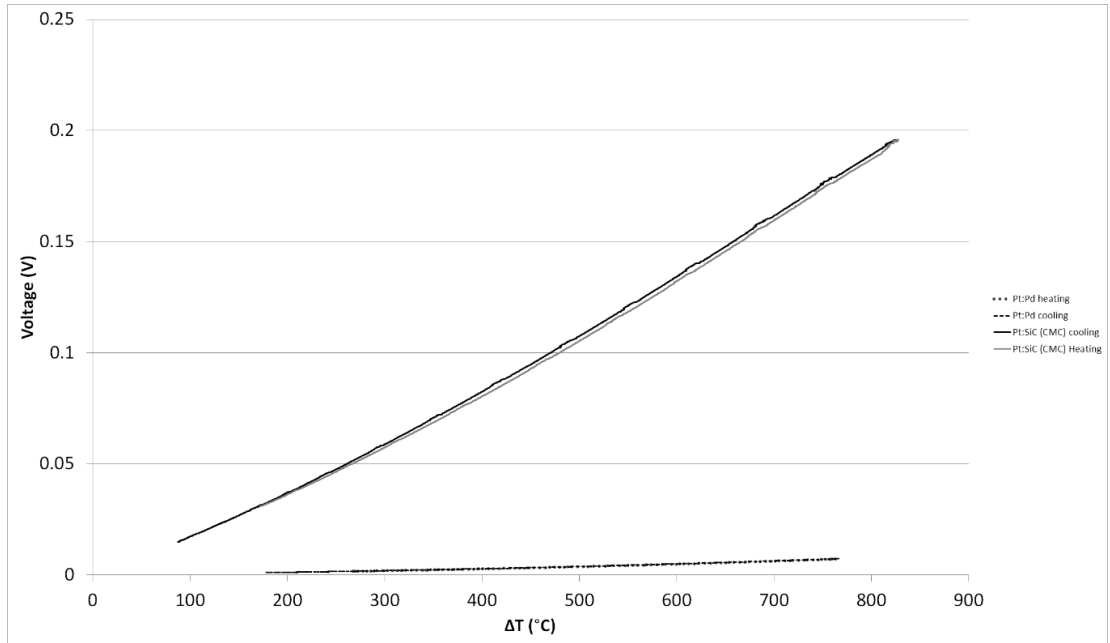


Figure 7: Thermoelectric response of a Pt:SiC CMC thermocouple and platinum:palladium thin film thermocouple upon heating and cooling; note the large difference in slopes for the two different thermocouples. There is almost no hysteresis between heating/cooling.

Thermoelectric response of Pt:SiC CMC thermocouples having different SiC fiber weaves is shown in Figure 8. The weave directions were parallel to, perpendicular to and at a 45° angle relative to the long axis of the CMC beams as shown in Figure 2b. The Pt:SiC CMC thermocouples here did not have the benefit of an oxygen diffusion barrier. When the CMC beams had SiC fibers perpendicular to the long axis of the beam, a maximum thermoelectric power of 148 $\mu\text{V}/^\circ\text{K}$ was realized when the hot junction reached a temperature of 510°C, which was the smallest response of all fiber orientations but still much larger than any response generated by Pt:Pt thermocouples

(~12 $\mu\text{V}/\text{K}$)[2]. The drift rate at this temperature was 2.68C/hr, which is extremely low when compared to most thin film thermocouples. When the CMC substrate had a 45° diagonal SiC fiber weave relative to the long axis of the CMC beam, a maximum thermoelectric power of 207 $\mu\text{V}/^\circ\text{K}$ was realized when the hot junction reached a temperature of 510°C. The drift rate at this temperature was 4.93 C/hr, which was the highest among all the substrates tested. When the CMC substrate had a parallel SiC fiber weave relative to the long axis of the CMC beam, a maximum thermoelectric power of 251 $\mu\text{V}/^\circ\text{K}$ was realized when the hot junction reached a temperature of 530°C. The drift rate at this temperature was 2.64 C/hr, which was the lowest seen among all the substrates tested. Therefore, the orientation with the largest thermoelectric power was the CMC beam with a SiC fiber weave parallel to the long axis of the CMC beam. The results shown in Figures 6 through 8 suggest that fiber orientation had a major effect on thermoelectric properties and that the SiC fibers played a large role than the SiC matrix in determining the overall thermoelectric properties. If the SiC matrix contributed to a greater extent than the SiC fibers, there would not be a strong correlation between the SiC fiber orientation and overall thermoelectric properties. Wrbanek et. al. showed that conductive oxides produce much greater thermoelectric powers [18] than the Pt:SiC CMC thermocouple but the thermocouples described here had the advantage of using the substrate material itself.

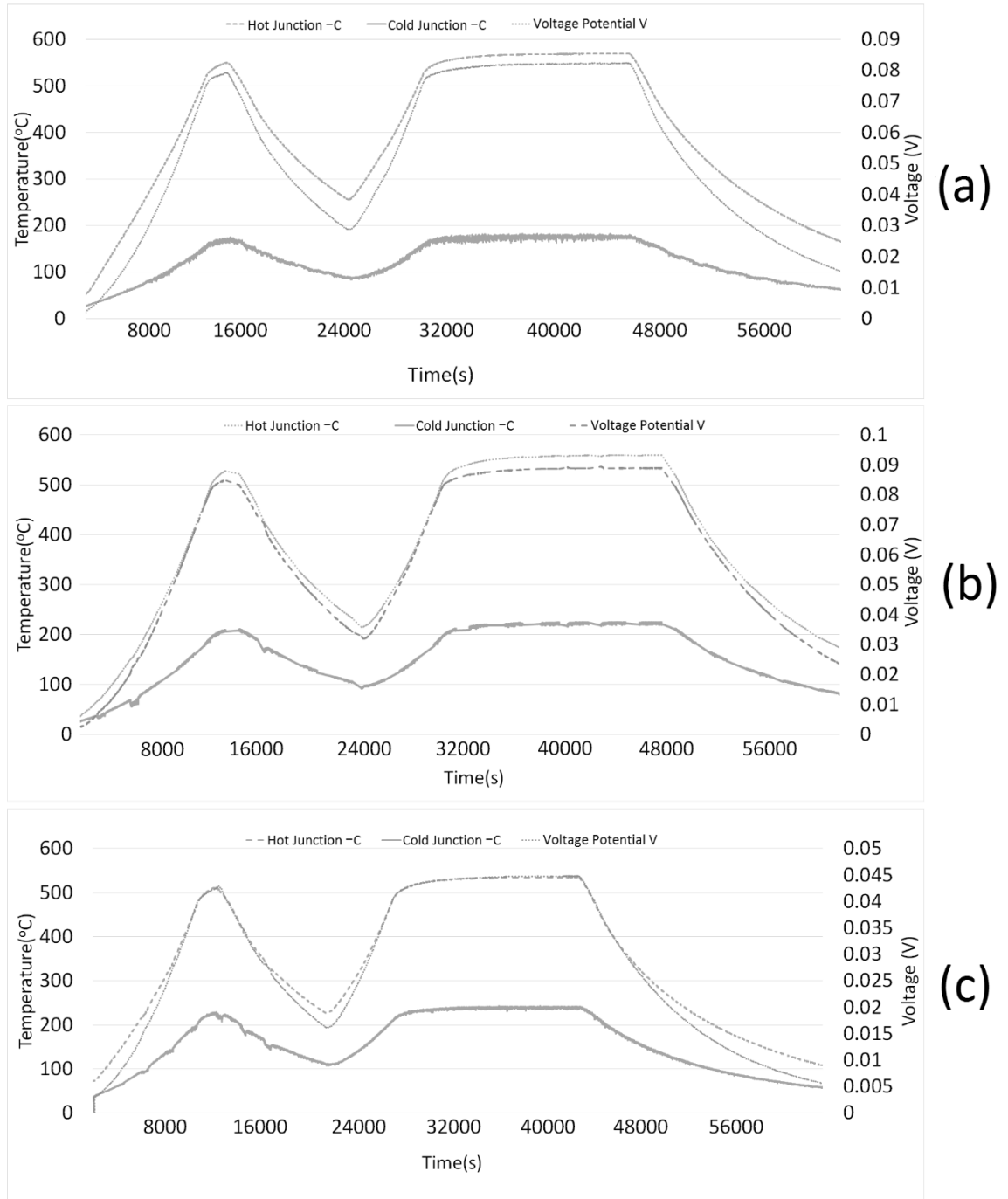


Figure 8: (a) Thermoelectric response of a Pt:SiC CMC thermocouple with a SiC fiber weave that was at 45° diagonal relative to the long axis of the CMC beam, (b)

Thermoelectric response of a Pt:SiC CMC thermocouple with a parallel SiC fiber weave relative to the

Table 1: Thermoelectric powers and drift rates of Pt:SiC CMC thermocouples with fiber orientation fibers perpendicular, parallel, and at a 45o to the long axis of the CMC substrate.

| Fiber relative to long axis | Maximum voltage output ($\mu V/k$) | Drift rate (K/hr) |
|-----------------------------|---|--------------------------|
| Parallel | 148.6 | 2.68 |
| 45° | 207 | 4.93 |
| Perpendicular | 251.6 | 2.64 |

The thermoelectric responses for the various SiC fiber orientations proved to be very stable as evidenced by the low drift rates observed for these thermocouples relative to thin film thermocouples. Although the temperatures were intentionally kept relatively low, the drift in the thermoelectric response of these Pt:SiC CMC thermocouples was likely due to oxidation to some extent via oxygen diffusion through the platinum interconnect thin film. Oxidation at the Pt:SiC interface occurs as a function of time at temperature and results in the formation of a thin SiO₂ layer between the platinum and SiC-SiC CMC. This oxide layer in turn degrades the ohmic contact between the platinum and SiC-SiC CMC and alters the measured emf. At higher temperatures

($T > 1000^\circ\text{C}$) the oxide layer becomes thick enough to form a rectifying contact and the signal becomes highly unstable. When this occurs, the resistance was measured to confirm that the ohmic nature of the Pt:SiC junction was still preserved. This suggested that the measured emf was due to the Pt:SiC CMC thermocouple and was not altered by an oxide. In addition to forming a rectifying contact, other structural changes in the platinum film such as grain growth, pore growth, and dewetting of the thin film can also lead to signal drift [1,2]. The improved stability over thin film thermocouples was attributed to the fact that the bulk SiC properties contribute to the overall sensor performance or thermoelectric response rather than those of the thin films, including the electrical stability of the SiC fibers in the SiC matrix.

Oxygen diffusion through the platinum interconnect film can compromise the thermoelectric properties of the Pt:SiC CMC thermocouple as well as its ability to perform as a high temperature sensor. Past research [1,2] on high temperature thin film strain gages suggested that ITON or indium tin oxynitride thin films could be an effective oxygen diffusion barrier to protect the Pt-SiC interface from oxidation at elevated temperatures. Towards this end, an ITO film was reactively sputtered in the presence of nitrogen to form an oxynitride layer over the Pt:SiC CMC junction. The associated partial pressures pressures were 7.2 mtorr Ar and 1.8 mTorr nitrogen. A 2 μm thick oxynitride film could be grown in approximately 5 hours after which the film was annealed in a tube furnace in flowing nitrogen (5 hours) at 500°C . To insure that the surface of the ITO film would be saturated with nitrogen and that the interstitial sites in the ITO film would be occupied by nitrogen, the as-sputtered films were annealed in nitrogen. This resulted in an expanded surface layer, which put the

surface in residual compression and enhanced the oxygen diffusion barrier. Figure 9 shows the drift of a Pt:SiC CMC thermocouple employing an oxynitride diffusion barrier at temperatures known to cause failure in a Pt:SiC CMC thermocouple without a barrier. It can be seen that the thermocouple with a barrier has greater stability than Pt:SiC CMC thermocouples without an oxygen diffusion barrier (Figures 8). Drift rates were extremely small, indicating that the ITON film performs exceptionally well as a diffusion barrier. Also, resistance measurements were made to confirm that the ohmic nature of the Pt:SiC contact was maintained.

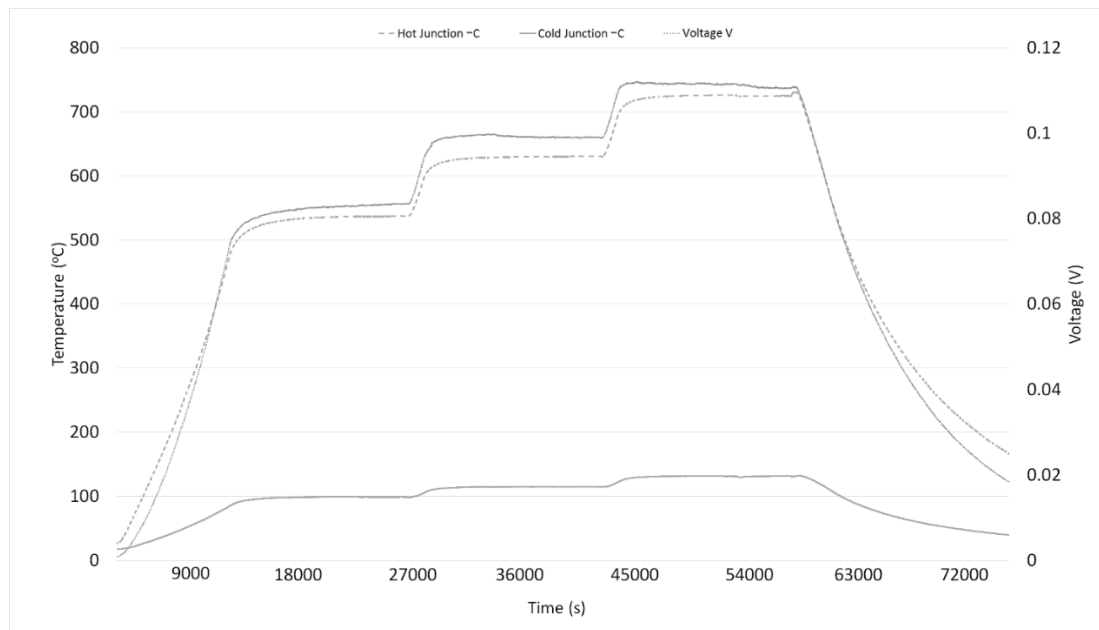


Figure 9: Thermoelectric response of a Pt:SiC CMC thermocouple at 530, 630, and 730°C fabricated with an ITON diffusion barrier.

2.5 Conclusions

Novel thermocouples utilizing the SiC-SiC CMC itself as one thermoelement and platinum as the other thermoelement were fabricated on SiC-SiC CMC's. Results indicate that these thermocouples have thermoelectric powers that are almost two orders of magnitude greater than those generated with type K wire thermocouples, which translates into much higher resolution sensors. The results also suggest that there is an effect of SiC fiber orientation on thermoelectric properties of the CMC and that the SiC fibers themselves contribute to the overall properties to a greater extent than the matrix phase SiC. Not only were these Pt:SiC CMC thermocouples more responsive than other types of thermocouples but they were considerably more stable than thin film thermocouples based on the observed drift rates. Pt:SiC CMC thermocouples with an oxygen diffusion barrier were also fabricated and increased the operating temperature of the sensors. When an oxygen diffusion barrier was employed at elevated temperatures ($T > 1000\text{C}$), platinum-silicides formed at the Pt:SiC interface. Since the Pt:SiC CMC thermocouples are limited to temperatures less than 1000C due to the formation of silicides future research to find a suitable diffusion barrier to prevent silicide formation will be a necessary. With the successful implementation of ITON diffusion barriers, Pt:SiC CMC thermocouples are a viable solution for surface temperature measurement of SiC-SiC CMC's in harsh conditions. Lastly, these results suggest this novel approach to temperature measurement could be extended to include embedded sensors in SiC-SiC CMC's.

List of References

- [1] I.M. Tougas, M. Amani, O.J. Gregory, “Metallic and Ceramic Thin Film Thermocouples for Gas Turbine Engines,” *Sensors*, vol. 13, pp. 15324-15347, 2013.
- [2] I.M. Tougas, and O.J. Gregory, “Thin film platinum-palladium thermocouples for gas turbine engine applications,” *Thin Solid Films*, vol. 539, pp. 345-349, 2013.
- [3] National Institute of Standards and Technology Type J Thermocouple Reference Tables. Available at: https://srdata.nist.gov/its90/type_j/300to600.html (accessed 31 March 2017).
- [4] National Institute of Standards and Technology Type K Thermocouple Reference Tables. Available at: https://srdata.nist.gov/its90/type_k/300to600.html (accessed 31 March 2017).
- [5] National Institute of Standards and Technology Type E Thermocouple Reference Tables. Available at: https://srdata.nist.gov/its90/type_e/300to600.html (accessed 31 March 2017).
- [6] National Institute of Standards and Technology Type N Thermocouple Reference Tables. Available at: https://srdata.nist.gov/its90/type_n/300to600.html (accessed 31 March 2017).
- [7] National Institute of Standards and Technology Type R Thermocouple Reference Tables. Available at: https://srdata.nist.gov/its90/type_r/600to900.html (accessed 31 March 2017).

- [8] National Institute of Standards and Technology Type S Thermocouple Reference Tables. Available at: https://srdata.nist.gov/its90/type_s/600to900.html (accessed 31 March 2017).
- [9] National Institute of Standards and Technology, Thermocouple Reference Tables Type B. Available at: https://srdata.nist.gov/its90/type_b/300to600.html (accessed 31 March 2017).
- [10] M.-A. Nicolet, "Diffusion Barriers in Thin Films," *Thin Solid Films*, vol. 52, pp. 415-443, 1978.
- [11] T.C. Chou, "High temperature reactions between SiC and platinum," *J. Mater. Sci.* vol. 26, pp. 1412-1420, 1991.
- [12] T.C. Chou, "Anomalous solid state reactions between SiC and Pt," *J. Mater. Res.*, Vol. 5, pp. 601-608, 1990.
- [13] L.E. Tanner, H. Okamoto, "The Pt-Si (Platinum-Silicon) System," *J. Phase Equilibria.*, vol. 12, pp. 571-574, 1991.
- [14] M.R. Rijnders, A.A. Kodentsov, J.A. Van Beek, J. van den Akker, F.J.J van Loo, "Pattern formation in Pt-SiC diffusion couples," *Solid State Ionics*, vol. 95, pp. 51-59, 1997.
- [15] J.A. DiCarlo, H. Yun, "Methods For Producing Silicon Carbide Architectural Preforms," U.S. Patent 7,687,016 issued March 30, 2010.
- [16] J.A. DiCarlo, H. Yun, "Methods For Producing High-Performance Silicon Carbide Fibers, Architectural Preforms, And High-Temperature Composite Structures," U.S. Patent 8,894,918 issued November 25, 2014.

- [17] R.R. Naslain, "SiC-Matrix Composites: Nonbrittle Ceramics for Thermostructural Application," *Int. J. App. Ceramics*, vol. 2(2), pp. 75-84, 2005.
- [18] J.D. Wrbanek, G.C. Fralick, D. Zhu, "Ceramic thin film thermocouples for SiC-based ceramic matrix composites," *Thin Solid Films*, vol. 520, pp. 5801-5806, 2012.

CHAPTER 3

ITO:SiC CMC Thermocouples for CMC Engine Components

Submitted for publication in IEEE Electron Device Letters

Kevin Rivera and Otto J. Gregory

Department of Chemical Engineering, University of Rhode Island, Kingston RI

3.1 Abstract

Measuring the temperature of components within a gas turbine engine hot section is crucial but current temperature sensors are not compatible with ceramic matrix composites (CMCs) which are replacing super nickel alloys. An ITO:SiC ceramic matrix thermocouple has been developed for temperature measurement of SiC-SiC CMCs. The thermocouple has the unique property of using the SiC-SiC CMC itself as one of the thermoelements as it is an extrinsic semiconductor. Using the CMC substrate improves its temperature sensitivity and the maximum thermoelectric potential is measured at $272\mu\text{V/K}$ which is an order of magnitude larger compared to type-k thermocouple. N₂ anneals at 500°C were used to improve high temperature stability of the ITO thin films and testing has shown that the ITO:SiC CMC thermocouple is able to survive temperatures nearing 700°C. The average measurement drift rate is 3.47°C/hr at these temperatures but decreased after subsequent thermal cycling due to oxide passivation of the ITO. Performance, fabrication details and challenges with this approach are discussed.

3.2 Introduction

Temperature measurement is the most typical engineering data points collected during the validation phase of an engine but with ceramic matrix composites (CMCs), which already have begun replacing certain super nickel alloy components, current techniques for temperature measurement are not compatible with the CMCs since welding to their surfaces is not possible without damaging their structural integrity. Next generation gas turbine engines will begin to heavily use these CMCs as a replacement for nickel based superalloys because of their superior thermomechanical

properties and ability to withstand higher temperatures which will increase engine thermal efficiencies [1].

Temperature measurement is typically conducted with bulk wire sensors that are welded onto the surface of the component of interest but with this not being a suitable option for CMCs, other solutions have to be sought. Temperature measurement using thin-films as thermocouple elements and RTDs has been researched heavily [2] but developing robust and reliable solutions is not simple since thin-films are easily susceptible to oxidation and dewetting effects [3] and their performance is very sensitive to metallurgical changes in their microstructure.

Thermocouples based on ITO have been shown to perform at temperatures near 1500°C when they are protected using oxygen barriers and annealed in nitrogen and air atmospheres but tend to suffer from large measurement drift values [4]. These thermocouples are successful but require a large enough sputtering chamber in order to deposit them depending on the engine component.

PN diodes have been developed as a potential high temperature measurement sensor and have the advantage of being relatively small and simple in principle. These diodes also have high sensitivity at around 3.5mV/°C compared to 41µV/°C for type-K thermocouples. This diode removes the necessity for amplifying circuits or cold junction compensation. Some drawbacks include the limited temperature range (20-600°C) and the numerous fabrications steps involved [5].

Noble metal thin-film thermocouples (TFTCs) have been attempted with varying degrees of success. PtRh:ITO TFTCs have been developed but suffer from high signal drift from 800-1000°C due to preferential oxidation of Rh [6]. Pt:Pd

TFTCs have also been developed and are very stable until 700-800°C when the Pd begins to aggressively oxidize [7]. Pt:Au TFTCs have great success since they avoid oxidation all together but are limited by the melting point of Au which is near 1000°C [8].

Previous work has been done to develop thermocouples using the p-type SiC-SiC CMCs and Pt thin films. The Pt:SiC CMC thermocouples were able to survive to 550°C when no protective barrier coatings were used. At temperatures beyond 550°C oxidation of the SiC-SiC CMC at the Pt:SiC CMC interface occurred leading to the formation of a rectifying contact [9]. At higher temperatures the use oxygen barriers was required and with them, operational temperature increased to 700°C. Above 700°C the Pt would react with the SiC-SiC CMC and form Pt silicides which formed a rectifying contact at the interface [10]. To circumvent this silicide reaction an additional barrier was employed and the thermocouple was able to survive up to 900°C but not any higher due to multiple junctions being created between the barriers, Pt thin film, and SiC-SiC CMC leading to an incoherent signal [10].

In this study, thermocouples utilizing ITO as one thermoelement and the p-type SiC-SiC CMC as the other have been developed and have been evaluated up to 660°C. The drift characteristics at these temperatures have been determined as well.

3.3 Experimental

3.3.1 Fabrication Process

The SiC-SiC CMC substrates were first heat treated at 1000°C for 10h to remove any surface impurities and to grow a passivating oxide layer. For sensor fabrication the substrates were first coated with 20um of mullite dielectric and the dielectric

coating was heat treated first on a Fischer Scientific hotplate at 100, 200 and 300 for 30 min each and placed in a Deltech tube furnace with a ramp rate of 4°C/min until it reached 1000°C and it was held there for 15h to allow sintering of the mullite dielectric for a complete heat treatment. Mullite was used since it has a similar coefficient of thermal expansion as the SiC-SiC CMC substrates at elevated temperatures.

Photolithographic techniques were used in order to pattern the coated SiC-SiC CMC substrates using a Dupont MX5040 negative photoresist. Once patterned, the substrates were placed in an MRC 822 sputtering system and high purity ITO (90:10) was sputtered in a 9mTorr argon atmosphere for 5h to achieve a film thickness of 5µm. The samples were removed several hours after, re-patterned and Pt was sputtered for the bond pads as a highly conductive contact material (Fig.10). Using Pt was ideal since it forms an ohmic contact to ITO. All the thin-films were annealed in N₂ for 5h at 500°C in order to relieve film stresses caused during sputtering from point defects and trapped argon as well as to promote crystallinity and homogeneity in the films. 0.2mm diameter Pt wires were bonded to the Pt thin film bond pads using Pt paste (Heraeus CL11-5100) and heat treated to promote a sintered finish. An open air anneal is typically done with ceramic thermocouples [11] but it was omitted in these tests because the testing temperatures were kept relatively low.

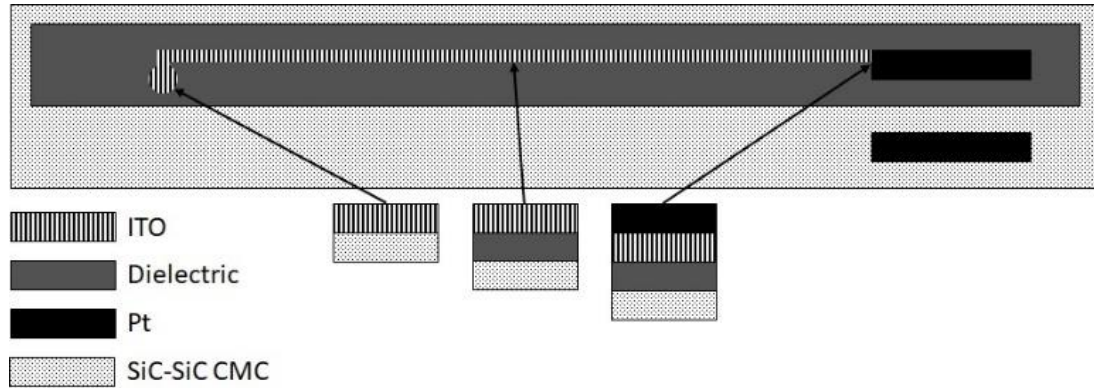


Figure 10: Schematic of the ITO:SiC CMC thermocouple.

3.3.2 Testing Procedures

All ITO:SiC CMC thermocouple hot junctions were heated in an Mellen tube furnace. A ceramic heat shield was used to introduce a temperature gradient across the long axis of the thermocouple and a hollow aluminum block connected to a chilled water supply was used to maintain the cold junction at as low a temperature as possible. Type-K thermocouples were used to measure the temperatures at both the hot and cold junctions. An Omega Personal Daq54 system was used to record thermocouple and voltage data (Fig.11). The furnace was generically programmed as follows: ramp to desired temperature and ramp down to 200°C. This was done for temperature ranging from 400 – 700°C in 100°C increments. Measurement drift in for the ITO:SiC CMC thermocouples was determined by holding the hot junction at a particular temperature for several hours.

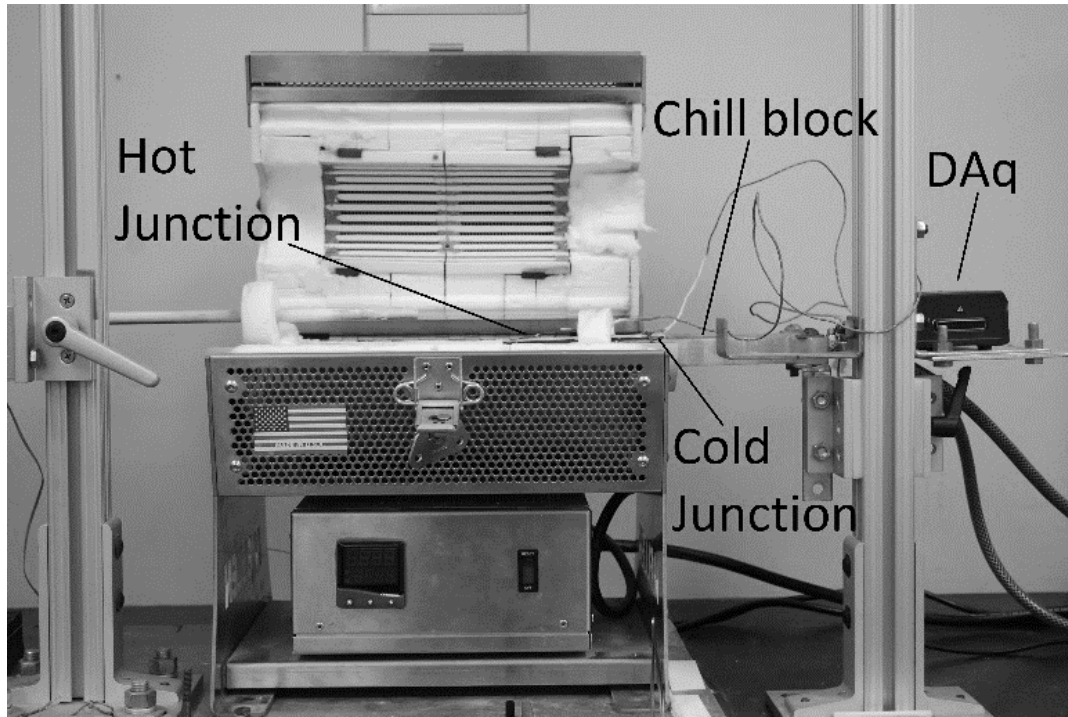


Figure 11: Testing apparatus used for the thermocouples. The aluminum chill block induces a cold junction and the free floating end of the thermocouple is inserted into a tube furnace. Data is collected using a personal Daq54.

3.3.3 Thermoelectric Characterization

Thermoelectric potential of the ITO:SiC CMC thermocouples was measured using eq.1.

$$V_T = \frac{\Delta V}{\Delta T} \quad (1)$$

where ΔV is the voltage drop across the thermocouples and ΔT is the temperature difference between the hot and cold junctions. Temperature drift was measured using eq.2.

$$T_D = \frac{\Delta V}{V_0} \cdot \frac{T_C}{\Delta t} \quad (2)$$

here ΔV is the voltage drop across the thermocouple, V_0 is the initial voltage measured at the start of the temperature hold, T_C is the temperature at which the hot junction is held at, and Δt is the elapsed time of the temperature hold.

3.4 Results

3.4.1 Thermoelectric Performance

The thermocouple was tested from 20–660°C and the furnace was programmed to cycle at 400, 500, 600, and 700°C but the cycles were seen at 434, 505, 584, 660°C and its thermoelectric potential was measured at 272 μ V/K (Fig.12). Overall the performance did not deteriorate over the course of testing which was noted by the low hysteresis (Fig.13). As temperatures exceeded 400°C a small amount of hysteresis could be seen but this is due to the oxidation of indium and tin in the ITO thin films caused by the absence of an open air anneal before testing. Temperatures higher than 660°C were tested in order to evaluate the stability of the ITO:SiC CMC thermocouple and it was determined that any temperatures above 700°C caused sensor failure (Fig. 14). This failure was brought about by the oxidation of the SiC-SiC CMC at the ITO:SiC CMC contact areas by oxygen diffusion through the ITO thin film at high temperatures.

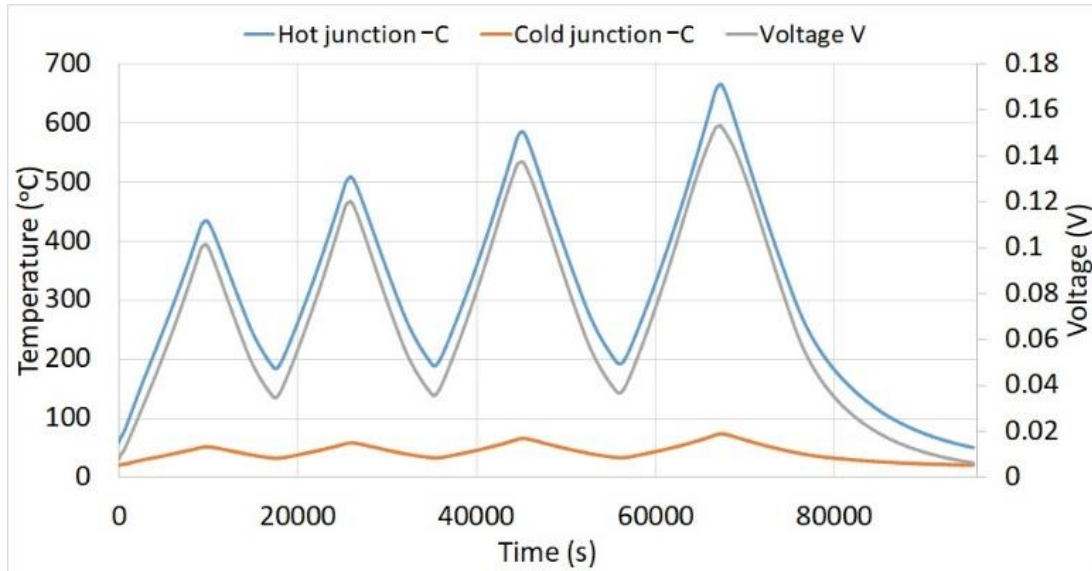


Figure 12: Furnace test for the ITO:SiC CMC thermocouple. Temperature ramps from 20-660°C.

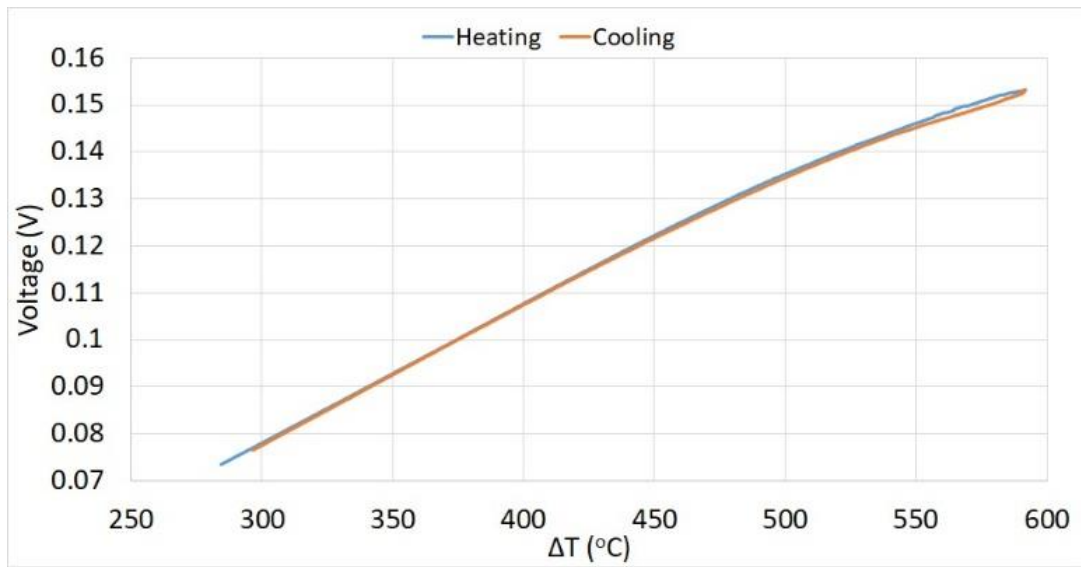


Figure 13: Hysteresis upon heating and cooling. Minimal hysteresis occurs at high temperature.

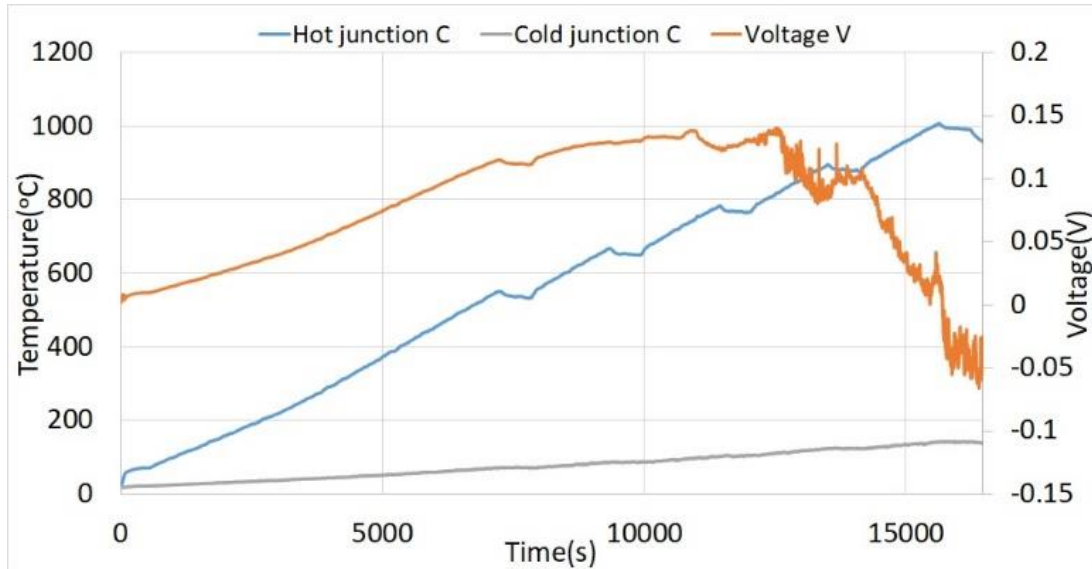


Figure 14: Temperature limit testing for the ITO:SiC CMC thermocouple. Oxidation at the ITO:SiC CMC contact area causes oxidation and sensor failure past 700°C.

3.4.2 Thermocouple Measurement Drift

The ITO:SiC CMC thermocouple was heated to 600°C and held at temperature for 10h and had an overall measurement drift of 3.47°C/hr (Fig.15). The value was high due to the lack of a prior air anneal and continued oxidation of the indium and tin in the ITO. The lack of an air anneal also caused inhomogeneity in the ITO films along the temperature gradient imposed on the longitude of the CMC substrate. Normally an air anneal is crucial for ITO being used at high temperatures for sensing applications.

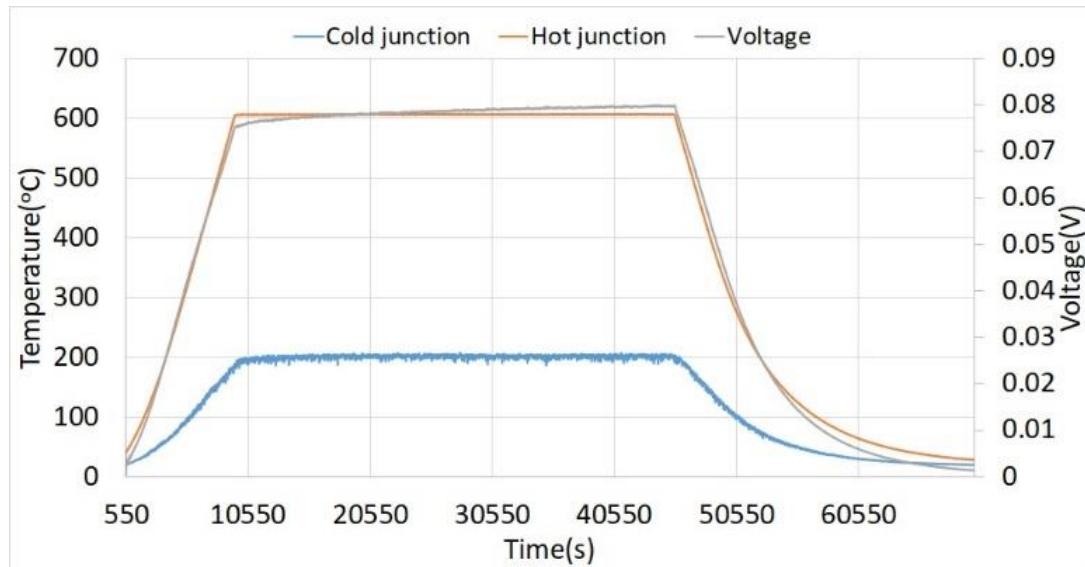


Figure 15: Measurement drift test conducted at 600°C.

3.5 Conclusions

An ITO:SiC CMC thermocouple was fabricated as a compatible solution for the SiC-SiC CMC components that will be used in gas turbine engine hot sections to measure surface temperatures. The ITO:SiC CMC thermocouples were able to survive to 660°C and produced 272 μ V/K. It is important to note that temperatures higher than 700°C caused sensor failure but in future sensors an oxynitride layer will be added over the ITO thin films in order to prevent oxygen diffusion in the SiC-SiC CMC in the ITO:SiC CMC contact areas.

List of References

- [1] R. R. Naslain, "SiC-Matrix Composites: Nonbrittle Ceramics for Thermostructural Applications," *Int. J. of Ceramic Tech.*, vol. 2, pp. 75-84, 2005.

- [2] M. Imran, A. Bhattacharyya, "Effect of Thin Film Thickness and Materials on the Response of RTDs and Microthermocouples," *IEEE Sens. J.*, vol. 6, pp. 1459-1467, 2006.
- [3] I. M. Tougas, M. Amani, O. J. Gregory, "Metallic and Ceramic Thin Film Thermocouples for Gas Turbine Engines," *Sensors*, vol. 13, pp. 15324-15347, 2013.
- [4] O. J. Gregory, T. You, "Ceramic Temperature Sensors for Harsh Environments," *IEEE Sens. J.*, vol. 5, pp. 833-838, 2005.
- [5] N. Zhang, C. Lin, D. G. Senesky, A. P. Pisano, "Temperature sensor based on 4H-silicon carbide pn diode operational from 20°C to 600°C," *Applied Physics Letters*, vol. 104, pp. 1-3, 2014.
- [6] X. Zhao, H. Wang, Z. Zhao, W. Zhang, H. Jiang, "Preparation and Thermoelectric Characteristics of ITO/PtRh:Pt:Rh Thin Film Thermocouple," *Nanoscale Research Letters*, pp. 1-6, 2017.
- [7] I. M. Tougas, O. J. Gregory, "Thin film platinum-palladium thermocouples for gas turbine engine applications," *Thin Solid Films*, vol. 539, pp. 345-349, 2013.
- [8] N. P. Moiseeva, "The Prospects for Developing Standard Thermocouples of Pure Metals," *Measurement Techniques*, vol. 47, pp. 915-919, 2004.
- [9] K. Rivera, T. Muth, J. Rhoat, M. Ricci, O. J. Gregory, "Novel temperature sensors for SiC-SiC CMC engine components," *J. Mater. Res.*, vol. 32, pp.3319-3325, 2017.

- [10] K. Rivera, M. Ricci, O. Gregory, "Diffusion barrier coatings for CMC thermocouples," *Surface & Coatings Technology*, vol. 336, pp. 17-21, 2018.
- [11] X. Zhao, H. Li, K. Yang, S. Jiang, H. Jiang, W. Zhang, "Annealing effects in ITO based ceramic thin film thermocouples," *J. of Alloys and Compounds*, vol. 698, pp. 147-151, 2017.

CHAPTER 4

Embedded Thermocouples for CMC Engine Components

Published in IEEE Sensors 2017, December 2017

Kevin Rivera, Matthew Ricci, and Otto J. Gregory

Department of Chemical Engineering, University of Rhode Island, Kingston RI

K. Rivera, M. Ricci, O.J. Gregory, “Embedded thermocouples for CMC engine components,” IEEE Sensors 2017, pp. 1-3.

4.1 Abstract

Nickel-based super alloys have been the mainstay for gas turbine components comprising the hot section. However, due to their superior thermomechanical properties, SiC-SiC ceramic matrix composites (CMC) are replacing nickel-based superalloy components. This requires that the CMC components be instrumented to determine structural integrity. Traditional wire thermocouples report reliable data but are not suited for the conditions in the gas turbine engine since they affect gas flow and vibrational modes during operation. Thin-film thermocouples provide a true surface temperature measurement but there are reliability issues with thin-film thermocouples such as selective oxidation, dewetting, and metallurgical changes as well as small diffusional distances. Sensors utilizing the bulk semiconducting properties of SiC in the CMC have been developed. High purity sputtered platinum is coupled with SiC in the base CMC to form a new class of thermocouples which produced thermoelectric powers of $250\mu\text{V}/^\circ\text{K}$ at $\sim 1000^\circ\text{C}$. These thermocouples are able to survive high temperature by using sputtered diffusion barrier coatings. Performance of this new class of thermocouples will be presented and the potential for embedded thermocouples for advanced CMC will be discussed.

4.2 Introduction

Next generation gas turbine engines will utilize ceramic matrix composites or CMC components rather than traditional nickel based superalloys due to their superior thermomechanical properties [1]. CMC based components will permit higher engine operating temperatures and thus allows higher thermal efficiencies [1]. Advanced instrumentation for these CMC components is needed to verify structural models and

the structural integrity of the components. Wire sensors for temperature measurement have been used extensively for nickel based superalloys since they can be welded to the components but they can affect the gas flow path and vibrational modes during operation due to their bulky nature [1]. However, they cannot be welded to CMC components. Thin-film sensors can be deposited directly onto the surfaces of engine components, and do not affect the gas flow path and vibrational modes during operation. However, thin-film thermocouples are prone to selective oxidation, dewetting, and metallurgical changes in the films that lead to considerable signal drift [2].

Earlier research into thin-film temperature sensors focused on Pt/Pt-Rh thermocouples or Type S thermocouples since the wire version proved so successful but it was determined that preferential oxidation of the rhodium in the films would limit this approach since changes in composition at higher temperatures can lead to changes in thermoelectric output [3]. Pt:Pd thin film thermocouples had some promise since they are not alloys but again selective oxidation of the palladium at temperatures in the range 600-800°C occurred as well as dewetting of the films [2, 4]. Other noble metal thermocouples such as Au:Pt were attempted in order to circumvent oxidation at higher temperatures but these lacked the ability to reach temperatures above 1000°C and exhibited low thermoelectric outputs [2]. Pt:ITO thin film thermocouples were able to survive temperatures above 1000°C and produced very large Seebeck coefficients with little or no drift [5]. However, the Pt:SiC(CMC) thermocouples described here can yield even larger thermoelectric outputs with greater stability by combining the benefits of noble metal thin films and bulk semiconductor properties.

This new class of thermocouple produced thermoelectric powers as large as $250\mu\text{V}/^\circ\text{K}$ with minimal drift at elevated temperatures. The Pt:SiC(CMC) thermocouple utilizes the bulk properties of the SiC in the CMC and is able to function at temperatures $\sim 1000^\circ\text{C}$ when protective coatings were employed. Sputtered diffusion barriers were also employed to prevent adverse reactions at elevated temperature which alters the ohmic nature of the Pt:SiC contacts and thus, the stability of the contacts at elevated temperatures [6].

4.3 Experimental

4.3.1 Preparation of the CMC Substrate Overcoat

The as-received CMC's were heat treated at 1000°C for 15 hours in a Deltech furnace. A thin layer of dielectric cement was then applied to the surface of the CMC to provide electrical isolation between the sputtered Pt leads, bond pads and the CMC. The dielectric layer was heat-treated on a Fisher Scientific hotplate for 20 minutes at 100°C , 20 minutes at 200°C , 40 minutes at 300°C followed by a high temperature heat treatment at 1000°C for 10 hours in the Deltech furnace.

4.3.2 Pt:SiC (CMC) Thermocouple Fabrication

Via holes were created in the dielectric coating deposited over the CMC substrate and photolithography techniques were used to pattern leads and bond pads on the surface of the CMC substrate (Fig. 16). For high temperature applications, diffusion barrier coatings were sputter deposited to prevent adverse reactions as well as maintain the ohmic nature of the contact formed between the Pt and SiC CMC (Fig. 17).

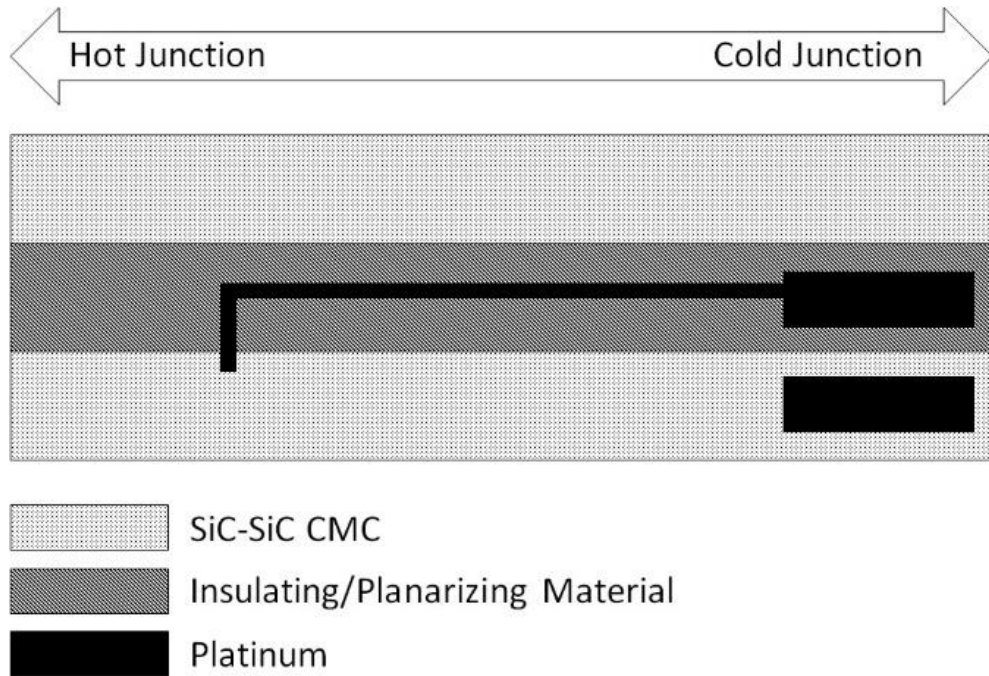


Figure 16: Schematic top-down view of a Pt:SiC(CMC) thermocouple.

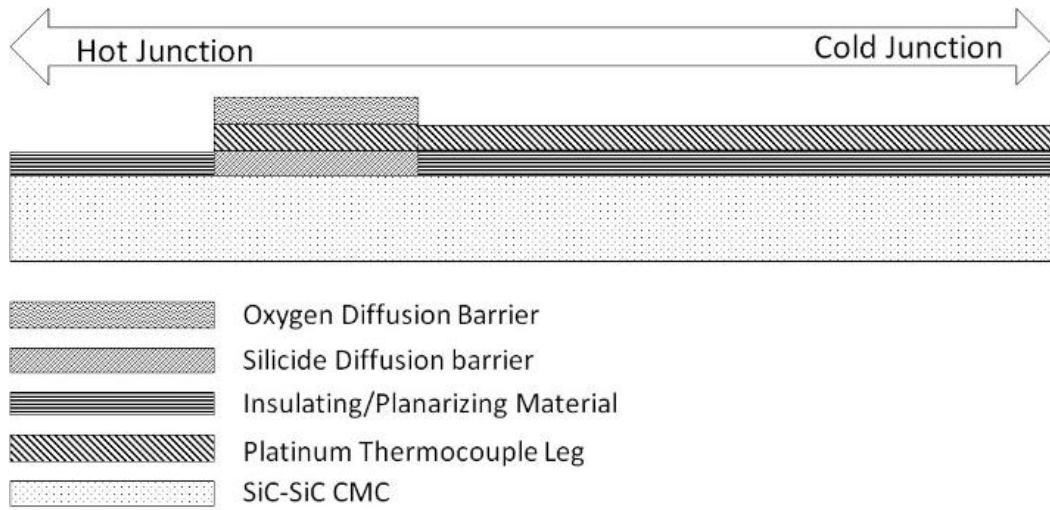


Figure 4.2:

Figure 17: Cross section of a Pt:SiC(CMC) thermocouple with barrier coatings.

4.3.3 SiC Fiber Orientation

The SiC-SiC CMC substrates used for thermoelectric testing had the same dimensions but utilized different SiC fiber orientations in the CMC. Four different orientations were used for testing: horizontal, 30° with respect to normal, 45° with respect to normal, and parallel to the long axis of the rectangular beam as shown in figure 3. The Pt:SiC(CMC) thermocouples were tested in a MHX tube furnace. The protocol for thermoelectric testing was as follows: ramp to 550°C at a rate of 4°C/min, hold for 20 minutes, ramp down to 200°C at a rate of 4°C/min, hold for 20 minutes, ramp to 550°C at a rate of 4°C/min, hold for 5 hours, and finally a ramp to 30°C at a rate of 4°C/min. This protocol was used to determine thermoelectric powers for each of the four orientations tested as well as the drift at 550°C.

4.3.4 Protective Barrier Testing

The protocol for testing the Pt:SiC(CMC) thermocouples with barrier coatings was as follows: ramp to temperature 1 at a rate of 4°C/min, hold for 5 hours, ramp to temperature 2 at a rate of 4°C/min, hold for 5 hours, ramp to temperature 3 at a rate of 4°C/min, hold for 5 hours and then a ramp back down to room temperature at a rate of 4°C/min. This test was used to determine thermoelectric properties as well as drift properties of the Pt:SiC(CMC) thermocouples at each temperature. The thermocouples were mounted on an aluminum chill block to maintain a cold junction for each test (fig. 19).

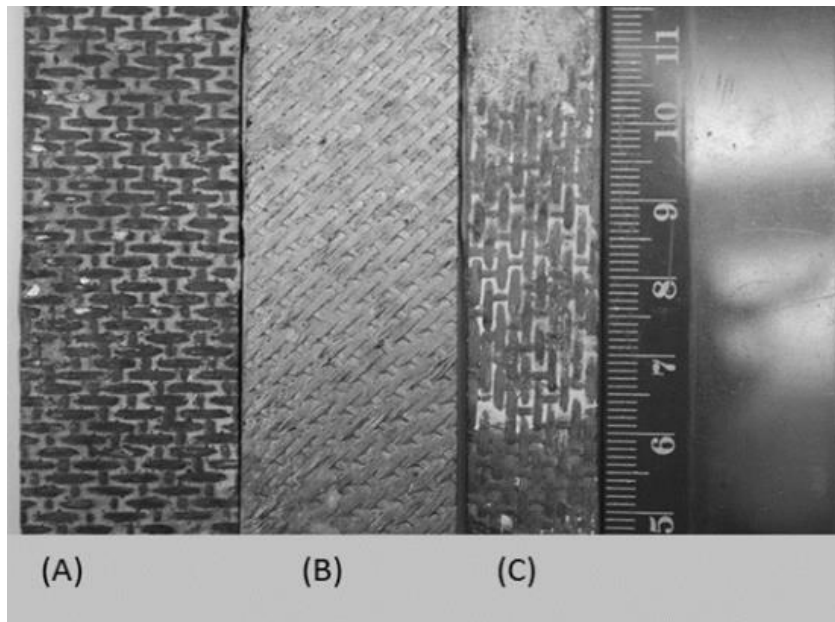


Figure 18: Photograph of different SiC fiber orientations in CMC. Note orientation (a) is horizontal, (b) at 45o to normal, and (c) parallel to the long axis of the substrate.

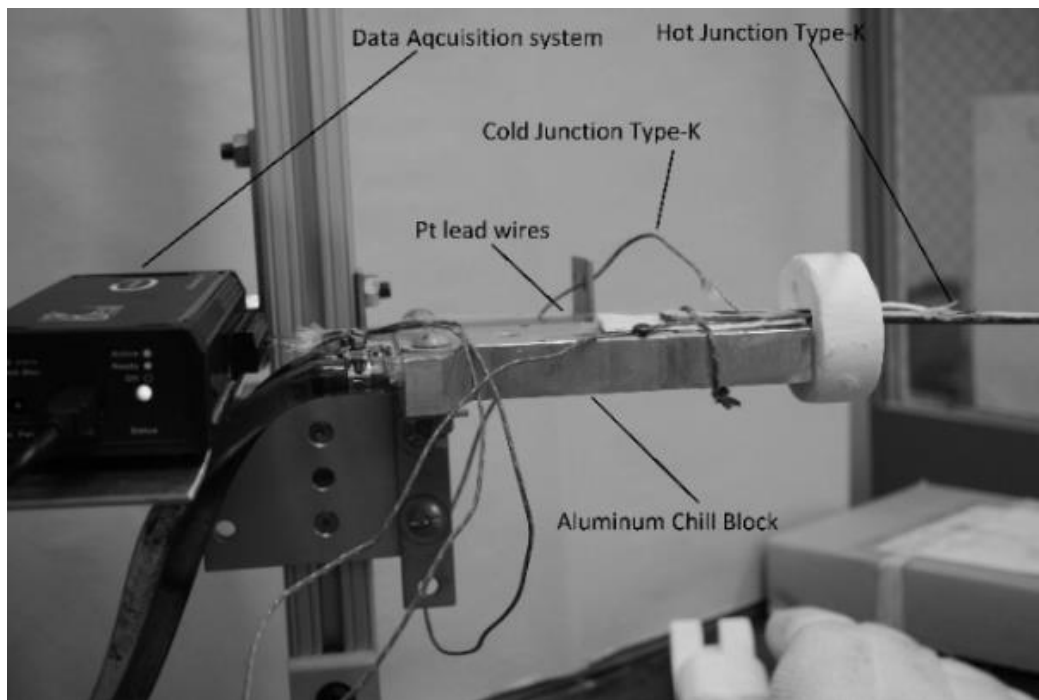


Figure 19: Photo of apparatus used for thermocouple testing and calibration.

4.4 Results

4.4.1 SiC Fiber Orientation Effect Testing

The results of the thermoelectric tests performed on the Pt:SiC(CMC) thermocouples with different SiC fiber orientations (Fig. 18) are presented in Table 2. The Pt:SiC(CMC) thermocouples fabricated on CMC beams having SiC fibers oriented horizontally with respect to the long axis yielded a maximum thermoelectric output of $148.6\mu\text{V}/^\circ\text{K}$ and a drift rate of $2.68^\circ\text{C}/\text{hr}$. The thermocouples fabricated on CMC beams with fibers oriented 30° relative to the long axis yielded thermoelectric outputs of $170\mu\text{V}/^\circ\text{K}$ and a drift rate of $2.12^\circ\text{C}/\text{hr}$. The CMC beams with SiC fibers oriented at 45° relative to the long axis produced a thermoelectric power of $207\mu\text{V}/^\circ\text{K}$ with a drift rate of $1.98^\circ\text{C}/\text{hr}$. And Pt:SiC(CMC) thermocouples utilizing CMC beams with the fibers parallel to the long axis of the substrate produced thermoelectric powers of $251.6\mu\text{V}/^\circ\text{K}$ with a drift rate of $1.8^\circ\text{C}/\text{hr}$.

Table 2: Tabulated results for SiC fiber orientation testing.

| Fiber orientation | Voltage ($\mu\text{V}/^\circ\text{K}$) | Drift rate ($^\circ\text{C}/\text{hr}$) |
|-------------------|--|---|
| Horizontal | 148.6 | 2.68 |
| 30° | 170 | 2.12 |
| 45° | 207 | 1.98 |
| Parallel | 251.6 | 1.8 |

4.4.2 Protective Barrier Testing

When the Pt:SiC(CMC) thermocouples were tested without any diffusion barrier coatings applied to the Pt:SiC junctions, a maximum operating temperature of 550°C was reached before failure and a thermoelectric voltage of 250 μ V/°K was generated (Figure 20). Higher temperatures were not possible in this case due to the diffusion of oxygen through the platinum film [7] which reacts with the SiC in the CMC to form SiO₂ at the Pt:SiC interface. As a result of this reaction, the contact does not remain ohmic. When an InON coating was employed as a diffusion barrier, a maximum operating temperature of 700°C was reached before failure and a thermoelectric power of 250 μ V/°K was attained (Figure 21). Any attempt at heating to higher temperatures caused the platinum in the junction to react with the SiC in the CMC and form platinum silicides [8,9]. When an ITON coating was used as an oxygen diffusion barrier and Ni:ITO was used as a diffusion barrier to prevent platinum silicide formation (Figure 22), the same thermoelectric power and drift rate were attained at temperatures ~900°C.

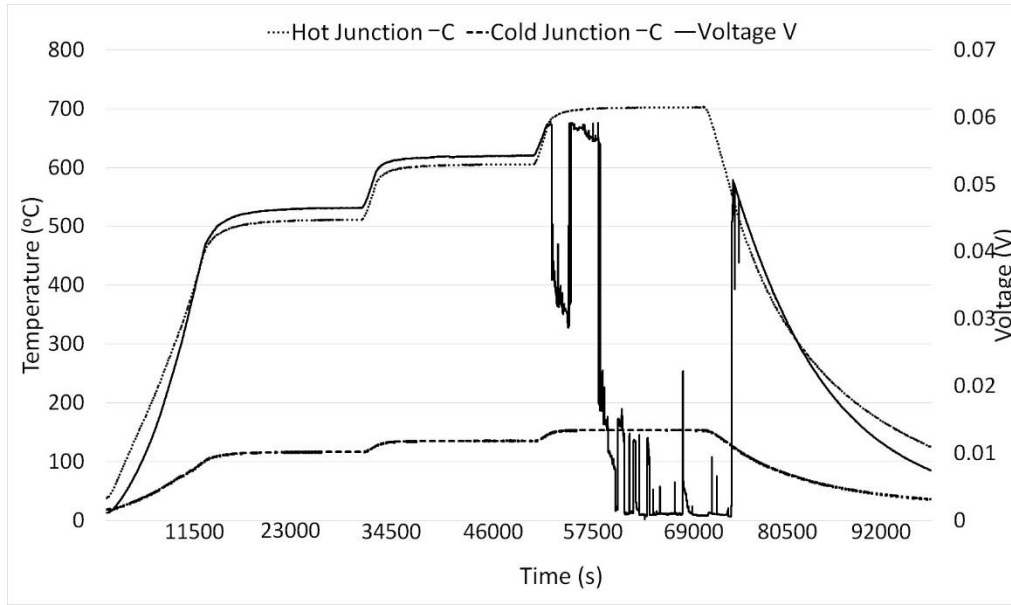


Figure 20: Pt:SiC(CMC) thermocouple with no diffusion barrier coating.

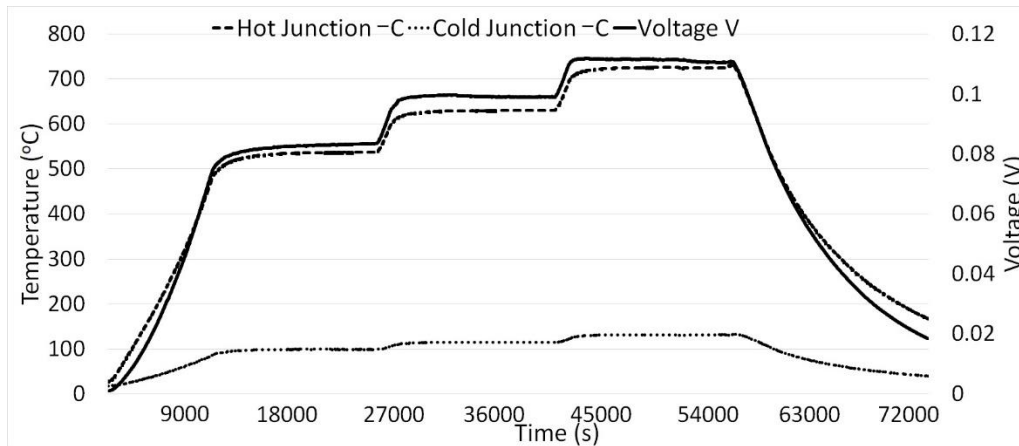


Figure 21: Pt:SiC(CMC) thermocouple utilizing an InON oxygen barrier coating.

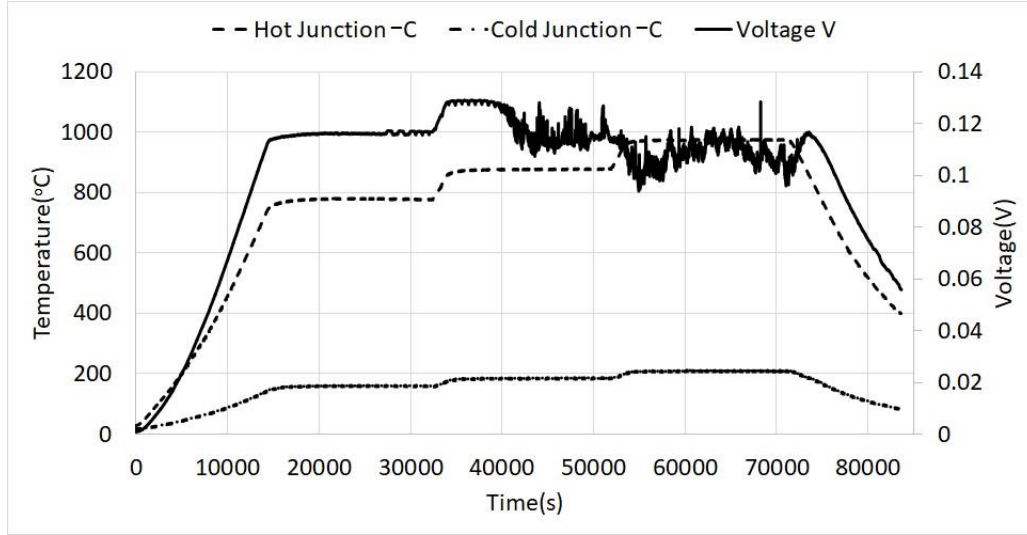


Figure 22: Pt:SiC(CMC) thermocouple utilizing ITON oxygen and Ni:ITO platinum silicide barrier coatings.

4.4.3 Governing Equations

To determine thermoelectric voltage, the following equation was used

$$V = \frac{\Delta V}{\Delta T} \quad (1)$$

where ΔT is the temperature difference between the hot and cold junctions and ΔV is the voltage difference measured at temperature. To estimate drift rate, the following equation was used

$$d = \frac{\Delta V}{V_r} \cdot \frac{T}{\Delta t} \quad (2)$$

where ΔV is the voltage difference measured at temperature, V_r is the reference voltage, T is the constant temperature that is held and Δt is the time elapsed during the hold period.

4.5 Conclusions

Temperature sensors utilizing the bulk properties of the SiC comprising the CMC were developed for advanced components comprising the hot section of gas turbine engines. The temperature sensors produced larger thermoelectric powers than Pt:ITO thin-film thermocouples [5] while maintaining minimal drift. At temperatures greater than 550°C, adverse reactions prompted the need for diffusion barrier coatings to prevent oxidation of the SiC in the Pt:SiC junction and the formation of platinum silicides. When diffusion barrier coatings were employed, the Pt:SiC(CMC) thermocouples could be cycled to ~900°C without failure. In the future, the same approach will be used to form embedded strain gages with superior piezoresistive properties.

List of References

- [1] I.M. Tougas, M. Amani, O.J. Gregory, "Metallic and ceramic thin film thermocouples for gas turbine engines," *Sensors*, vol. 13, pp. 15324-15347, 2013.
- [2] N.P. Moiseeva, "The prospects for developing standard thermocouples of pure metals," *Measurement Techniques*, vol. 47, pp. 915-919, 2004.
- [3] K.G. Kreider, G. Greg, "High temperature materials for thin-film thermocouples on silicon wafers," *Thin Solid Films*, vol. 376, pp. 32-37, 2000.
- [4] I.M. Tougas, O.J. Gregory, "Thin film platinum-palladium thermocouples for gas turbine applications," *Thin Solid Films*, vol. 539, pp. 345-349, 2013.

- [5] X. Chen, O.J. Gregory, M. Amani, "Thin-film thermocouples based on the system $\text{In}_2\text{O}_3\text{-SnO}_2$," *J. Am. Ceram. Soc.*, vol. 94, pp. 854-860, 2011.
- [6] M.A. Nicolet, "Diffusion barriers in thin films," *Thin Solid Films*, vol. 52, pp. 415-443, 1978.
- [7] L.R. Velho, R.W. Barlett, "Diffusivity and solubility of oxygen in platinum and Pt-Ni alloys," *Metallurgical Transactions*, vol. 3, pp. 65-72 , 1972.
- [8] T.C. Chou, "High temperature reactions between SiC and platinum," *J. Mater. Sci.*, vol 26, pp. 1412-1420, 1991.
- [9] T.C. Chou, "Anomalous solid state reaction between SiC and Pt," *J. Mater. Res.*, vol. 5, pp. 601-608, 1990.

CHAPTER 5

Diffusion Barrier Coatings for CMC Thermocouples

Published in Surface & Coatings Technology, 2018

Kevin Rivera, Matthew Ricci, and Otto Gregory

Department of Chemical Engineering, University of Rhode Island, Kingston RI

K. Rivera, M. Ricci, O.J. Gregory, “Diffusion barrier coatings for CMC thermocouples,” Surface & Coatings Technology, vol. 336, pp. 17-21

5.1 Abstract

A platinum:silicon carbide thermocouple has been developed to measure the surface temperature of ceramic matrix composites (CMC) with high resolution. Platinum was deposited by rf sputtering onto a SiC-SiC CMC substrates coated with a dielectric, such that the SiC-SiC CMC was one thermoelement and the platinum film was another thermoelement comprising the Pt:SiC(CMC) thermocouple. The purpose of the dielectric was to electrically isolate the platinum leads from the SiC-SiC CMC. The thermoelectric output, hysteresis and drift of the Pt:SiC(CMC) thermocouples were measured at temperatures ranging from 600°C to 1000°C. The thermoelectric powers generated by the Pt:SiC thermocouples were an order in magnitude greater than conventional Pt:Pt or Type K thermocouples. Thermoelectric powers as large as 250 μ V/°K were reported for these thermocouples, as compared to thermoelectric powers of 10 μ V/°K reported for Pt:Pt and Type K thermocouples. The results presented within show that the Pt:SiC(CMC) thermocouples exhibit excellent stability at high temperatures, relatively low drift rates, and little hysteresis during thermal cycling. However, the Pt:SiC junctions were prone to oxidation effects as well as the formation of platinum silicides at high temperature, which can compromise the junction and lead to excessive drift. Therefore, a number of diffusion barrier coatings were applied to the Pt:SiC junctions in an attempt to improve stability and lower drift in this promising new class of thermocouples.

5.2 Introduction

At the present time, gas turbine engine components are comprised largely of nickel based superalloys but future engine designs will utilize components made of lighter, and stronger ceramic matrix composites (CMC), that have superior thermomechanical properties. These CMC's are less prone to fatigue failure [1, 2] and can survive higher operating temperatures. Utilizing CMC's in the engine hot section can therefore increase engine efficiency and improve fuel economy. However, any instrumentation used to monitor temperature and loads of CMC jet engine parts must also survive the harsh conditions in the engine hot section in order to be a viable solution for instrumenting these advanced materials. Temperatures in the hot section of gas turbine engine exceed 1000°C and it is critical to accurately measure surface temperatures, in order to evaluate the structural integrity of these engine components.

Wire thermocouples affect the gas flow patterns through the engine as well as the vibrational modes of thin cross section engine components, due to their bulky nature [1]. Thin film thermocouples can avoid these shortcomings of wire thermocouples since they have almost no thermal mass and are deposited onto the surface of an engine part [1, 3]. However, thin films are prone to selective oxidation, dewetting, metallurgical changes, and the small diffusional distances mean that thin film leads and junctions can degrade quickly at elevated temperatures [4].

A platinum:silicon carbide thermocouple or Pt:SiC(CMC) thermocouple has been developed which utilizes the bulk semiconducting properties of the SiC in the CMC. This thermocouple solves many of the issues associated with films thermocouples used in high temperature applications. Pt:Pt thin film thermocouples,

for example degraded above 900°C due to oxidation of the Pd. Au:Pt thin film thermocouples do not oxidize but are limited to 1000°C due to alloying/dealloying effects [1,5-8]. The Pt:SiC junction in these thermocouples is susceptible to oxidation effects and the formation of platinum silicides at high temperature but these are mitigated by using protective coatings [9].

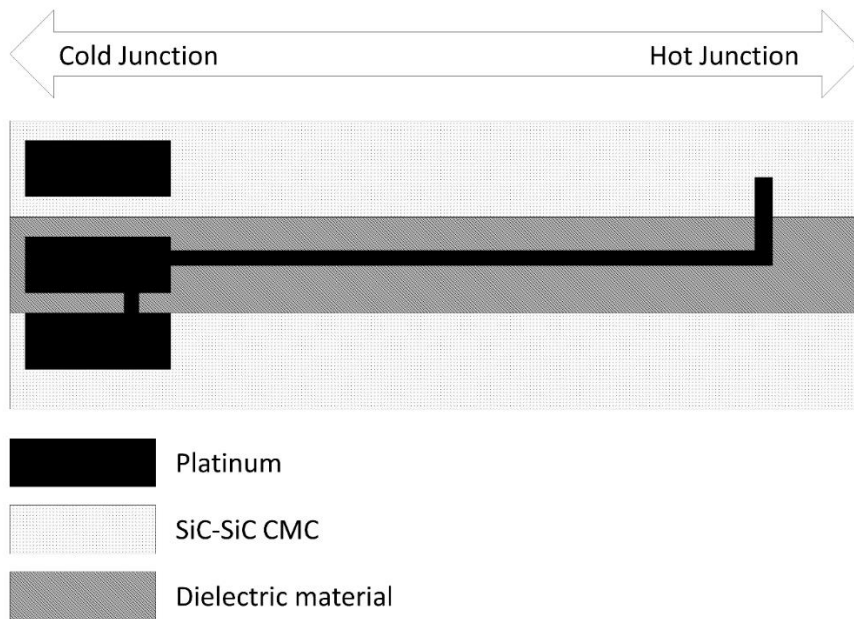


Figure 23: Schematic of a Pt:SiC(CMC) thermocouple (top-view).

The Pt:SiC(CMC) thermocouple consists of a several platinum thin films (bondpads and legs) that are connected to the SiC base material in the ceramic matrix composite (CMC) through vias created in the dielectric coating (Figure 23), thus forming the Pt:SiC (CMC) thermocouple. The Pt:SiC junction in the Pt:SiC(CMC) thermocouple can suffer from oxidation at elevated temperatures, as oxygen can readily diffuse through the platinum thin film [10], altering the ohmic nature of the contact between the platinum and SiC, ultimately forming a rectifying or Schottky

contact. The formation of an SiO₂ layer at the junction is responsible for this but can be prevented by utilizing a suitable oxygen diffusion barrier that limits oxygen ingress. When the diffusion of oxygen is mitigated by the use of protective coatings, the thermodynamics shifts in favor of platinum silicide formation [11-13]. Thus, another diffusion barrier is needed to prevent the reaction between the platinum and the SiC CMC substrate. With suitable diffusion barriers, the Pt:SiC (CMC) thermocouple will be a robust temperature sensor that can reliably survive temperatures of 1000°C or greater. The performance of the Pt:SiC (CMC) thermocouple is superior to other thermocouples in that it yields thermoelectric powers of ~200uV/°K with minimal drift, which is almost two orders of magnitude greater than thermoelectric power generated by Pt:Pd thin film thermocouples and Type K wire thermocouples [1, 4-6, 14].

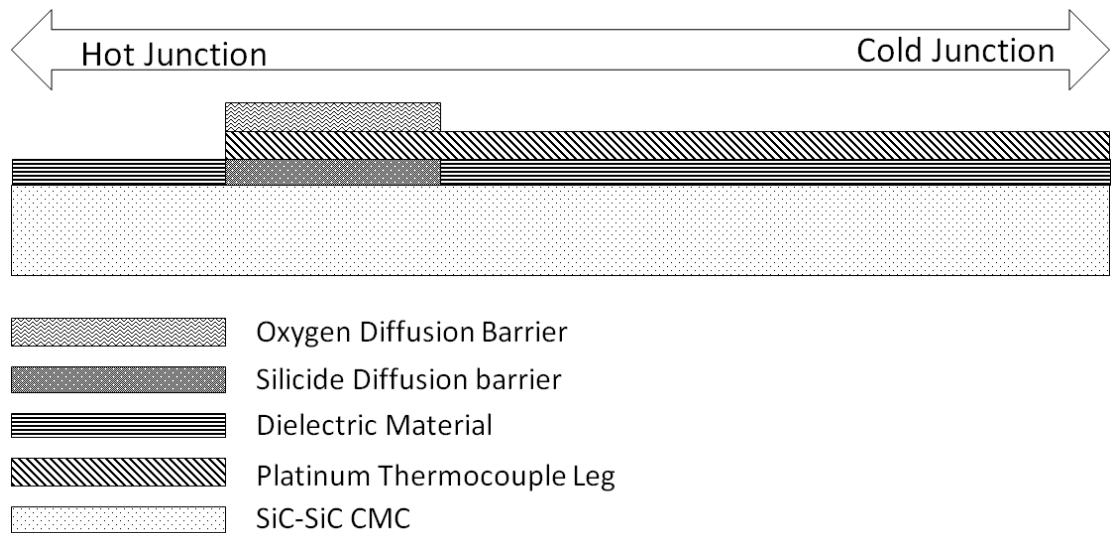


Figure 24: Schematic cross section of a Pt:SiC(CMC) thermocouple (cross section) showing the various sputtered films that serve as diffusion barriers and thermocouple legs (side view).

5.3 Experimental

5.3.1 Fabrication

The Pt:SiC(CMC) thermocouples are fabricated on bare SiC-SiC CMC surfaces which incorporate a thin dielectric coating, applied as a cement. Platinum thin films are connected to the SiC base material in the ceramic matrix composite (CMC) by rf sputtering through vias created in the dielectric coating. Figure 23 shows the top view of a typical Pt:SiC(CMC) thermocouple and Figure 24 shows the side view of the various layers comprising the diffusion barriers, protective coatings and thermocouple legs. The substrate was heat treated to 1000°C in air for 15 hours in order to grow a surface oxide onto which the dielectric coating was applied.

The dielectric used for most of the investigation was mullite, which was applied to the CMC surface in the form of cement. The cement was heated at 100°C for 20 minutes, 200°C for 20 minutes, 300°C for 40 minutes on a FischerScientific™ hot plate, followed by heating to 1000°C for 10 hours in a Deltech tube furnace. After heat treatment, vias in the dielectric layer were formed to make contact to the SiC. Etching in buffered HF solution was used to insure that a clean SiC surface free of oxides was formed at the Pt:SiC junction. Photolithography was used to pattern the thermocouple legs and bond pads. For this purpose, a dry negative photoresist (Dupont MX5050™ Durham, NC) was placed on the surface of the dielectric coated substrate and heated at 100°C for one minute in order to promote adhesion. A mylar mask with the desired artwork was placed on the surface of the negative photoresist and an AOI Aligner™ with a 350nm ultraviolet light was used to transfer the thermocouple pattern to the photoresist. The substrate was then developed in an ammonium hydroxide based

developer solution. Buffered HF was then used in the areas designated for Pt:SiC junctions in order to ensure a very clean surface before sputter deposition.

Indium tin oxide (ITO) was used as the platinum silicide barrier due to its good electrical conductivity, which allowed the ohmic contact at the junction to be maintained. The ITO diffusion barrier films were sputtered through the via formed in the dielectric and onto the freshly etched SiC surface. The ITO platinum silicide barrier was sputtered for 6 hours at 300W using a forward voltage of 1000V, resulting in a film thickness of 4 μ m. All platinum films were then deposited at 250W using a forward voltage of 1100V to yield a 2 μ m thick film. To prepare the protective indium oxynitride (InON) diffusion barrier films over the Pt-SiC junction, indium oxide was sputtered for 5 hours in a nitrogen rich plasma at 300W using a forward voltage of 800V to achieve a 20 μ m thick film. The platinum silicide diffusion barrier and platinum films were sputtered in pure argon at 9 mTorr. The InON diffusion barrier was sputtered in a nitrogen rich plasma (argon:nitrogen ratio of 8:2), at a total pressure of 10 mTorr. After each thin film deposition, the substrate was nitrogen annealed in a tube furnace at a temperature of 550°C in order to densify the film by releasing any argon gas that was trapped during deposition [1,5].

5.3.2 Thermocouple Testing

The apparatus used for thermocouple testing is shown in Figure 25. Here, a Deltech furnace was ramped to 800°C, 900°C, and 1000°C at a rate of 40C/min and was held for 5 hours at each temperature before a final ramp to room temperature. This was the preferred test method for evaluating the thermoelectric response of the Pt:SiC(CMC) thermocouples, employing both oxygen and silicide diffusion barriers.

Pt:SiC(CMC) thermocouples that only employed an oxygen diffusion barrier were tested at temperatures ranging from 500–720°C. Pt:SiC(CMC) thermocouples that did not utilize any protective coatings or diffusion barriers were ramped directly to a maximum temperature of 550°C. To calculate the thermoelectric power of the Pt:SiC(CMC) thermocouple, the following eq. 1 was used:

$$A = \frac{\Delta V}{\Delta T} \quad (1)$$

where ΔV is the difference between the reference voltage (measured at room temperature) and the voltage measured at the desired temperature, and ΔT is the difference between the temperatures measured at the hot and cold junctions. In order to measure the drift rate of the thermocouple (ΔV as a function time at a constant temperature) the following equation was used:

$$r = \frac{\Delta V}{V_r} \cdot \frac{T_c}{\Delta t} \quad (2)$$

where T_c is the hold temperature, Δt is the time the sensor was held at temperature, ΔV is the difference in voltage between the voltage at the beginning of the temperature hold and the voltage at the end of the temperature hold, and V_r is the voltage at the beginning of the temperature hold.

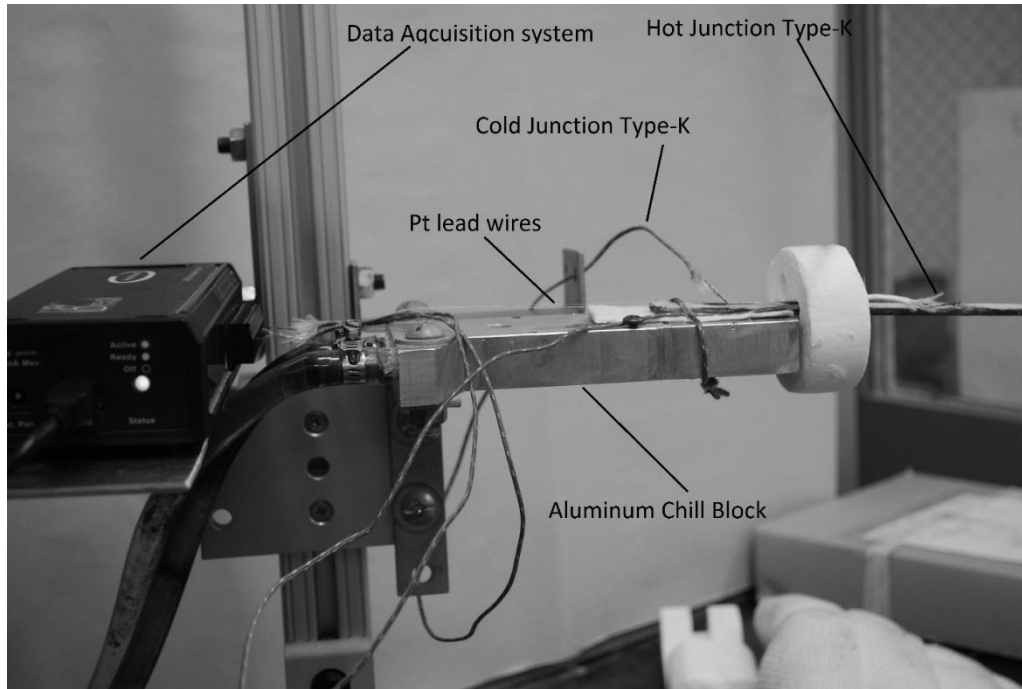


Figure 25: Apparatus used for testing Pt:SiC(CMC) thermocouples.

5.4 Results and Discussion

5.4.1 Pt:SiC (CMC) TC with No Diffusion Barriers

Pt:SiC(CMC) thermocouples prepared without a protective coating were only able to achieve a hot junction temperature of 550°C before failure. A thermoelectric power of 250 μ V/°K was attained for this thermocouple at 550°C, as shown in Figure 26. Even at these moderate temperatures, oxygen could readily diffuse through the platinum film forming the junction and a drift rate that increased with increasing temperature was observed [10]. The oxidation-induced drift produced a drift rate of 2.68°C/hr at 550C but this rate was still low enough that the thermocouple could still function properly.

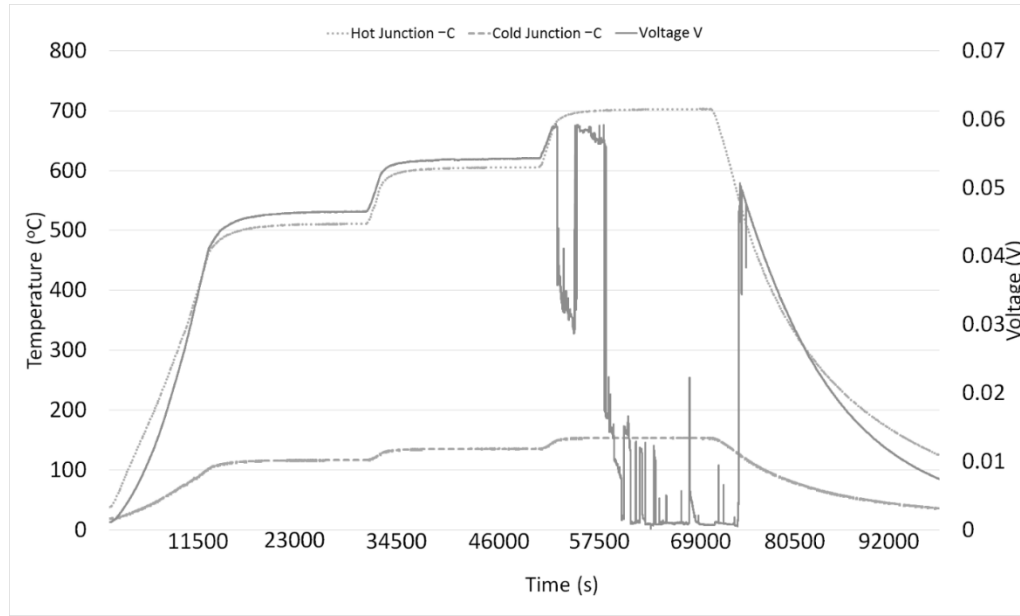


Figure 26: Thermoelectric response of a Pt:SiC(CMC) thermocouple with no diffusion barriers.

5.4.2 Pt:SiC (CMC) TC with An Oxygen Barrier

Oxygen diffusion barriers based on indium oxynitride (InON) were investigated as protective coatings for the Pt:SiC(CMC) thermocouples. In_2O_3 was reactively sputtered in an argon/nitrogen plasma, to form the InON coatings on the Pt:SiC junctions, which served as an oxygen diffusion barrier. Pt:SiC(CMC) thermocouples employing the oxynitride coatings were able to achieve a hot junction temperature of 720°C without failure (Figure 27). As shown in Figure 27, a thermoelectric power of $200\mu\text{V}/^\circ\text{K}$ was achieved at 720°C and the drift rate of this sensor was substantially reduced relative to the Pt:SiC(CMC) thermocouples that employed Pt:SiC junctions without barriers; i.e. a drift rate of $0.31^\circ\text{C}/\text{hr}$ was observed at 700°C but the thermocouple did not survive higher temperatures due to the

formation of platinum silicides that form in the absence of oxygen at these elevated temperatures. Pt₃Si and other platinum silicides can form at higher temperatures [11, 12] but the environmental conditions were such that the formation of platinum carbides was not thermodynamically feasible [15].

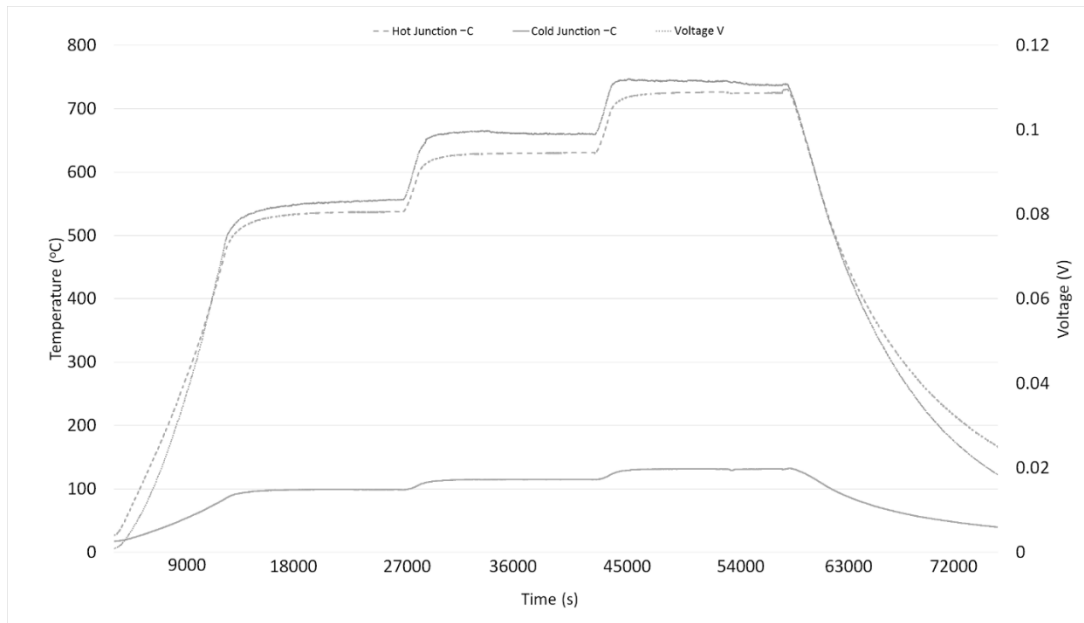


Figure 27: Thermoelectric response of a Pt:SiC(CMC) thermocouple Utilizing an InON oxygen diffusion barrier.

5.4.3 Pt:SiC (CMC) TC with Oxygen and Platinum Silicide Barriers

Pt:SiC(CMC) thermocouples were fabricated utilizing both oxygen and platinum silicide diffusion barriers. For these thermocouples an InON barrier was used to prevent the diffusion of oxygen. Several additional silicide diffusion barriers films were evaluated in terms of their ability to prevent the interdiffusion of platinum and silicon to form platinum silicides. Initially, an InON/W:ITO coating was investigated as a silicide diffusion barrier to prevent the Pt:SiC junction from being compromised. A Pt:SiC(CMC) thermocouple utilizing an InON film as the oxygen diffusion barrier

and W:ITO as the platinum silicide barrier was able to achieve a hot junction temperature of 800°C before failure and a drift rate of 0.217 °C/hr at 800°C. When InON was used as the oxygen diffusion barrier, and Ni:ITO as a platinum silicide diffusion barrier, thermocouples utilizing this combination of coatings were able to achieve a hot junction temperature of 900°C before failure with a drift rate of 1.47°C/hr. Finally, ITO films were investigated as platinum silicide diffusion barriers and indium tin oxynitride (ITON) films were investigated as oxygen diffusion barriers (Figure 28). Hot junction temperatures on the order of 950°C were attained with a drift rate of 0.027°C/hr. This is close to the target temperature of 1000°C for these Pt:SiC(CMC) thermocouples (1000°C), and represents a 400°C improvement in operating temperature relative to the unprotected Pt:SiC(CMC) thermocouples.

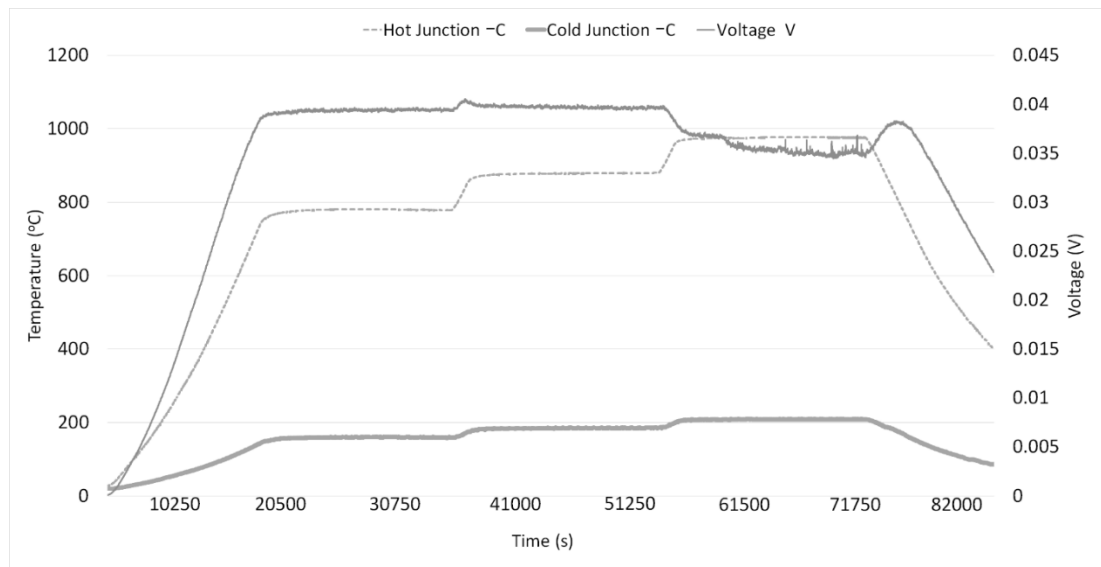


Figure 28: Thermoelectric response of a Pt:SiC(CMC) thermocouple that utilizes a ITON oxygen diffusion barrier and ITO platinum silicide diffusion barrier.

5.5 Conclusions

When the Pt:SiC(CMC) thermocouples without protective coatings were evaluated in terms of thermoelectric response, thermocouple failure occurred at 600°C. This failure was attributed to the increased rate of oxygen diffusion through the platinum contact. As oxygen diffused through the platinum contact, it reacts with the SiC at the Pt:SiC interface to form SiO₂. At lower temperatures, the rate of oxygen diffusion was small enough to allow the sensor to function with minimal drift but at higher temperatures the rate increased substantially and an oxide layer formed between the Pt and SiC CMC, causing the formation of a rectifying or Schottky contact formed as a result. When InON coatings were employed as diffusion barriers, the resulting thermocouples could operate at temperatures more than 200°C higher than those without diffusion barriers. In this case, the diffusion of oxygen through the platinum contact was limited but at higher operating temperatures and in the absence of oxygen, the thermodynamics shifted toward the formation of platinum silicides, which became thermodynamically favorable. The platinum silicides, although much more conductive than SiO₂, still managed to change the nature of the Pt-SiC contact from one that was ohmic in nature to one that was Schottky like.

ITON and ITO thin films were investigated as diffusion barriers and when these were incorporated into Pt:SiC CMC thermocouples, a maximum operating temperature of 950°C was achieved. These temperature sensors could perform at typical hot section temperatures but better diffusion barrier films will be needed to increase the operating temperature beyond 1000°C. Thin film thermocouples based on

Pt:ITO are stable in air at temperatures up to 1200°C, and exhibit large thermoelectric powers with low drift [16,17] but the Pt:SiC(CMC) thermocouples described here have the advantage of utilizing bulk SiC thermoelectric properties for their stability and thus have the potential to go well beyond these temperatures.

List of References

- [1] I.M. Tougas, M. Amani, O.J. Gregory, “Metallic and Ceramic Thin Film Thermocouples for Gas Turbine Engines,” *Sensors*, vol.13, 15324-15347, 2013.
- [2] R.R. Naslain: Sic-Matrix Composites, “Nonbrittle Ceramics for Thermostructural Application,” *Int. J. App. Ceramics*, vol. 2, 75-84, 2005.
- [3] J.D. Wrbanek, G.C. Fralick, D. Zhu,”Ceramic thin film thermocouples for SiC-based ceramic matrix composites,” *Thin Solid Films*, vol. 520, 5801-5806, 2012.
- [4] K.G. Krieder, G. Greg, “High temperature materials for thin-film thermocouples on silicon wafers,” *Thin Solid Films*, vol. 376, 32-37, 2000.
- [5] I.M. Tougas, and O.J. Gregory, “Thin film platinum-palladium thermocouples for gas turbine engine applications,” *Thin Solid Films*, vol. 539, 345-349, 2013.
- [6] N.P. Moiseeva, “The Prospects for Developing Standard Thermocouples of Pure Metals,” *Measurement Techniques*, vol. 47, 915-919, 2004.
- [7] K.D. Hill, “An investigation of palladium oxidation in the platinum/palladium thermocouple system,” *Metrologia*, vol. 39, 51-58, 2002.

- [8] K.G. Kreider, F. DiMeo, "Platinum/palladium thin-film thermocouples for temperature measurements on silicon wafers," *Sensors and Actuators A*, vol. 69, 46-52, 1998.
- [9] M.-A. Nicolet, "Diffusion Barriers in Thin Films," *Thin Solid Films*, vol. 52, 415-443, 1978.
- [10] L.R. Velho, R.W. Barlett, "Diffusivity and Solubility of Oxygen in Platinum and Pt-Ni Alloys," *Metallurgical Transactions*, vol. 3, 65-72, 1972.
- [11] T.C. Chou, "High temperature reactions between SiC and platinum," *J. Mater. Sci.*, vol. 26, 1412-1420, 1991.
- [12] T.C. Chou, "Anomalous solid state reactions between SiC and Pt," *J. Mater. Res.*, vol. 5, 601-608, 1990.
- [13] L.E. Tanner, H. Okamoto, "The Pt-Si (Platinum-Silicon) System," *J. Phase Equilibria*, vol. 12, 571-574, 1991.
- [14] Y.A. Abdelaziz, F.M. Megahed, M.M. Halawa "Stability and calibration of platinum/palladium thermocouples following heat treatment," *Measurement*, vol. 35, 413-420, 2004.
- [15] M.R. Rijnders, A.A. Kodentsov, J.A. Van Beek, J. van den Akker, F.J.J van Loo, "Pattern formation in Pt-SiC diffusion couples," *Solid State Ionics*, vol. 95, 51-59, 1997.
- [16] X. Chen, O.J. Gregory, M. Amani, "Thin-Film Thermocouples Based on the System $\text{In}_2\text{O}_3\text{-SnO}_2$," *J. Am. Ceram. Soc.*, vol. 94, 854-860, 2011.
- [17] O.J. Gregory, Q. Lao, E.E. Crisman, "High temperature stability of indium tin oxide thin films," *Thin Solid Films*, vol. 406, 286-293, 2002.

CHAPTER 6

Advanced Sensors for CMC Engine Components

Published in ICACC 2018, September 2018

Kevin Rivera, Matthew Ricci, Otto Gregory

Department of Chemical Engineering, University of Rhode Island, Kingston RI

K. Rivera, M. Ricci, O.J. Gregory, “Advanced Sensors for CMC Engine Components,” ICACC 2017 proceedings, vol. 2, pp. 1-4

6.1 Abstract

Next generation gas turbine engines used for propulsion purposes will utilize ceramic matrix composite (CMC) components in the engine hot section to achieve higher engine operating temperatures and higher thermal efficiencies. Within the engine hot section, rotating components can experience temperatures above 1000°C and g-forces over 50,000g. Therefore, it is important to monitor temperature and strain of these CMC components under these harsh conditions, such that structural models can be verified and new designs can be evaluated. However, conventional wire instrumentation is not well suited for such applications since the sensors and leads cannot be welded to the CMC components and the CMC surfaces cannot be altered. Temperature and strain sensors have been developed for SiC-SiC CMC's, which rely on the semiconducting properties of the SiC-SiC substrate itself to generate large and reliable resistive, piezoresistive, and thermoelectric responses with the added advantage of minimal intrusion, negligible mass, and fast response times. At temperatures $> 1000^{\circ}\text{C}$, oxidation, small diffusional distances, and microstructural changes can lead to signal drift and thus coatings were developed to ensure the integrity of the semiconductor:metal contacts in these sensors. Results of temperature and strain testing will be presented as well as the fabrication steps used to make the sensors.

6.2 Introduction

Future gas turbine engines will utilize ceramic matrix composites or CMC components rather than traditional nickel based superalloys due to their superior

thermomechanical properties [1]. CMC based components will permit higher engine operating temperatures and thus allows higher thermal efficiencies [1]. Advanced instrumentation for these CMC components is needed to verify structural models and the structural integrity of the components. Wire sensors for temperature measurement have been used extensively for nickel based superalloys engine components since they can be welded on but they can affect the gas flow path and vibrational modes during operation due to their bulky nature [1]. However, they cannot be welded to CMC components. Thin-film sensors can be deposited directly onto the surfaces of engine components, and do not affect the gas flow path and vibrational modes during operation. However, thin-film sensors are prone to selective oxidation, dewetting, and metallurgical changes in the films that lead to considerable signal drift [2].

6.2.1 Temperature sensors

Earlier research into thin-film temperature sensors focused on Pt/Pt-Rh thermocouples or Type S thermocouples since the wire version proved so successful but it was determined that preferential oxidation of the rhodium in the films would limit this approach since changes in composition at higher temperatures can lead to changes in thermoelectric output [3]. Pt:Pd thin film thermocouples had some promise since they are not alloys but again selective oxidation of the palladium at temperatures in the range 600-800°C occurred as well as dewetting of the films [2,4]. Other noble metal thermocouples such as Au:Pt were attempted in order to circumvent oxidation at higher temperatures but these lacked the ability to reach temperatures above 1000°C and exhibited low thermoelectric outputs [2]. Pt:ITO thin film thermocouples were

able to survive temperatures above 1000°C and produced very large Seebeck coefficients with little or no drift [5]. However, Pt:SiC(CMC) thermocouples have been developed which yield even larger thermoelectric outputs with greater stability by combining the benefits of noble metal thin films and bulk semiconductor properties. This new class of thermocouple produced thermoelectric powers as large as 250 μ V/K with minimal drift at elevated temperatures. The Pt:SiC(CMC) thermocouple utilizes the bulk properties of the SiC-SiC in the CMC and is able to function at temperatures \sim 1000°C when protective coatings were employed. Sputtered diffusion barriers were also employed to prevent adverse reactions at elevated temperature which alters the ohmic nature of the Pt:SiC contacts and thus, the stability of the contacts at elevated temperatures [6]. Past work concerning the measurement of a piece of materials resistance to monitor structural damage in have been conducted with large success [7,8] and more recently SiC-SiC CMC resistivity has been measured to evaluate structural damages caused by exposure to temperatures above 1000°C and high strain [9,10]. A resistive temperature device (RTD) has also been developed where the active resistive element is the SiC-SiC CMC which is doped with boron and has a negative temperature coefficient of resistance (TCR) in order to measure high temperatures.

6.2.2 Strain gages

Pd:Cr strain gages were investigated because of their structural stability and linear strain behavior at elevated temperatures [11] but had low gage factors and could only operate at temperatures just above 1000°C in open air. Indium tin oxide (ITO) thin

film strain gages were shown to perform at temperatures up to 1500°C and have gage factors of 130 but had high signal drift at high temperatures due to the large negative TCR of the ITO [12]. A much more stable version of the ITO strain gage was developed with a near zero TCR but produced gage factors of around 5 due to the inclusion of Pt to balance the TCR [13]. Piezoresistive properties of various SiC polymorphs with p or n dope loadings have been studied extensively [14,15] and are well understood for n-type but p-types are still being studied. A strain gage in which the active strain element is the p-type SiC-SiC CMC has been developed which takes advantage of the SiC-SiC CMC piezoresistive properties and exhibits a gage factor of ~20.

6.3 Experimental

6.3.1 Preparation of the CMC Substrate Overcoat

The as-received CMC's were heat treated at 1000°C for 15 hours in a Deltech furnace. A thin layer of dielectric cement was then applied to the surface of the CMC to provide electrical isolation between the sputtered Pt leads, bond pads and the CMC. The dielectric layer was heat-treated on a Fisher Scientific hotplate for 20 minutes at 100°C, 20 minutes at 200°C, and 40 minutes at 300°C followed by a high temperature heat treatment at 1000°C for 10 hours in the Deltech furnace.

6.3.2 Pt:SiC(CMC) Thermocouple Fabrication

Via holes were created in the dielectric coating deposited over the CMC substrate and photolithography techniques were used to pattern leads and bond pads on the surface of the CMC substrate (Fig. 29). For high temperature applications, diffusion

barrier coatings were sputter deposited to prevent adverse reactions as well as maintain the ohmic nature of the contact formed between the Pt and SiC-SiC CMC (Fig. 30).

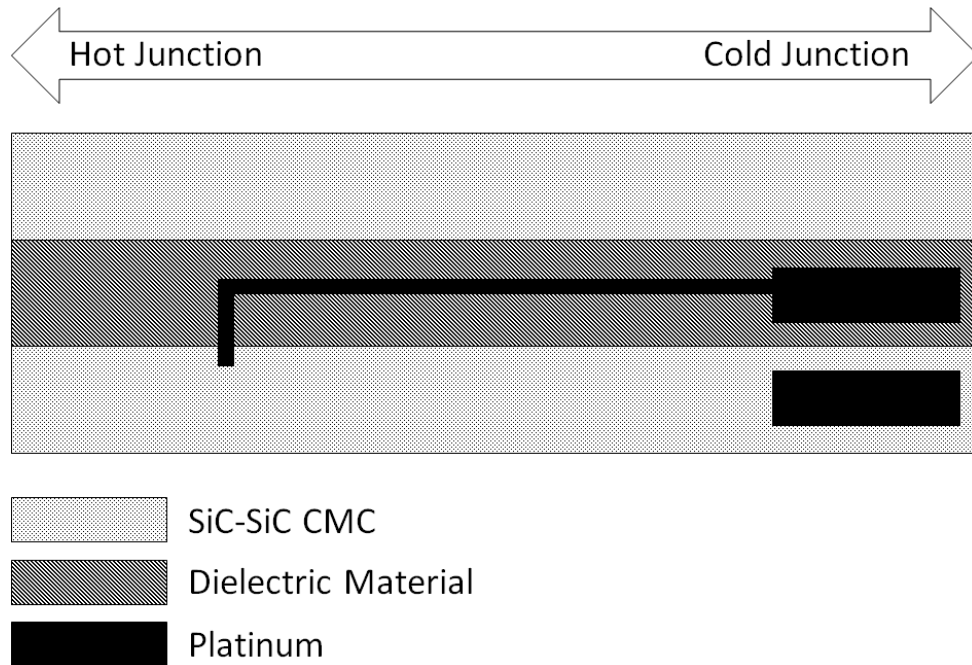


Figure 29: Schematic top-down view of a Pt:SiC(CMC) thermocouple.

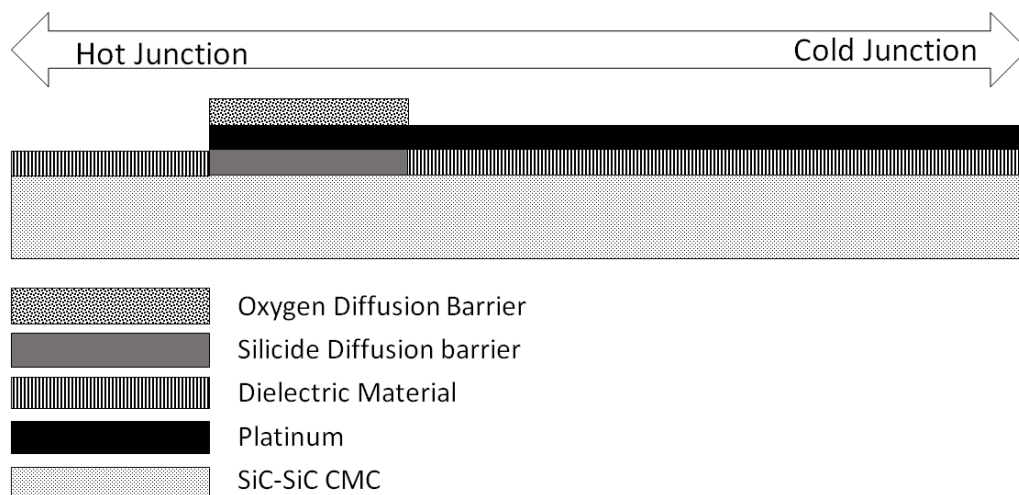


Figure 30: Cross section of a Pt:SiC(CMC) thermocouple with barrier coatings.

6.3.3 SiC-SiC CMC RTD and Strain Gage Fabrication

A four-terminal design was implemented (Fig. 31) in order to measure a voltage drop and remove any contact resistance from the measurement. In the case of higher temperature testing ($>1000^{\circ}\text{C}$), diffusion barrier coatings were employed to prevent the ohmic contact between the metal:semiconductor from becoming rectifying.

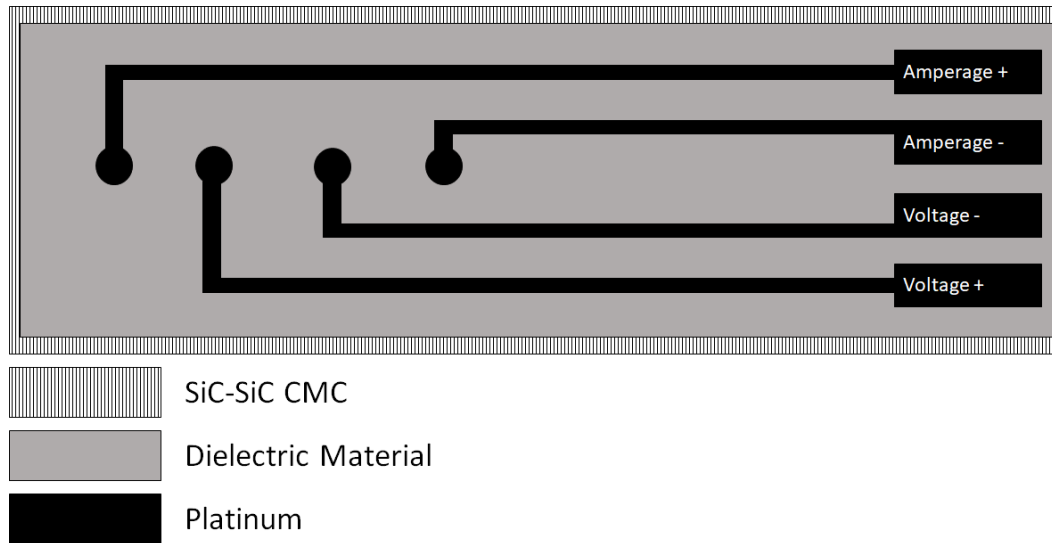


Figure 31: Schematic view of the design shared by SiC-SiC CMC RTD and strain gage.

6.3.4 Sensor Testing Procedures

The protocol for testing the Pt:SiC(CMC) thermocouples with barrier coatings and SiC-SiC CMC RTDs was as follows: ramp to the first setpoint temperature at a rate of $4^{\circ}\text{C}/\text{min}$, hold for 5 hours, ramp to the second setpoint temperature at a rate of $4^{\circ}\text{C}/\text{min}$, hold for 5 hours, ramp to the third setpoint temperature at a rate of $4^{\circ}\text{C}/\text{min}$,

hold for 5 hours and then a ramp back down to room temperature at a rate of 4°C/min. This test was used to determine thermoelectric and TCR properties of the Pt:SiC(CMC) thermocouples and SiC-SiC CMC RTDs respectively as well as their signal drift properties. The thermoelectric potential was measured using eq.1.

$$V_{TE} = \frac{\Delta V}{\Delta T} \quad (1)$$

Where ΔV is the voltage potential measured and ΔT is the temperature difference between the thermocouple hot and cold junction. Thermocouple temperature drift was measured using eq.2.

$$T_d = \frac{\Delta V}{V_o} \cdot \frac{T}{\Delta t} \quad (2)$$

Where V_o is the voltage measured at the beginning of the test hold period, T is the hold period temperature and Δt is the amount of time held. TCR of the SiC-SiC CMC RTD was determined using eq.3.

$$\alpha = \frac{\Delta R}{R_o \Delta T} \quad (3)$$

where ΔR is the difference between the resistance at a temperature and the reference resistance at room temperature, R_o is the reference resistance, and ΔT is the difference between the test temperature and the reference temperature. The SiC-SiC CMC strain gages were held in a custom built four-point testing setup and strained using an Instron and strained at a controlled frequency. A constantan strain gage was mounted

on the center of the SiC-SiC CMC strain gage surface using an adhesive. The outer two wire leads of the SiC-SiC CMC strain gage connected to a Keithley 224 constant current source set to 0.001A. The middle two wire leads connected to a PDAQ54 system to measure a voltage drop. The student strain gage wire leads connected directly to a Vishay P3 strain indicator to measure the applied strain. Gage factor for the SiC-SiC CMC strain gage was determined using eq.4.

$$GF = \frac{\Delta R}{R_o} \cdot \frac{1}{\Delta \epsilon} \quad (4)$$

Where ΔR is change in resistance, R_o is the initial resistance before the applied strain, and $\Delta \epsilon$ is the applied strain.

6.4 Results and Discussion

6.4.1 Thermocouples with Protective Barrier Testing

When the Pt:SiC(CMC) thermocouples were tested without any diffusion barrier coatings applied to the Pt:SiC junctions, a maximum operating temperature of 550°C was reached before failure and a thermoelectric voltage of 250uV/K was generated with drift rate of 1.8°C/hr (Fig. 32). Higher temperatures were not possible in this case due to the diffusion of oxygen through the platinum film [16] which reacted with the SiC-SiC in the CMC to form SiO₂ at the Pt:SiC interface. As a result of this reaction, the contact did not remain ohmic. When an InON coating was employed as a diffusion barrier, a maximum operating temperature of 700°C was reached before failure and a thermoelectric power of 250uV/K was attained (Fig. 33). Any attempt at heating to

higher temperatures caused the platinum in the junction to react with the SiC-SiC in the CMC and form platinum silicides [17,18]. When an ITON coating was used as an oxygen diffusion barrier and ITO was used as a diffusion barrier to prevent platinum silicide formation, the thermocouples were able to operate successfully at temperatures $\sim 1000^{\circ}\text{C}$ (Fig. 34).

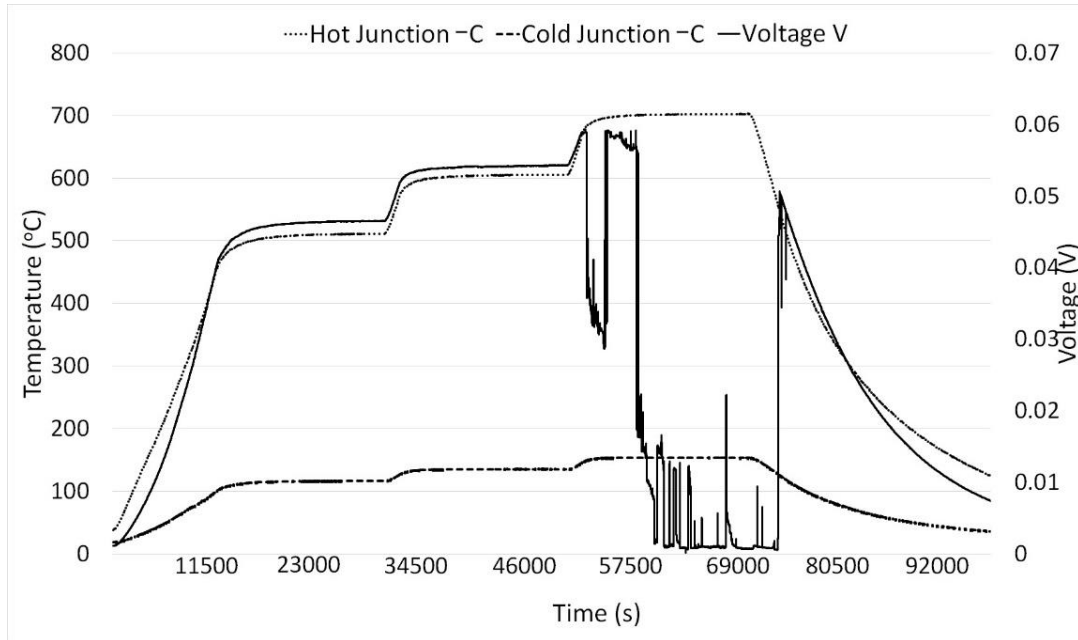


Figure 32: Pt:SiC(CMC) thermocouple with no diffusion barrier coating

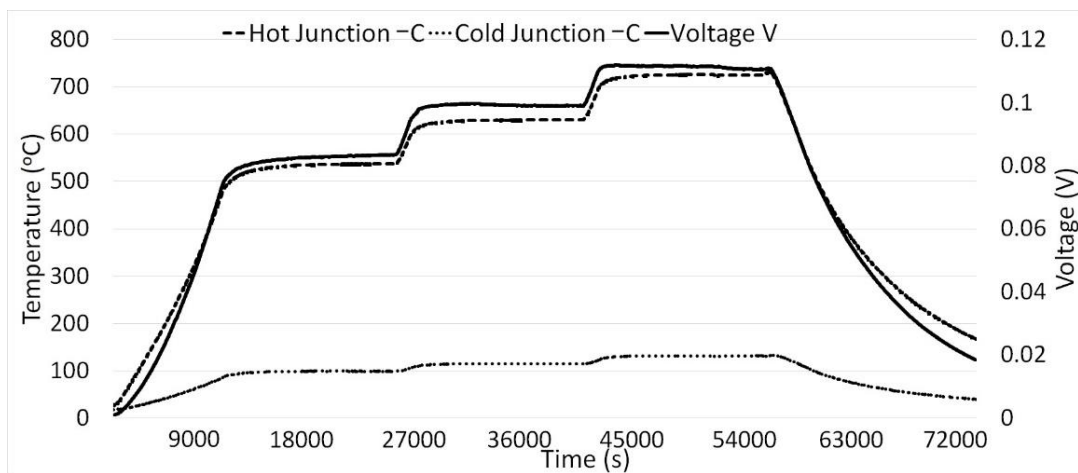


Figure 33: Pt:SiC(CMC) thermocouple utilizing a InON oxygen barrier coating

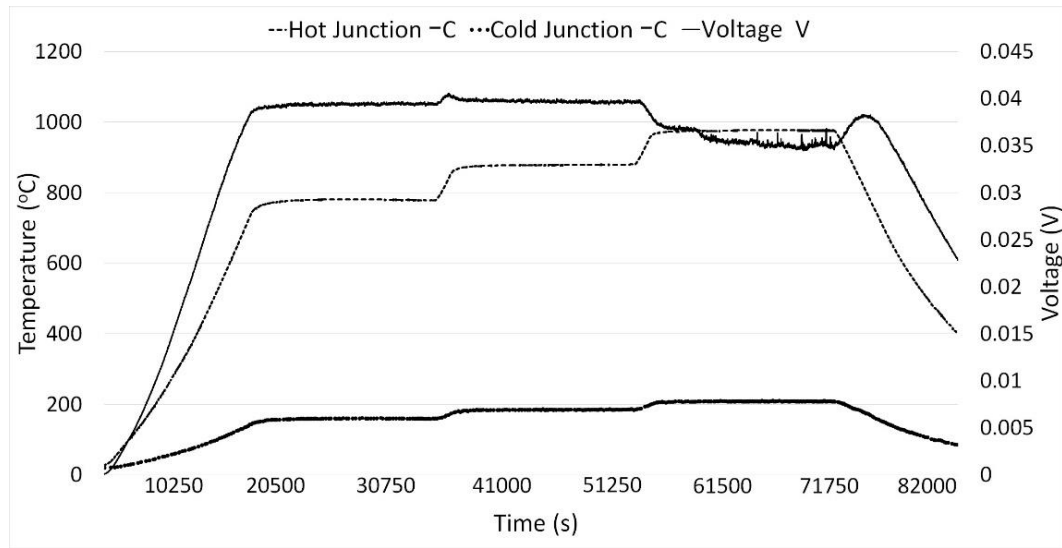


Figure 34: Pt:SiC(CMC) thermocouple utilizing ITON oxygen and ITO platinum silicide barrier coatings

6.4.2 SiC-SiC CMC RTD Testing

SiC-SiC CMC RTD testing was conducted and the TCR was found to be generally nonlinear (Fig. 35). Using the four-terminal design it was determined that diffusion barriers were not needed since the contact resistance was eliminated. For low temperature testing (100-250°C) the resistance of the SiC-SiC CMC RTD changed from 255-225Ω which gave a TCR of 0.000794°C⁻¹.

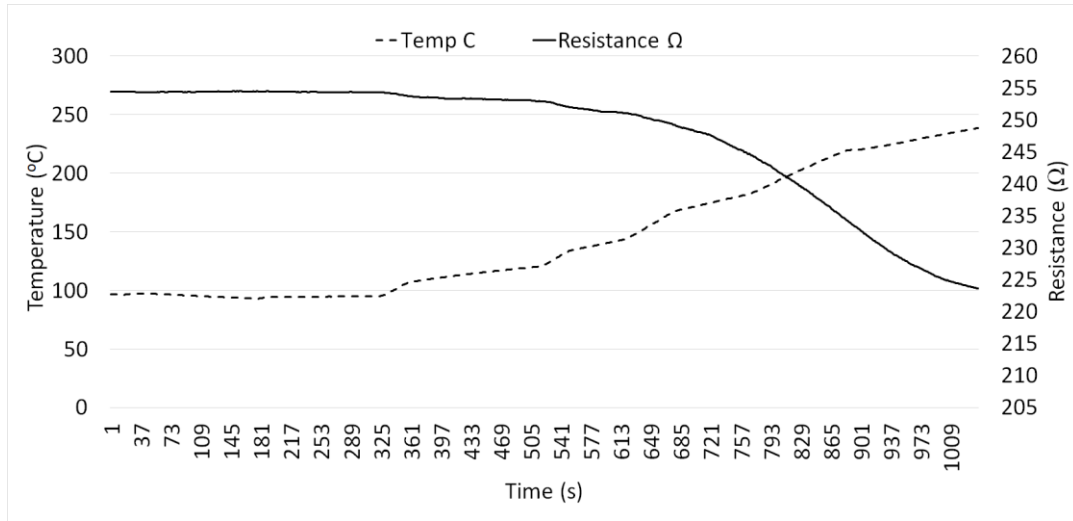


Figure 35: RTD testing from 100-250°C.

6.4.3 SiC-SiC CMC Strain Gage

When the SiC-SiC CMC strain gage was tested at 20°C with 1200 $\mu\epsilon$ loads applied every 10 seconds, a change in resistance of 4 Ω was measured resulting in a gage factor of 20 (Fig. 8).

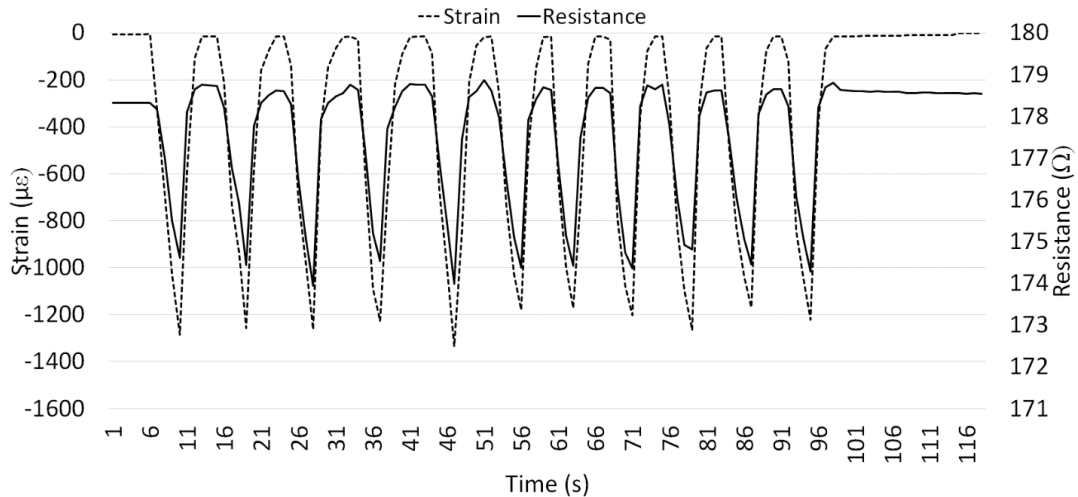


Figure 36: SiC-SiC CMC strain gage test using an excitation current of 0.05A.

6.5 Conclusions

Thermocouples utilizing the bulk properties of the SiC-SiC comprising the CMC were developed for advanced components comprising the hot section of gas turbine engines. The thermocouples produced larger thermoelectric powers than Pt:ITO thin-film thermocouples [5] while maintaining minimal drift. At temperatures greater than 550°C, adverse reactions prompted the need for diffusion barrier coatings to prevent oxidation of the SiC in the Pt:SiC junction and the formation of platinum silicides. When diffusion barrier coatings were employed, the Pt:SiC(CMC) thermocouples could be cycled to ~1000°C without failure. RTDs and strain gages in which the active resistive element is the SiC-SiC CMC have been demonstrated with TCRs and gage factors on the order of 0.000794°ppm/C and 20 respectively. The sensors developed in this study displayed either partial or full self-sensing capability and were able to produce large signals due greatly in part to the semiconducting properties of the SiC-SiC CMC material.

List of References

- [1] I.M. Tougas, M. Amani, O.J. Gregory, “Metallic and ceramic thin film thermocouples for gas turbine engines,” *Sensors*, vol. 13, pp. 15324-15347, 2013.
- [2] N.P. Moiseeva, “The prospects for developing standard thermocouples of pure metals,” *Measurement Techniques*, vol. 47, pp. 915-919, 2004.

- [3] K.G. Kreider, G. Greg, "High temperature materials for thin-film thermocouples on silicon wafers," *Thin Solid Films*, vol. 376, pp. 32-37, 2000.
- [4] I.M. Tougas, O.J. Gregory, "Thin film platinum-palladium thermocouples for gas turbine applications," *Thin Solid Films*, vol. 539, pp. 345-349, 2013.
- [5] X. Chen, O.J. Gregory, M. Amani, "Thin-film thermocouples based on the system $\text{In}_2\text{O}_3\text{-SnO}_2$," *J. Am. Ceram. Soc.*, vol. 94, pp. 854-860, 2011.
- [6] M.A. Nicolet, "Diffusion barriers in thin films," *Thin Solid Films*, vol. 52, pp. 415-443, 1978.
- [7] J.F.Lei, H.A. Will, "Thin-film thermocouples and strain-gauge technologies for engine applications," *Sens. Act. A*, vol. 65, pp. 187-19, 1998.
- [8] O.J. Gregory, T. You, "Piezoresistive Properties of ITO Strain Sensors Prepared with Controlled Nanoporosity," *J. of the Electrochemical Soc.*, vol. 151, pp. 198-203, 2004.
- [9] O. Gregory, Q. Lou, "A self-compensated strain gage for use at elevated temperatures," *Sens. Act. A*, vol. 88, pp. 234-240, 2001.
- [10] T.C. Chou, "Anomalous solid state reaction between SiC and Pt," *J. Mater. Res.*, vol. 5, pp. 601-608, 1990.
- [11] C.E. Smith, G.N. Morscher, Z.H. Xia, "Monitoring damage accumulation I ceramic matrix composites using electrical resistivity," *Scripta Materialia*, vol. 59, pp. 463-466, 2008.
- [12] L.R. Velho, R.W. Barlett, "Diffusivity and solubility of oxygen in platinum and Pt-Ni alloys," *Metallurgical Transactions*, vol. 3, pp. 65-72, 1972.

- [13] T.C. Chou, "High temperature reactions between SiC and platinum," *J. Mater. Sci.*, vol 26, pp. 1412-1420 , 1991.
- [14] H. Phan, P. Tanner, D.V. Dao, L. Wang, N. Nguyen, Y. Zhu, S. Dimitrijevic, "Piezoresistive Effect of p-Type Single Crystalline 3C-SiC Thin Film," *IEEE Electron Device Letters*, vol. 35, pp. 399-401, 2014.
- [15] R.S. Okojie, "Characterization of highly doped n- and p-type 6H-SiC piezoresistors," *IEEE Transactions on Electron Devices*, vol. 45, pp. 785-790, 1998.
- [16] C.E. Smith, G.N. Morscher, Z.H. Xia, "Electrical Resistance as a Nondestructive Evaluation Technique for SiC/SiC Ceramic Matrix Composites Under Creep-Rupture Loading," *Int. J. Appl. Ceram. Technol.*, Vol 8, pp. 298-307, 2011.
- [17] B. Fankhanel, E. Muller, U. Mosler, W. Siegel, "SiC-fibre reinforced glasses – electrical properties and their applications," *J. ECS*, vol. 21, pp. 649-657, 2001.
- [18] H. Mei, L. Cheng, "Damage analysis of 2D C/SiC composites subjected to thermal cycling in oxidizing environments by mechanical and electrical characterization," *Materials Letters*, vol. 59, pp. 3246-3251, 2005.

CHAPTER 7

Strain Gages for CMC Engine Components

Published in IEEE Sensors Letters, August 2018

Kevin Rivera, and Otto J. Gregory

Department of Chemical Engineering, University of Rhode Island, Kingston RI

K. Rivera, O. J. Gregory, "Strain Gages for SiC-SiC CMC Ceramic Matrix Composite Engine Components," IEEE Sensors Letters, vol. 2, pp. 1-4

7.1 Abstract

As more and more SiC–SiC ceramic matrix composites or CMC’s are being used in the hot sections of gas turbine engines, there is a greater need for in-situ strain measurement in these harsh conditions. Thin film strain sensors are ideally suited for this task since they have minimal mass and are nonintrusive. However, if the bulk piezoresistive properties of SiC-SiC CMC’s could be used instead of the thin film piezoresistive properties, superior resolution and stability could be realized. Toward this end, we have fabricated strain gages in which the active strain element is the SiC-SiC CMC itself. As a result of this approach, a Pt:SiC CMC strain gage capable of operating at 500°C for prolonged periods was demonstrated. The large piezoresistive responses associated with the SiC fibers and SiC matrix resulted in gage factors larger than 100. Performance of the Pt:SiC CMC strain gages under both tension and compression are reported and the IV characteristics of the strain gages as well as the piezoresistive response as a function of temperature are presented. In addition, the potential for embedded strain gages in advanced CMC engine components will be discussed.

7.2 Introduction

Components within the hot section of gas turbine engines, such as the blades and disks can experience extremely large g-forces and high temperatures. Silicon carbide ceramic matrix composites (CMCs) are being considered for components in the engine hot section because they are refractory, creep and oxidation resistant, and thus, will result in higher thermal efficiencies by increasing the maximum engine operating temperature [1].

To monitor the structural integrity of CMC components, they need to be instrumented with strain gages that are both stable and sensitive: i.e. exhibit a repeatable, measurable output as a function of deformation. Strain gages employed within the engine environment should have negligible mass and an extremely low profile, so that they do not affect vibrational patterns and the gases flowing through the engine. They should also be able to withstand very high temperatures for prolonged periods with little signal drift. Standard wire strain gages are bulky and in most cases have to be welded to the surface of the engine components. Welding is commonly used with metallic engine components as well as embedded gages but SiC-SiC CMC's cannot be welded or machined, thus, other solutions for strain measurement must be considered. Thin film strain gages offer an excellent alternative but their performance is greatly affected by oxidation, diffusion effects, and alterations in their microstructure [2].

Pd-Cr thin film strain gages exhibit nearly linear changes in resistance as a function of strain and can be used at temperatures up to 1050°C. However, severe limitations in performance are encountered at temperatures beyond 1050°C due to thin film issues [3]. More recently indium tin oxide (ITO) strain gages have been used for these applications due to their high temperature chemical and electrical stability. ITO based strain gages are not prone to oxidative effects and operate at temperatures above 1500°C. They have gage factors of 100 but suffer from signal drift due to their large negative temperature coefficient of resistance (TCR) [4]. This signal drift can be mitigated by creating low TCR nanocomposites such as Pt:ITO which have nearly zero drift because of the constituents having nearly equal and opposite TCR's but a

reduced gage factor is seen [5].

Thick film strain gages have several advantages over thin film strain gages since they are able to withstand severe oxidation better, experience smaller temperature effects, they can be applied onto components which are too large to fit within typical deposition chambers required for sputtering and are much simpler to deposit [6].

Extremely large gage factors have been measured by Zhang and Ivanko [7, 8] but their strain gages cannot survive or sustain these gage factors at high temperatures and in the harsh conditions of a gas turbine engine. Large gage factors would be preferential within a gas turbine engine to verify structural models and monitoring structural integrity of the components.

Semiconductor strain gages are ideally suited for strain applications because of their high sensitivity [9-10]. SiC has over two hundred different polymorphs with very different chemical and mechanical properties [11]. Both poly and single crystalline SiC with assorted p or n-type loadings have been tested to understand its piezoresistive behavior. Gage factors of 30 to -20 were found experimentally, depending on the direction the SiC was strained [12-14]. P and n-type semiconductors have negative TCRs but experience opposite changes in resistance as a function of applied strain. The mechanism for resistance change upon strain is very well understood for n-type [15] semiconductors but not nearly as well for p-type semiconductors [16]. A great deal of work has been done in both experimentation and modeling to gain a better understanding of the piezoresistance effect in p-type semiconductors [13, 17]. SiC has a bandgap of 3.3eV and the type used in this study has a boron coating on the fibers to enhance its high temperature oxidation resistance but this coating also increases the

electrical conductivity of the SiC. Consequently, this makes the SiC-SiC CMC's an excellent choice for high temperature sensor applications and can overcome some limitations of instrumenting CMC's with thick and thin film sensors. It is also nearing the required maturity to soon be implemented in future gas turbine engines.

The goal of this work was to create a high-resolution strain gage that was stable at elevated temperatures and that relied on bulk properties instead of thin film properties. A Pt:SiC CMC strain gage capable of operating at 500°C for prolonged periods was demonstrated. Eventually, Pt:SiC CMC strain gages capable of operating at temperatures greater than 1000°C is anticipated. Performance of the Pt:SiC CMC strain gages under tension and compression were evaluated and the IV characteristics of the strain gage as a function of temperature were determined to characterize the metal:semiconductor contacts.

7.3 Experimental Results

7.3.1 Strain Gage Fabrication

As-received SiC-SiC CMCs (19cm x 2.5cm x 0.3 cm) were heated in an MHI tube furnace at 1000°C for 20 hr to clean them and grow a stable oxide. A 20µm thick layer of mullite dielectric was applied using a doctor blade technique to create a smooth surface and heat treated to 100 °C, 200 °C, 300°C for 30 minutes each and a final heat treatment at 1000°C for 15 hr using a Deltech tube furnace. Photolithography techniques were employed using a dry photoresist (Dupont MX5050) to which the strain gage pattern was applied over the dielectric (Fig. 37). Via holes were created in the dielectric where the SiC-SiC CMC makes contact to the thin film leads and the surface of the SiC-SiC CMC in these areas was etched using a dilute HF mixture.

High purity platinum was then RF sputtered directly into the windows created in the photoresist for 1 hr at 300W and a forward voltage of 1200V in 9mTorr high purity argon gas. The platinum films, 2.5 μ m thick, were then annealed in nitrogen to remove any trapped argon and point defects formed during the sputter process.

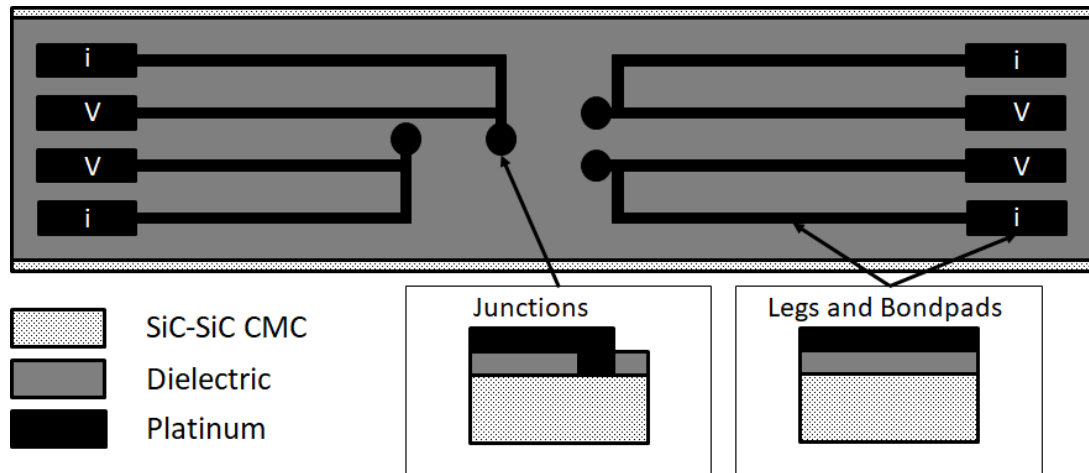


Figure 37: Pt:SiC CMC strain gage design showing the two outer leads (current) and two inner leads (voltage). The pattern on the left is sensitive to longitudinal strain and the pattern on the right is sensitive to transverse strain.

7.3.2 Electrical Characterization of Contacts

In order to pass an excitation current through Pt:SiC CMC strain gages and extract the output signal, it was critical to electrically characterize the metal:semiconductor interface (Fig. 38). A Van der Pauw technique [18] was used to ensure that the Pt:SiC CMC contacts were ohmic in nature and non-rectifying. The strain gage was heated in a Lindberg TF55035A tube furnace to determine the IV characteristics at temperatures ranging from 20-510°C. The strain gage was tested in both forward and reverse bias

and both behaviors were found to be linear, which indicated that the Pt:SiC CMC contacts were ohmic in nature. Beyond 550°C, the behavior was rectifying, which indicated that a Schottky barrier had formed.

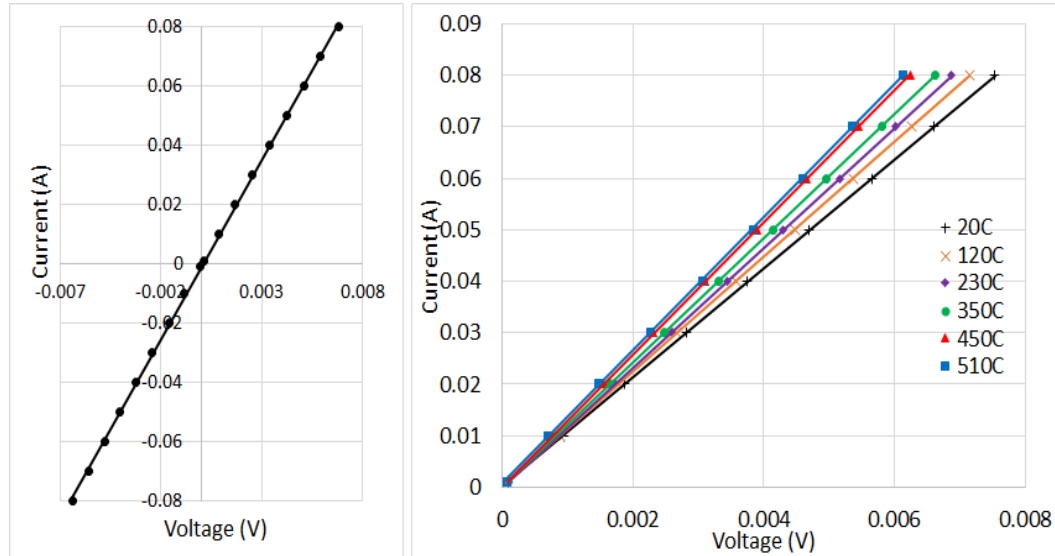


Figure 38: I-V characteristics of a Pt:SiC CMC contact. The I-V characteristic in the forward bias and reverse bias conditions for the Pt:SiC-SiC CMC contacts at 20°C (left) and the I-V curve for the forward bias condition at temperatures ranging from 20°C-510°C

7.3.3 Piezoresistance

Two techniques were used to apply strain to the Pt:SiC CMC strain gages. One was a four-point bend method described by ASTM C1341 to ensure uniform strain across the surface and the other was a cantilever loading method, which allowed the strain gage to be tested at elevated temperatures. The four-point method testing setup used an Instron tensile testing machine to load the beam and therefore, was only used for

room temperature piezoresistance measurements. The cantilever-load method was used for high-temperature piezoresistance measurements, since the fixture was able to fit within the hot zone of a tube furnace. Two lag screws were used to keep the Pt:SiC CMC strain gage in place and the strain gage was excited using a rigid alumina rod that was oscillated by a small rotating steel cylinder mounted on a high torque DC motor. A two wire Kelvin clamp method was used to measure strain performance at lower temperatures and a 4-wire method was utilized for higher temperature testing to eliminate contact resistance (Fig. 37). The Pt:SiC CMC strain gages were excited using 10mA (Keithly 224 constant current source), and were connected to a PDAQ54 to measure voltage drop across the strain gage. A student strain gage was mounted at the center of the strain gage on the surface using an epoxy in order to measure applied strain during testing and interfaced with a Vishay P3 strain indicator to collect strain data.

The two main factors that affect overall resistance change during strain are a geometric effect as well as changes in resistivity of the active strain element. Eq. 1 shows this relationship for strain gages.

$$GF = 1 + 2\nu + \frac{\Delta\rho}{\rho_0 \epsilon} \quad (1)$$

where $\Delta\rho$ is the change in resistivity, ρ_0 is the initial resistivity at room temperature, ϵ is the applied strain, and ν is the poisson ratio. The first two terms are due to a geometric effect and the last term is due to piezoresistivity, which for semiconductors is the dominant term. Gage factor was calculated using a derived version of (1).

$$GF = \frac{\Delta R}{R_o \varepsilon} \quad (2)$$

where ΔR is the change of resistance and R_o is the initial resistance at room temperature. To determine the strain gage output drift over a prolonged period at a constant applied strain rate and constant temperature for the Pt:SiC CMC strain gage eq. 3 was used

$$\varepsilon_d = \frac{\Delta R}{R_i} \cdot \frac{\varepsilon_c}{\Delta t} \quad (3)$$

where ΔR is the change in resistance, R_i is the initial resistance at the start of the hold period, ε_c is the constant applied strain rate, and Δt is the elapsed hold time.

The cantilever-load method was used to determine gage factor at elevated temperatures. Here, a continuous excitation current of 10mA was used to excite the strain gage. When the Pt:SiC CMC strain gage was tested under $-600\mu\varepsilon$ of compression, a gage factor of 112 was measured (Fig. 3). Under $300\mu\varepsilon$ of tension the gage factor was 50. Transverse gage factors were also determined using the same method and they were equal and opposite to the longitudinal gage factors in both tension and compression. These gage factors are large compared those reported for SiC in literature but we hypothesize that the SiC fibers in the CMC carry a majority of the current and that the grains are highly crystalline and oriented in the direction of drawing with a high degree of anisotropy which should result in large gage factors. The SiC matrix is also a potentially contributing to the bulk piezoresistive properties but these have not been documented to date so their role is not certain. In general the gage factor was nonlinear as strain was applied but had a region within $50-125\mu\varepsilon$ where the gage factor was relatively linear (Fig. 39). From $20-230^\circ\text{C}$ the gage factor

increased but at temperatures beyond, the gage factor diminished to about 1 (Fig. 40).

The Pt:SiC CMC strain gages exhibited large changes in resistance when strained but did not fully return to their original resistance, due to damage accumulation in the SiC fibers. Through non-destructive evaluation Smith has shown that the majority of current in the SiC CMCs is carried by the fibers and any damage will show up as a resistance change [19]. At 500°C, the drift rate in compression and TCR were $-0.0492\mu\epsilon/\text{hr}$ and $-0.0006435^\circ\text{C}^{-1}$ respectively.

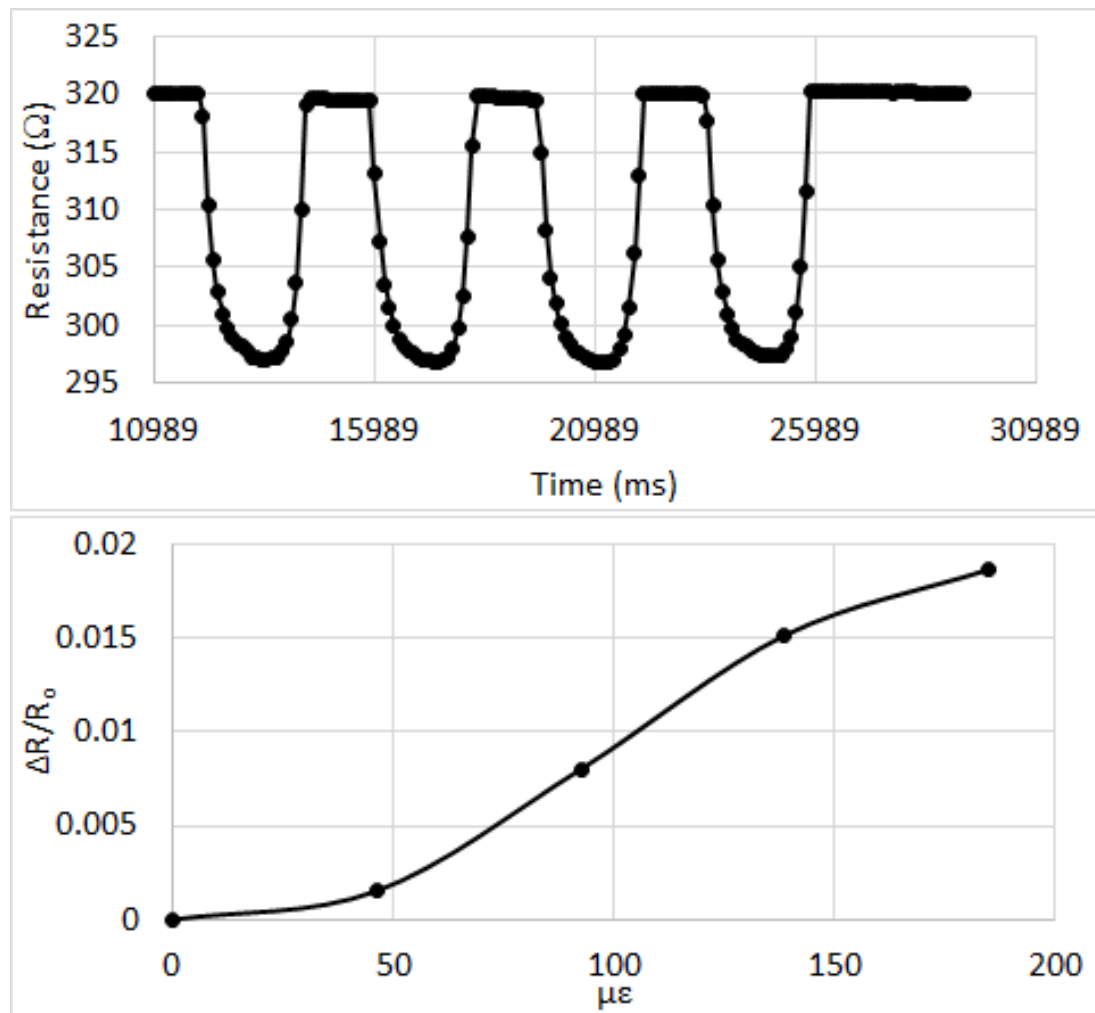


Figure 39: (Bottom) Plot showing resistance change as a function of applied strain in tension, Note; slight non-linear resistance change with applied strain. (Top) Portion of a test for a Pt:SiC CMC strain gage strained at $-600\mu\epsilon$ and 20°C . Gage factor of 112 is

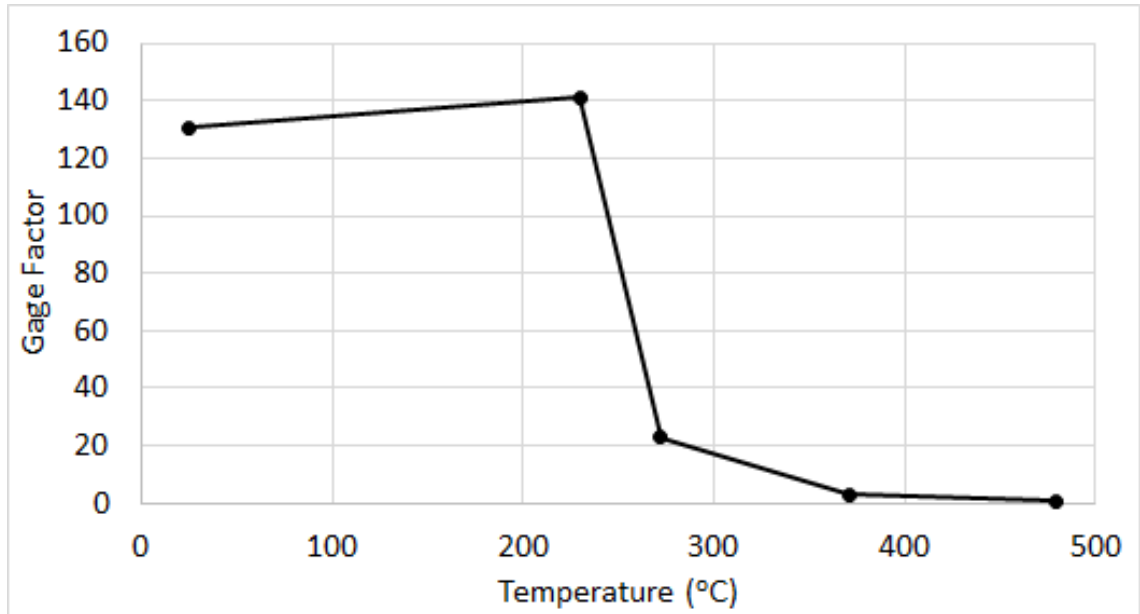


Figure 40: The effect of temperature on the gage factor for the Pt:SiC CMC strain gage under compressive strain.

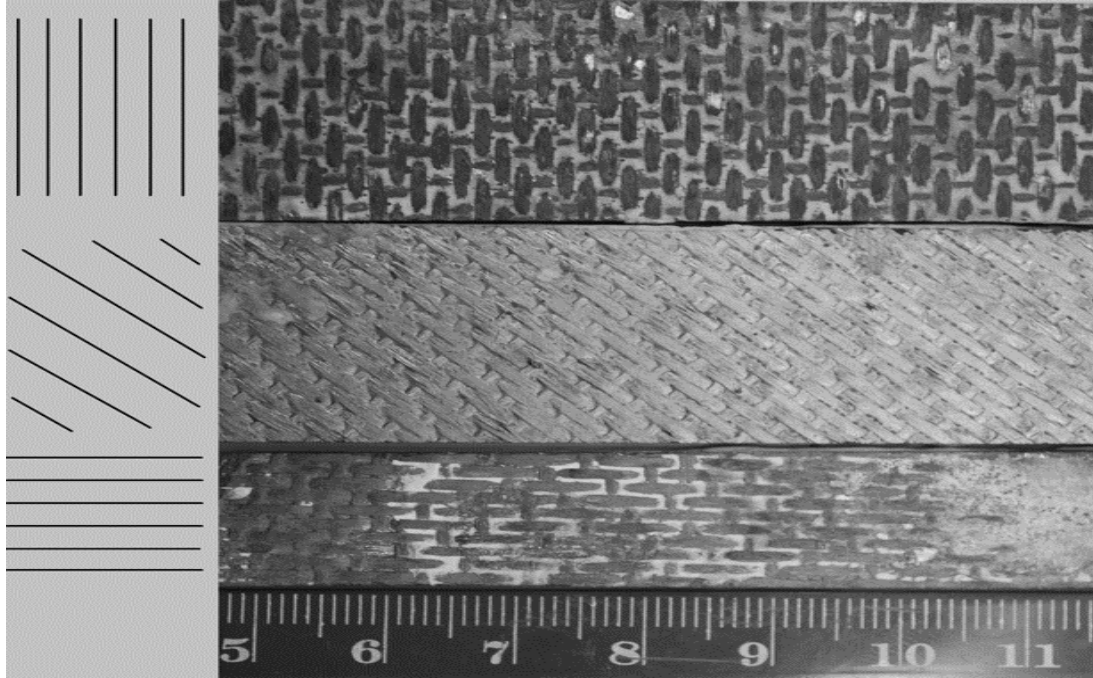


Figure 41: Photograph of SiC-SiC CMC substrates with differing fiber orientations. Relative to the long axis (Top) is 90°, (Middle) is 45°, and (Bottom) is parallel.

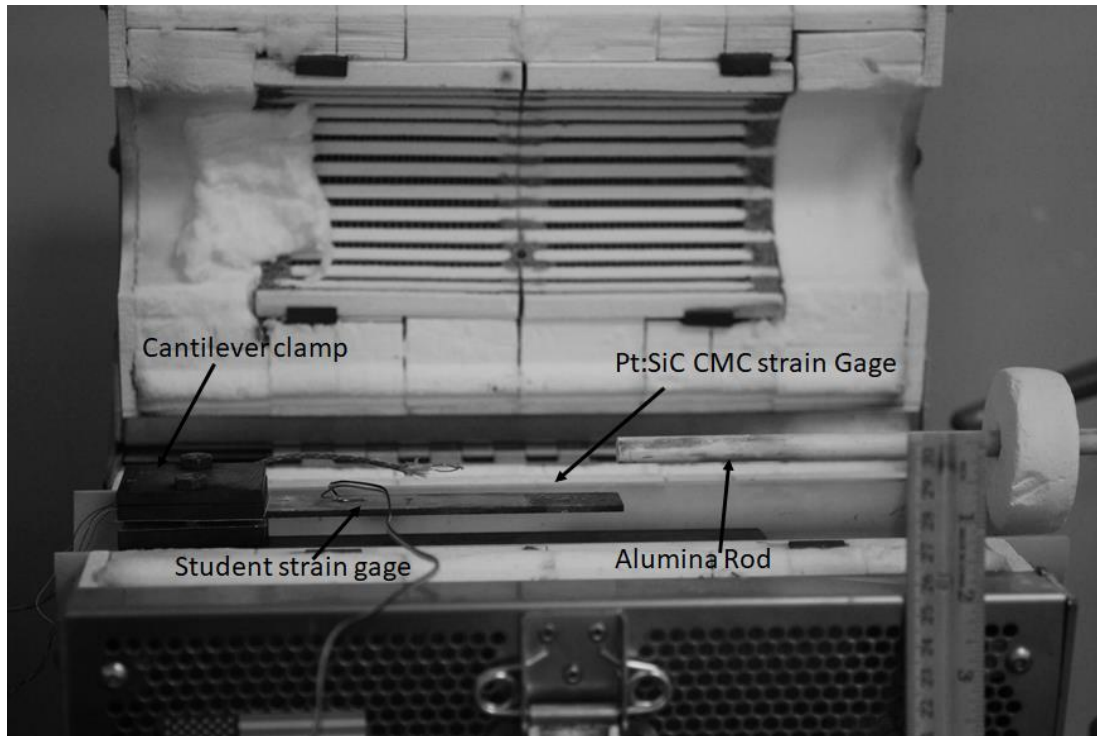


Figure 42: Photograph showing the testing tube furnace holding a Pt:SiC CMC strain gage in a cantilever fixture.

7.3.4 SiC CMC Fiber Directionality Effect

The SiC-SiC CMC substrates are comprised of polycrystalline SiC fibers encased within a polycrystalline SiC matrix. The SiC fibers were oriented in different directions within the matrix for different substrates (Fig. 41) and in previous work, thermocouples in which the SiC-SiC CMC was an active thermoelement saw a noticeable effect on overall thermoelectric performance based on the orientation of the SiC embedded fibers [20]. Gage factors for Pt:SiC CMC strain gages fabricated on SiC-SiC CMC substrates with different fiber orientations at room temperature are shown in Table 3. The ASTM C1341 method was used because the strain could be

applied uniformly across the surface but this method resulted in lower gage factors than those measured using the cantilever load method at similar applied strain. An excitation current of 10mA was used for this method and the strain was applied relative to the long axis of the beam; i.e. for the ASTM C1341 method when the strain gage was fabricated on a beam with fibers parallel to the long axis, a gage factor of 13 was measured, whereas the beam with a 45° fiber orientation had a gage factor of 20. The beam with a 90° fiber orientation had a gage factor of 28. The opposite trend was observed when the Pt:SiC CMC strain gages were tested using the cantilever load method (Fig. 42). In the latter case, the largest gage factors were achieved when the SiC fibers were parallel to the long axis of the beam and smaller gage factors were observed when the fibers were oriented at 90° to the long axis of the beam. These results were anticipated when the cantilever load method was utilized. When the CMC beams with the SiC fibers oriented at 90° with respect to the long axis of the beam were tested, the smallest gage factors were recorded; i.e. this orientation was least sensitive to applied strain. The opposite trend was observed when the ASTM method was used since the direction of applied strain was normal to the directions associated with the cantilever method. Overall, the effect of fiber directionality could be seen but it was not nearly as dramatic as the effect seen with thermoelectric performance of the CMC thermocouples.

Table 3: Embedded SiC fiber orientation effect on gage factor using the four point ASTM C1341 and cantilever load methods at room temperature.

| Fiber orientation | $\Delta R/R_0$ | $\mu\epsilon$ | Gage factor |
|-------------------|----------------|---------------|-------------|
| Parallel* | -0.008692 | -667 | 13.03 |
| 45°* | -0.023 | -1172 | 19.62 |
| 90°* | -0.028 | -1004 | 27.89 |
| Parallel** | -0.003938 | -140 | 28.13 |
| 45°** | -0.003701 | -197 | 18.79 |
| 90°** | -0.002264 | -275 | 8.23 |

*ASTM C1341 method.

**Cantilever load method.

7.4 Conclusion

Pt:SiC CMC strain gages exhibited relatively large gage factors at low temperatures ($G \sim 100$) but as expected, the gage factors decreased with increasing temperature. The study shows that more work has to be done to understand this behavior in order to make the Pt:SiC CMC strain gage a practical option for use in gas turbine engines.

Previous work with Pt:SiC CMC thermocouples showed that diffusion barriers were necessary when temperatures greater than 550°C are anticipated, due to the formation of SiO₂ on the SiC-SiC CMC surface by oxygen diffusion through the platinum thin film at the metal:semiconductor interface [20]. A consequence of this is the formation of a rectifying contact, which compromised the thermoelectric output and stability. In order to mitigate the formation of a Schottky barrier, diffusion barrier coatings were used to preserve the integrity of the metal:semiconductor contact [21]. In the future, the same approach will be taken to improve the stability of Pt:SiC CMC

strain gages. Diffusion barrier coatings will be reactively sputtered onto the Pt:SiC CMC contacts to prevent oxygen diffusion. With these protective coatings, the Pt:SiC CMC strain gages will be able to operate at temperatures well above 550°C.

List of References

- [1] Naslain R R, “SiC-Matrix Composites:Nonbrittle Ceramics for Thermo-Structural Application,” *Int. J. Appl. Ceram. Technol*, vol. 2, pp. 75-84, 2005.
- [2] Tougas M I, Amani M, Gregory O J, “Metallic and Ceramic Thin Film Thermocouples for Gas Turbine Engines,” *Sensors*, vol. 13, pp. 15324-15347, 2013.
- [3] Lei J, Will H A, “Thin-film thermocouples and strain-gauge technologies for engine applications,” *Sens. Acts. A*, vol. 65, pp. 187-193, 1997
- [4] Gregory O J, Luo Q, Crisman E E, “High temperature stability of indium oxide thin films,” *Thin Solid Films*, vol. 406, pp. 286-293, 2002
- [5] Gregory O J, Chen X, “A Low TCR Nanocomposite Strain Gage for Temperature Aerospace Applications,” *IEEE Sensors 2017*, pp. 624-627, 2007.
- [6] White N M, Turner J D, “ Thin-film sensors: past, present and future,” *Meas. Sci. Technol*, vol. 8, pp. 1-20, 1997.
- [7] Zhang S, Cai L, Miao J, Wang T, Yeom J, Sepulveda N, Wang C, “Fully Printer Silver-Nanoparticle-Based Strain Gauges with Record High Sensitivity,” *Adv. Electron. Mater.*, vol. 3, pp.1-6, 2017.

- [8] Ivanco J, Halahovets Y, Vegso K, Klackova I, Kotlar M, Vojtko A, Micusik M, Jergel M, Majkova E, "Cyclopean gauge factor of the strain-resistance transduction of indium oxide films," *Mater. Sci. Eng.*, vol. 108, pp. 1-7, 2016.
- [9] Smith C S, "Piezoresistance Effect in Germanium and Silicon," *Phys. Rev.*, vol. 94, pp. 42-49, 1954.
- [10] Kanda Y, "Piezoresistance effect in silicon," *Sens. Acts. A*, vol. 28, pp. 83-91, 1991.
- [11] Ching W Y, Xu Y, Rulis P, Ouyang L, "The electronic structure and spectroscopic properties of 3C, 2H, 4H, 6H, 15R and 21R polymorphs of SiC," *Mat. Sci. Eng. A*, vol. 422, pp. 147-156, 2005.
- [12] French P J, Evans G R, "Piezoresistance in Polysilicon and its Applications to Strain Gauges," *Solid-State Electronics*, vol. 32, pp. 1-10, 1989.
- [13] Phan H, Tanner P, Dao D V, Wang L, Nguyen N, Zhu Y, Dimitrijevic S, "Piezoresistive Effect of p-Type Single Crystalline 3C-SiC Thin Film," *IEEE Electronic Device Letters*, vol. 35, pp. 399-401, 2014.
- [14] Phan H, Dao D V, Nakamura K, Dimitrijevic S, Nguyen N, "The Piezoresistive Effect of SiC for MEMS Sensors at High Temperatures: A Review" *JMEMS*, vol 24, pp. 1663-1677, 2015.
- [15] Herring C, Vogt Erich, "Transport and Deformation-Potential Theory for Many-Valley Semiconductors with Anisotropic Scattering," *Phys. Rev.*, vol. 101, pp. 944-961., 1954.
- [16] Adams E N, "Elastoresistance in p-Type Ge and Si," *Phys. Rev.*, vol. 96, pp. 803-804, 1954.

- [17] Richter J, Pedersen J, Brandyge M, Thomsen E V, Hansen O, "Piezoresistance in p-type silicon revisited," *J. Appl. Phys.*, vol. 104, pp. 1-8, 2008.
- [18] Ramadan A A, Gould R D, Ashour A, "On the Van der Pauw method of resistivity measurements," *Thin Solid Films*, vol. 239, pp.272-275, 1994.
- [19] Smith C, Morscher, G N, Xia Z, "Electrical Resistance as a Nondestructive Evaluation Technique for SiC/SiC Ceramic Matrix Composites Under Creep-Rupture Loading," *Int. J. Appl. Ceram. Technol.*, vol. 8, pp. 298-307, 2010.
- [20] Rivera K, Muth T, Rhoat J, Ricci M, Gregory O J, "Novel temperature sensors for SiC-SiC CMC engine components," *J. Mater. Res.*, vol. 32, pp. 3319-3325, 2017.
- [21] Rivera K, Ricci M, Gregory O J, "Diffusion barrier coatings for CMC thermocouples," *Surface Coat. Technol.*, vol. 336, pp. 17-21, 2018.

CHAPTER 8

Resistance Temperature Detectors for CMC Engine Components

Submitted for publication in IEEE Electron Device Letters

Kevin Rivera and Otto J. Gregory

Department of Chemical Engineering, University of Rhode Island, Kingston RI

8.1 Abstract

Components within a gas turbine engine experience temperature upwards of 1200°C and g-forces greater than 50,000 and the nickel based superalloys are the current state of the art as far as material choice for these hot section components. Thus, there is a need for higher temperature components in order to achieve greater thermal efficiencies, which has prompted the need for more refractory materials to be used such as the ceramic matrix composites (CMCs). Thus, they that have been studied intensively over the past few decades. Measuring the temperature of these components is crucial during the engine development phase to evaluate structural models and temperature sensors such as thermocouples, resistance temperature detectors (RTDs) and thermistors are used but the sensors available are not compatible with the CMCs because they would have to be surface welded and thus alternative approaches for this problem have been sought. The CMC used in this study is comprised of SiC fibers in a SiC matrix. An RTD has been developed in which the SiC-SiC CMC is the active sensor element and can be used to measure temperatures up to 500°C. Beyond these temperatures a protective barrier coating has to be utilized.

8.2 Introduction

Temperatures in gas turbine engines can exceed 1200°C and super nickel alloys used within the hot section are being replaced with ceramic matrix composites (CMCs) in order to achieve higher temperatures and higher thermal efficiencies [1]. Temperature sensors such as thermocouples, thermistors and resistance temperature detectors (RTDs) can be used to measure temperatures but each choice has several advantages

and disadvantages. Conventional wire temperature sensors will have to be replaced by thin film or alternative solutions that are compatible with the CMCs since devices cannot be welded.

Thermocouples based on conductive oxides deposited on aluminum oxide have been demonstrated by Gregory [2] which are electrically and chemically stable in oxidizing environments at temperatures approaching 1500°C. Since these are based on conductive oxides, they are stable to very high temperature. The CMCs of interest in this study are comprised of SiC fibers encased in a SiC matrix. In previous work the substrate itself was used as one of the thermoelements in a thermocouple by coupling to with platinum leads and imposing a temperature gradient across the substrate [3]. These thermocouples can operate at temperatures nearing 1000°C when diffusion barrier coatings are employed to prevent oxygen ingress and adverse reactions. Thermistors are mostly used for low temperature applications (20-300°C) but certain devices have been developed to measure temperatures approaching 1300°C. Wang has shown lightly doped zirconia and calcium oxide thermistors that have highly stable changes in resistance as a function of temperature but still have a somewhat non-linear response [4]. Wire and thin film platinum RTDs have been tested at temperatures approaching 1000°C and thin film RTDs based on Au, Cu, and Ni have proved useful for lower temperature measurements [5].

A resistance temperature device in which the SiC-SiC CMC is the active resistor has been developed in this study. The RTDs maintain electrical and chemical stability to temperatures nearing 500°C but have require diffusion barrier coatings similar to the Pt:SiC CMC thermocouples that were mentioned previously when temperatures above

550°C were tested. The diffusion barriers preserve the ohmic nature at the film contacts. The RTD described within is a potential solution for temperature measurement of the SiC-SiC CMCs that allow the components to monitor their own temperature.

8.3 Experimental

8.3.1 Fabrication

The SiC-SiC CMC substrates were heated to 1000°C for 15hr to grow a stable oxide layer to improve adhesion of the dielectric coatings. A 20µm mullite coating was then applied to the surface and heat treated at 100 and 200°C for 20 minutes, 300 for 40 minutes on a hot plate and slowly ramped to 1000°C for 15hr in a tube furnace. Photolithography techniques were then used to pattern the substrate with the RTD pattern. The substrate was then placed in a sputtering chamber at 9mTorr with argon gas and sputtered with either Pt/Rh or indium tin oxide (ITO). High purity Pt/Rh was RF sputter deposited for 2.5 hours at 300W and a forward voltage of 1000V. ITO was RF sputter deposited for 10 hours at 350W and a forward voltage of 1100V. The resistance of the SiC-SiC CMC is much lower than the deposited Pt/Rh thin films and a four point resistance measurement design was used to eliminate the contact resistance of the thin films and to ensure that the positive TCR of the metal thin films would not overpower the negative TCR of the SiC-SiC CMC (Fig. 43).

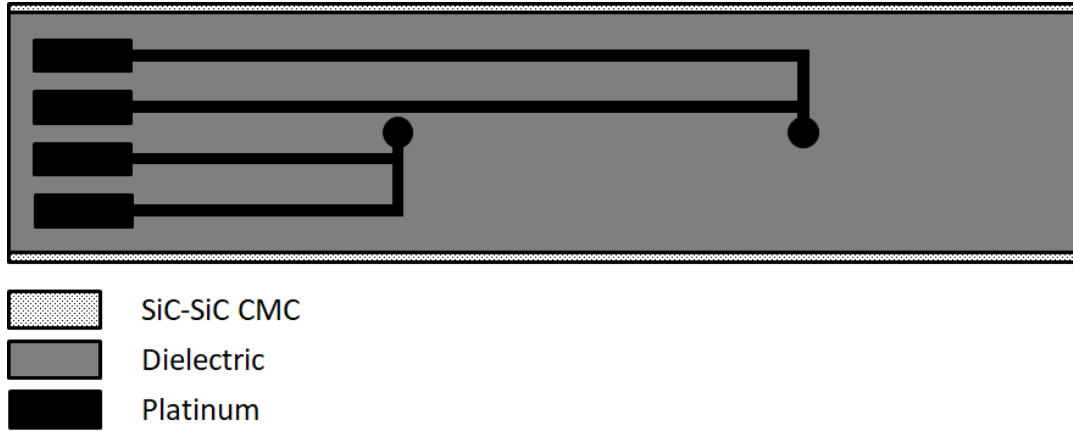


Figure 43: Pt/Rh:SiC CMC RTD design. Current is passed through the outer legs and the voltage drop is measured across the inner legs.

8.3.2 Governing Equations

To determine TCR of the RTD at a particular temperature a first order approximation was used shown in eq.1

$$\alpha = \frac{R_F - R_o}{R_o(T_F - T_o)} \quad (1)$$

where R_o is the initial resistance at the reference temperature T_o and R_F is the final resistance at T_F .

8.3.3 Diffusion Barrier Coatings

The ITO:SiC contacts were susceptible to oxygen diffusion and subsequent oxidation of the ITO at high temperatures. Once oxygen diffuses through the contact it can oxidize the SiC in the CMC and form a SiO_2 layer that causes the contact to become rectifying and eventually electrically insulating. Reactively sputtered coatings consisting of ITON (10 μm) were used to protect these contact areas.

8.3.4 Testing Procedure

When Pt or Pt/Rd thin films were used, a four-wire resistivity measurement was used as opposed to a 2-point measurement to eliminate contact resistance and avoid the changes in resistance contributed by the thin leads since they exhibit positive TCR. When conductive oxide thin films were used, a four-wire resistivity measurement was used but only two contact points were used since TCR of the conductive oxides is negative similar to the SiC in the CMC. In the four wire measurement, electrical current was passed along the outer leads and the voltage drop across the SiC-SiC CMC was measured at the inner leads.

8.4 Results

The Pt/Rh:SiC CMC RTD was thermally excited to 500°C and then cooled to 100°C. The RTD started off with a very low resistance due to the four point design used which eliminated the resistance of the Pt/Rh legs (Fig. 44). This low starting resistance made temperature measurement above 500°C difficult for the data acquisition because the change in resistance per unit change in temperature was minimized as the resistance decreased. The TCR of the Pt/Rh:SiC CMC RTD was due to the SiC-SiC CMC, which reflected experimental values for SiC found by Zhang et.al [6] (Fig. 45). The ITO:SiC CMC RTDs did not perform as well mainly due to a large temperature range over which the resistance remains near 50Ω (425-250°C). The resistance change from 250-150°C was more dramatic but contained much more noise compared to the Pt/Rh:SiC CMC RTD (Fig.46). The IV characteristics of the ITO:SiC contacts were evaluated using the Vanderpauw method and was determined that they

formed and ohmic contact (Fig. 47).

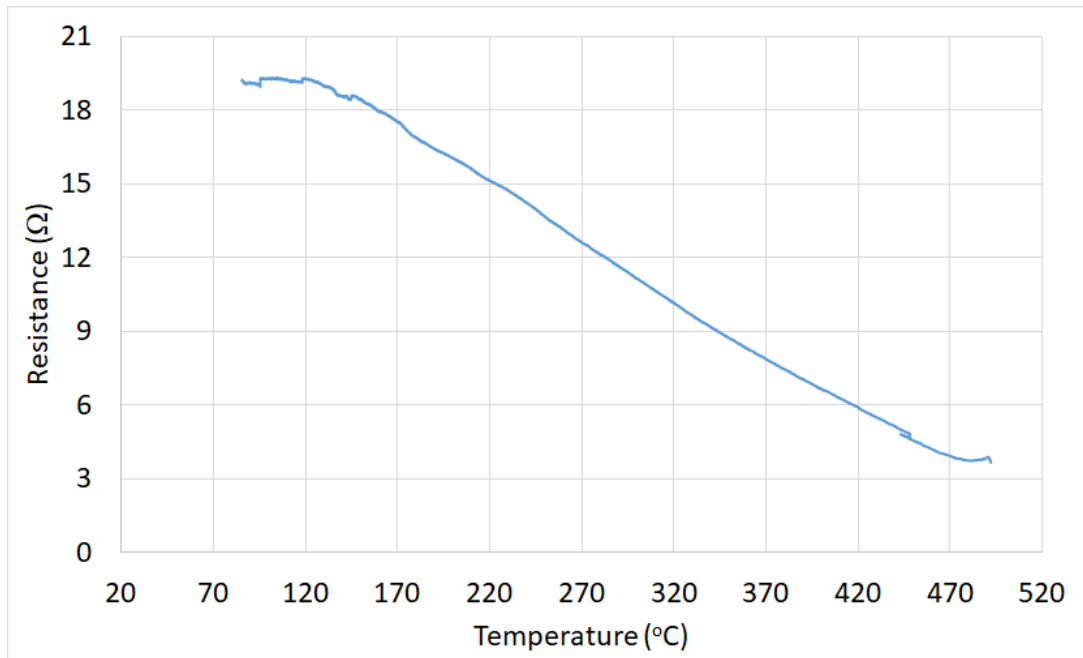


Figure 44: Electrical resistance as a function of temperature. Here a linear relationship between electrical resistance and temperature from 150°C to 450°C and nonlinear behavior was observed at temperatures lower than 150°C and higher than 450°C.

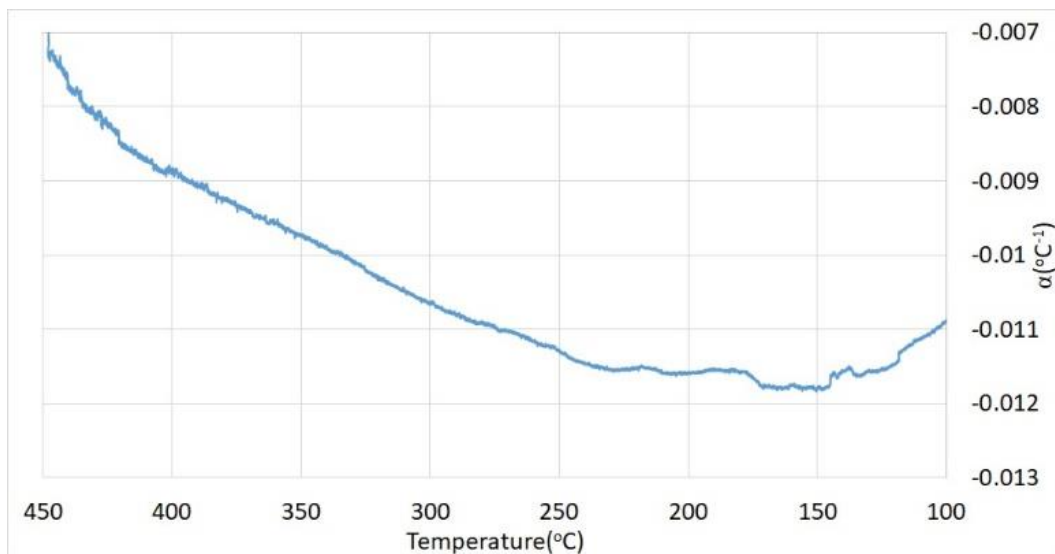


Figure 45: TCR of the Pt/Rh:SiC CMC RTD as a function of temperature.

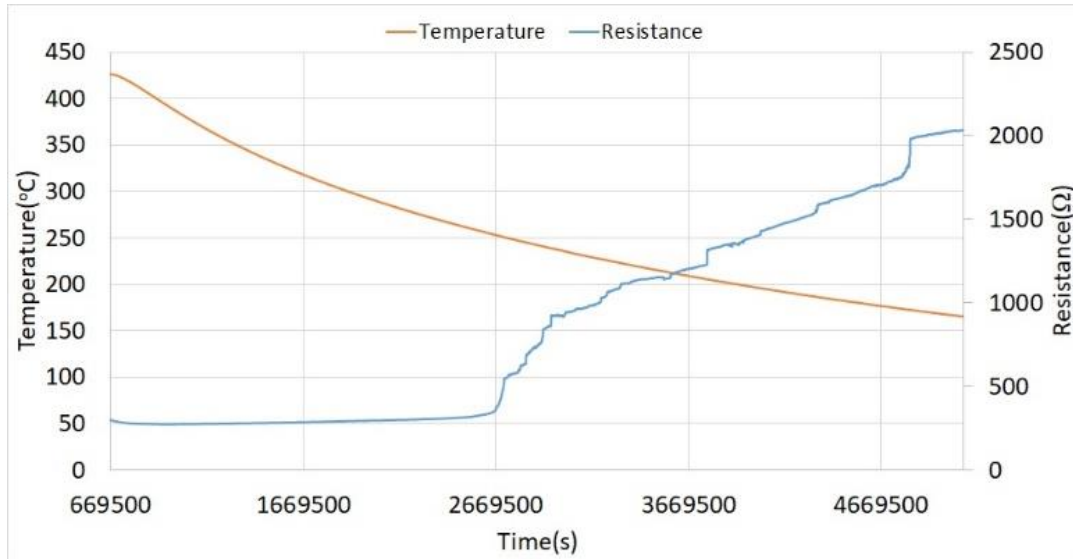


Figure 46: Ramp down of ITON/ITO:SiC CMC RTD. The contribution of the ITO film was observed from 425°C-250°C.

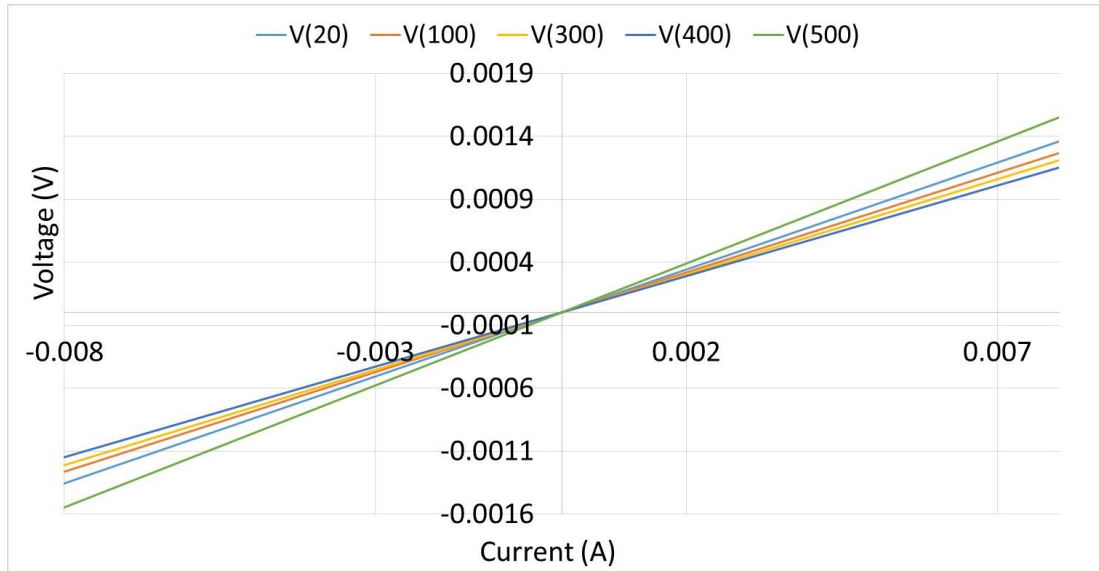


Figure 47: IV characteristics of an ITO:SiC CMC contact as a function of temperature using the Vanderpauw method. ITO forms an ohmic contact to the SiC-SiC CMC.

8.5 Conclusion

RTDs based on SiC-SiC CMCs have been developed but are somewhat limited. The Pt/Rh:SiC CMC RTDs were more stable in terms of performance compared to the ITO:SiC CMC RTDs. Because the Pt/Rh:SiC CMC RTDs had such a low initial resistance (20Ω), their temperature range was limited by the continuous decrease as the temperature was increased. The ITO films suffered from oxidation and high signal noise which makes them undesirable candidates for thin film leads for use in SiC-SiC CMCs. In the future work, the performance of the ITO:SiC CMCs will be improved by adding a layer of Pt or Pt/Rh underneath to stabilize the signal.

List of References

- [1] R.R. Naslain. "SiC-Matrix Composites: Nonbrittle Ceramics for Thermo-Structural Application," *Int. J. Appl. Ceram. Tech.*, vol. 2, pp. 75-84, 2005.
- [2] X. Chen, O.J. Gregory, M. Amani, "Thin-Film Thermocouples Based on the System $\text{In}_2\text{O}_3\text{-SnO}_2$," *J. Am. Ceram. Soc.*, vol. 94, pp. 854-860, 2011.
- [3] K. Rivera, M. Ricci, O.J. Gregory, "Diffusion barrier coatings for CMC thermocouples," *Surface & Coatings Technology*, vol. 336, ppg. 17-21, 2018.
- [4] C.C. Wang, S.A. Akbar, W. Chen, J.R. Schorr, "High-temperature thermistors based on yttria and calcium zirconate," *Sens. Acts. A*, vol. 58, pp. 237-243, 1997.

- [5] M. Imran, A. Bhattacharyya, "Effect of Thin Film Thickness and Materials in the Response of RTDs and Microthermocouples," *IEEE Sensors journal*, vol. 6, pp. 1459-1467, 2006.
- [6] J. Zhang, C. Carraro, R.T. Howe, R. Maboudian, "Electrical, Mechanical and metal contact properties of polycrystalline 3C-SiC films for MEMS in harsh environments," *Surface and Coatings Technology*, vol. 201, pp. 8893-8898, 2007.

CHAPTER 9

Conclusions

9.1 Thermocouples for CMC engine components

In this work different approaches were used to develop thermocouples that would be compatible with SiC-SiC CMCs. Pt:SiC CMC thermocouples could be used at temperatures up to 550°C but not beyond due these temperatures to oxidation and the ITO:SiC CMC thermocouples were limited to 660°C. In order to improve the operating temperature of the Pt:SiC CMC thermocouples, diffusion barriers consisting of reactively sputtered ITO in pressurized N₂ were deposited to prevent oxidation and oxygen diffusion and ITO was sputtered as a barrier to prevent the formation of platinum silicides at elevated temperatures. Overall these thermocouples could operate near 1000°C which is the largest temperature of interest. Temperatures beyond this resulted in failure of the protective barrier coatings and rendered the device useless.

9.2 Strain Gages for CMC engine components

Strain gages were developed that had gage factors larger than 100 but suffered from decreasing gage factors with increasing temperature. The current Pt:SiC CMC strain gage was limited to operational temperatures of 550°C.

9.3 Resistance Temperature Devices for CMC engine components

RTDs based on the SiC-SiC CMCs had not been explored in as much detail and proved to be a difficult to implement. The use of metal thin films in the RTDs required that four point measurement be used to eliminate any contact resistance and degradation due to the positive TCR of the metal and negative TCR of the SiC CMC

interferes with the behavior as a function of temperature would be highly nonlinear as a function of temperature electrical resistance of the positive TCR leads with the negative TCR of the SiC CMC made it difficult to generate calibration curves. These RTDs could function over a limited range but due to the low initial resistance this limited their temperature range. When conductive oxide films were used the four point measurement was not necessary since the ITO and SiC in the CMC both have negative TCRs. However these RTDs had a very large noise to signal ratio and were virtually unusable at high temperatures.

CHAPTER 10

Future work

10.1 High Temperature CMC Thermocouples

A severe limitation with the thermocouples developed in this work was the requirement of multiple protective barrier coatings when platinum thin films were used as one of the thermoelements but in future CMC thermocouples improvements will be made to the ITO:SiC CMC thermocouples discussed in chapter 3. The ITO:SiC CMC thermocouples also suffer from oxidation and require an oxygen barrier beyond 660°C but they have the advantage of not reacting with the SiC-SiC CMC. For future thermocouples thicker ITO films will be sputtered along with thick oxygen diffusion barriers in order to account for the large surface roughness of the SiC-SiC CMCs and high temperature air anneals will be done in addition to the N₂ anneals before testing in order to reduce inhomogeneity in the ITO thin films along the thermocouple temperature gradient.

10.2 High Temperature CMC Strain gages and RTDs

Both the CMC strain gages and RTDs have the advantage of utilizing the same designs so in future versions the design will be adjusted in order to improve performance (Fig. 48).

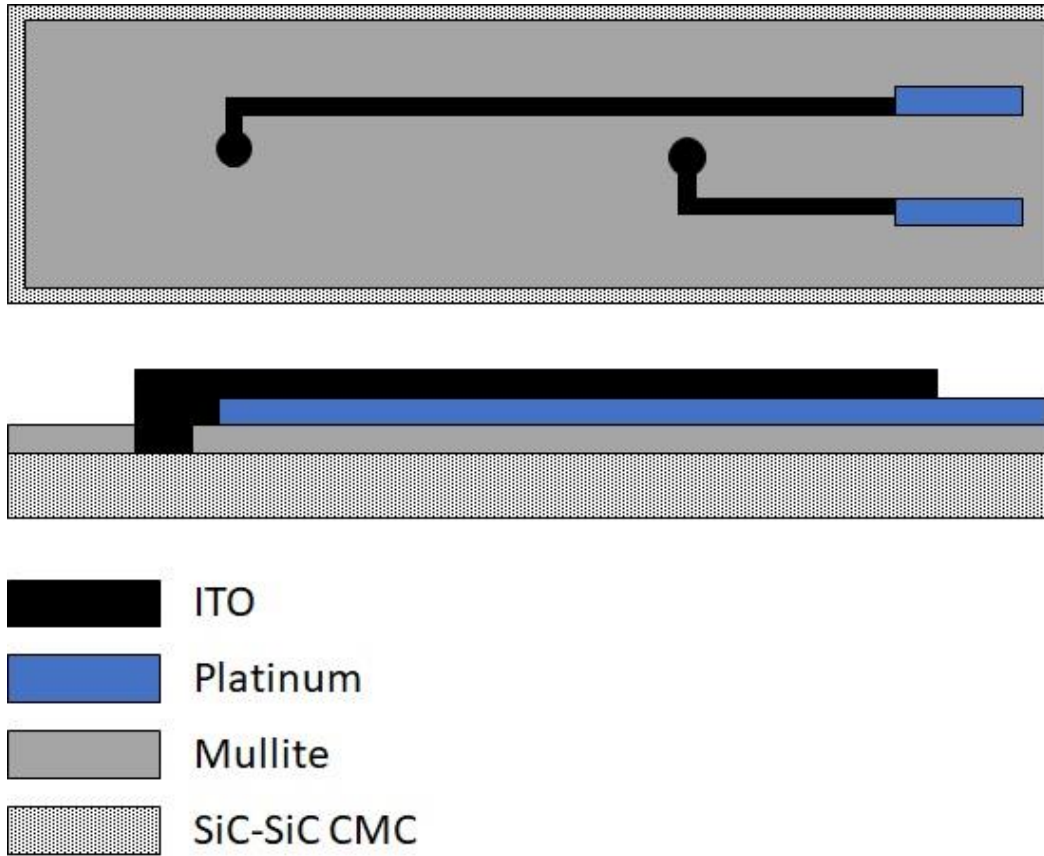


Figure 48: Concept for future RTD and strain gage showing a top and layered view.

APPENDICES

Begin typing or pasting your appendices here.

BIBLIOGRAPHY

- Abdelaziz, Y.A., Megahed, F.M., Halawa ,M.M., “Stability and calibration of platinum/palladium thermocouples following heat treatment,” *Measurement*, vol. 35, 413-420, 2004.
- Adams, E. N., “Elastoresistance in p-Type Ge and Si,” *Phys. Rev.*, vol. 96, pp. 803-804, 1954.
- Chen, X., Gregory, O.J., Amani, M., “Thin-film thermocouples based on the system $\text{In}_2\text{O}_3\text{-SnO}_2$,” *J. Am. Ceram. Soc.*, vol. 94, pp. 854-860, 2011.
- Ching, W. Y., Xu, Y., Rulis, P., Ouyang, L., “The electronic structure and spectroscopic properties of 3C, 2H, 4H, 6H , 15R and 21R polymorphs of SiC,” *Mat. Sci. Eng. A*, vol. 422, pp. 147-156, 2005.
- Chou, T.C., “High temperature reactions between SiC and platinum,” *J. Mater. Sci.*, vol 26, pp. 1412-1420, 1991.
- Chou, T.C., “Anomalous solid state reaction between SiC and Pt,” *J. Mater. Res.*, vol. 5, pp. 601-608, 1990.
- DiCarlo, J.A., Yun, H., “Methods For Producing Silicon Carbide Architectural Preforms,” U.S. Patent 7,687,016 issued March 30, 2010.
- DiCarlo, J.A., Yun, H., “Methods for Producing High-Performance Silicon Carbide Fibers, Architectural Preforms, And High-Temperature Composite Structures,” U.S. Patent 8,894,918 issued November 25, 2014.

- Fankhanel, B., Muller, E., Mosler, U., Siegel, W., "SiC-fibre reinforced glasses – electrical properties and their applications," *J. ECS*, vol. 21, pp. 649-657, 2001.
- French, P. J., Evans, G. R., "Piezoresistance in Polysilicon and its Applications to Strain Gauges," *Solid-State Electronics*, vol. 32, pp. 1-10, 1989.
- Gregory, O. J., You, T., "Ceramic Temperature Sensors for Harsh Environments," *IEEE Sens. J.*, vol. 5, pp. 833-838, 2005.
- Gregory, O.J., You, T., "Piezoresistive Properties of ITO Strain Sensors Prepared with Controlled Nanoporosity," *J. of the Electrochemical Soc.*, vol 151, pp. 198-203, 2004.
- Gregory, O. J., Lou, Q., "A self-compensated strain gage for use at elevated temperatures," *Sens. Act. A*, vol. 88, pp. 234-240, 2001.
- Gregory, O. J., Luo, Q., Crisman, E. E., "High temperature stability of indium oxide thin films," *Thin Solid Films*, vol. 406, pp. 286-293, 2002
- Gregory, O. J., Chen, X., "A Low TCR Nanocomposite Strain Gage for Temperature Aerospace Applications," *IEEE Sensors 2017*, pp. 624-627, 2007.
- Herring, C., "Transport and Deformation-Potential Theory for Many-Valley Semiconductors with Anisotropic Scattering," *Phys. Rev.*, vol. 101, pp. 944-961., 1954.
- Hill, K.D., "An investigation of palladium oxidation in the platinum/palladium thermocouple system," *Metrologia*, vol. 39, 51-58, 2002.
- Imran, M., Bhattacharyya, A., "Effect of Thin Film Thicknes and Materials on the Response of RTDs and Microthermocouples," *IEEE Sens. J.*, vol. 6, pp. 1459-1467, 2006.

- Ivanco, J., Halahovets, Y., Vegso, K., Klackova, I., Kotlar, M., Vojtko, A., Micusik, M., Jergel, M., Majkova, E., "Cyclopean gauge factor of the strain-resistance transduction of indium oxide films," *Mater. Sci. Eng.*, vol. 108, pp. 1-7, 2016.
- Kanda, Y., "Piezoresistance effect in silicon," *Sens. Acts. A*, vol. 28, pp. 83-91, 1991.
- Kreider, K.G., DiMeo, F., "Platinum/palladium thin-film thermocouples for temperature measurements on silicon wafers," *Sensors and Actuators A*, vol. 69, 46-52, 1998.
- Krieder, K.G., Greg, G., "High temperature materials for thin-film thermocouples on silicon wafers," *Thin Solid Films*, vol. 376, 32-37, 2000.
- Lei, J., Will, H. A., "Thin-film thermocouples and strain-gauge technologies for engine applications," *Sens. Acts. A*, vol. 65, pp. 187-193, 1998
- Mei, H., Cheng, L., "Damage analysis of 2D C/SiC composites subjected to thermal cycling in oxidizing environments by mechanical and electrical characterization," *Materials Letters*, vol. 59, pp. 3246-3251, 2005.
- Moiseeva, N.P., "The prospects for developing standard thermocouples of pure metals," *Measurement Techniques*, vol. 47, pp. 915-919, 2004.
- Naslain, R. R., "SiC-Matrix Composites: Nonbrittle Ceramics for Thermo-Structural Application," *Int. J. Appl. Ceram. Technol*, vol. 2, pp. 75-84, 2005.
- National Institute of Standards and Technology Type J Thermocouple Reference Tables. Available at: https://srdata.nist.gov/its90/type_j/300to600.html (accessed 31 March 2017).

National Institute of Standards and Technology Type K Thermocouple Reference Tables. Available at: https://srdata.nist.gov/its90/type_k/300to600.html (accessed 31 March 2017).

National Institute of Standards and Technology Type E Thermocouple Reference Tables. Available at: https://srdata.nist.gov/its90/type_e/300to600.html (accessed 31 March 2017).

National Institute of Standards and Technology Type N Thermocouple Reference Tables. Available at: https://srdata.nist.gov/its90/type_n/300to600.html (accessed 31 March 2017).

National Institute of Standards and Technology Type R Thermocouple Reference Tables. Available at: https://srdata.nist.gov/its90/type_r/600to900.html (accessed 31 March 2017).

National Institute of Standards and Technology Type S Thermocouple Reference Tables. Available at: https://srdata.nist.gov/its90/type_s/600to900.html (accessed 31 March 2017).

National Institute of Standards and Technology, Thermocouple Reference Tables Type B. Available at: https://srdata.nist.gov/its90/type_b/300to600.html (accessed 31 March 2017).

Nicolet, M.A., "Diffusion barriers in thin films," *Thin Solid Films*, vol. 52, pp. 415-443, 1978.

Okojie, R.S., "Characterization of highly doped n- and p-type 6H-SiC piezoresistors," *IEEE Transactions on Electron Devices*, vol. 45, pp. 785-790, 1998.

- Phan, H., Dao, D. V., Nakamura, K., Dimitrijević, S., Nguyen, N., “The Piezoresistive Effect of SiC for MEMS Sensors at High Temperatures: A Review” *JMEMS*, vol 24, pp. 1663-1677, 2015.
- Phan, H., Tanner P, Dao, D. V., Wang, L., Nguyen, N., Zhu, Y., Dimitrijević, S., “Piezoresistive Effect of p-Type Single Crystalline 3C-SiC Thin Film,” *IEEE Electronic Device Letters*, vol. 35, pp. 399-401, 2014.
- Ramadan, A. A., Gould, R. D., Ashour, A., “On the Van der Pauw method of resistivity measurements,” *Thin Solid Films*, vol. 239, pp.272-275, 1994.
- Richter, J., Pedersen, J., Brandyge, M., Thomsen, E. V., Hansen, O., “Piezoresistance in p-type silicon revisited,” *J. Appl. Phys.*, vol. 104, pp. 1-8, 2008.
- Rijnders, M.R., Kodentsov, A.A., Van Beek, J.A., van den Akker, J., Van Loo, F.J.J., “Pattern formation in Pt-SiC diffusion couples,” *Solid State Ionics*, vol. 95, 51-59, 1997.
- Rivera, K., Muth, T., Rhoat, J., Ricci, M., Gregory, O. J., “Novel temperature sensors for SiC-SiC CMC engine components,” *J. Mater. Res.*, vol. 32, pp. 3319-3325, 2017.
- Rivera, K., Ricci, M., Gregory, O. J., “Diffusion barrier coatings for CMC thermocouples,” *Surface Coat. Technol.*, vol. 336, pp. 17-21, 2018.
- Smith, C.E., Morscher, G.N., Xia, Z.H., “Monitoring damage accumulation in ceramic matrix composites using electrical resistivity,” *Scripta Materialia*, vol. 59, pp. 463-466, 2008.

- Smith, C., Morscher, G. N., Xia, Z., “Electrical Resistance as a Nondestructive Evaluation Technique for SiC/SiC Ceramic Matrix Composites Under Creep-Rupture Loading,” *Int. J. Appl. Ceram. Technol.*, vol. 8, pp. 298-307, 2011.
- Smith, C. S., “Piezoresistance Effect in Germanium and Silicon,” *Phys. Rev.*, vol. 94, pp. 42-49, 1954.
- Tanner, L. E., Okamoto, H., “The Pt-Si (Platinum-Silicon) System,” *J. Phase Equilibria*, vol. 12, 571-574, 1991.
- Tougas, I. M., Amani, M., Gregory, O. J., “Metallic and Ceramic Thin Film Thermocouples for Gas Turbine Engines,” *Sensors*, vol. 13, pp. 15324-15347, 2013.
- Tougas, I. M., O.J. Gregory, “Thin film platinum-palladium thermocouples for gas turbine applications,” *Thin Solid Films*, vol. 539, pp. 345-349, 2013.
- Velho, L. R., Barlett, R.W., “Diffusivity and Solubility of Oxygen in Platinum and Pt-Ni Alloys,” *Metallurgical Transactions*, vol. 3, 65-72, 1972.
- Wang, C. C., Akbar, S.A., Chen, W., Schorr, J.R., “High-temperature thermistors based on yttria and calcium zirconate,” *Sens. Acts. A*, vol. 58, pp. 237-243, 1997.
- White, N. M., Turner, J. D., “Thin-film sensors: past, present and future,” *Meas. Sci. Technol*, vol. 8, pp. 1-20, 1997.
- Wrbanek, J. D., Fralick, G.C., Zhu, D., “Ceramic thin film thermocouples for SiC-based ceramic matrix composites,” *Thin Solid Films*, vol. 520, pp. 5801-5806, 2012.

- Zhang, S., Cai, L., Miao, J., Wang, T., Yeom, J., Sepulveda, N., Wang, C., “Fully Printed Silver-Nanoparticle-Based Strain Gauges with Record High Sensitivity,” *Adv. Electron. Mater.*, vol. 3, pp.1-6, 2017.
- Zhang, J., Carraro, C., Howe, R.T., Maboudian, R., “Electrical, Mechanical and metal contact properties of polycrystalline 3C-SiC films for MEMS in harsh environments,” *Surface and Coatings Technology*, vol. 201, pp. 8893-8898, 2007.
- Zhang, N., Lin, C., Senesky, D. G., A. P. Pisano, “Temperature sensor based on 4H-silicon carbide pn diode operational from 20°C to 600°C,” *Applied Physics Letters*, vol. 104, pp. 1-3, 2014

Zhao, X., Li, H., Yang, K., Jiang, S., Jiang, H., Zhang, W., “Annealing effects in ITO based ceramic thin film thermocouples,” *J. of Alloys and Compounds*, vol. 698, pp. 147-151, 2017.

Zhao, X., Wang, H., Zhao, Z., Zhang, W., Jiang, H., “Preparation and Thermoelectric Characteristics of ITO/PtRh:Pt:Rh Thin Film Thermocouple,” *Nanoscale Research Letters*, pp. 1-6, 2017.